Electric Technology U.S.S.R.

ЭЛЕКТРИЧЕСТВО

Volume 2, 1961

Selected papers from
Elektrichestvo Nos. 4, 5 and 6, 1961

shed by

RGAMON PRESS NEW YORK LONDON OXFORD PARIS

for Pergamon Institute, Washington and Oxford

ELECTRIC TECHNOLOGY, U.S.S.R.

PERGAMON INSTITUTE

A DIVISION OF PERGAMON INTERNATIONAL CORPORATION, OPERATED IN THE PUBLIC SERVICE FOR THE FURTHERANCE AND DISSEMINATION OF SCIENTIFIC KNOWLEDGE

President of the Scientific Advisory Council:
Sir Robert Robinson, O.M., F.R.S.

Executive Director: Captain I. R. Maxwell, M.C.

122 *East 55th Street New York* 22, *N.Y.* (*Telephone No. Plaza* 39651).

Headington Hill Hall, OXFORD. (*Telephone No. Oxford* 64881)

Pergamon Institute can occasionally use additional translators for science and engineering material to assist with this programme of translation from Russian and other Slavonic languages.

Scientists and engineers who have a knowledge of Russian, and who are willing to assist with this work, should apply to the Administrative Secretary of the Institute. They should write to New York or Oxford for rates of payment and other details.

Four volumes per annum. Approximately 700 pages per annum.
Annual Subscription Rate £20 ($60).
Single volumes may be purchased for £6 ($14).

Orders should be sent to the distributors at either of the following addresses

Headington Hill Hall, Oxford
122 East 55th Street, New York 22, N.Y.

PUBLISHED BY

PERGAMON PRESS LTD.

NEW YORK · LONDON · OXFORD · PARIS

November 1961

A MAGNETIC ROTATING - ARC ARRESTER FOR COMBINED PROTECTION FROM INTERNAL SURGES AND LIGHTNING STRIKES ON 500 KV TRANSMISSION LINES*

V.P. SAVEL'EV, V.V. SHMATOVICH,
V.I. PRUZHININA and V.K. PUGACHEV

(Lenin All-Union Electrical Engineering Institute)

(Received 25 July 1960)

Introduction

Plans have been made to reduce the level of insulation on the equipment used in 500 kV a.c. transmission lines to 2.5 U_p. These plans are based on the use of appropriate arresters.

In 1957 the All-Union Electrical Engineering Institute developed a "tervite"** arrester for protection from internal surges which is known in the U.S.S.R. as the "commutation" arrester. It is quite capable of limiting internal surges to 2.5 U_p and its quenching voltage is 1.6 U_p [1]. But it affords no protection against direct lightning strikes with current surges up to 10 kA. This has entailed the use of a special lightning arrester which was also developed at the Institute and which is known as the "vilite" lightning arrester ("Vilite" is a Russian ceramic material which consists of SiC + clay and graphite, *Translator*). The operating resistors of this arrester have better non-linearity, but their current capacity is less and their quenching voltage is lower (1.3 U_p) [1,2].

But the use of two types of valve arrester involved isolating the lightning arrester from the effects of internal surges and this posed

---

* *Electrichestvo*, No.4, 13-20, 1961.

** Tervite is a special type of material used to make non-linear resistors (Translator).

very difficult technical problems. It was therefore decided to combine the functions of the separate "commutation" and "lightning" arresters in one combined magnetic rotating-arc arrester. This arrester was developed by the Institute* in 1958.

The limitation of internal surges

Internal overvoltages reach 3 to 4 U_p under the various fault conditions which occur on 500 kV transmission lines under transient conditions. The arrester should restrict the surge to 2.5 U_p or less and interrupt the current in the next half-period after its "free" (transient) component has decayed and the recovery voltage has dropped to the value of the quenching voltage of the arrester.

The need to restrict internal surges to 2.5 U_p determines both the puncture voltage of the arrester and the residual voltage on its operating resistance. The operating resistance of the arrester should be as large as possible since the current is then a minimum. This also means that the rupturing capacity of the sparkgaps need not satisfy such demanding conditions.

Calculations [3, 4], experiments on model 500 kV lines and field tests on a 400 kV network [5] all point to the conclusion that the most probable load on an arrester under transient conditions is an oscillatory decaying discharge lasting three half-periods**:

Half-periods	Amplitude, A	Length of wave, msec
1	1,500	2.5-3.5
2	700-800	5
3	250-350	5

But most research laboratories usually find one half-period of current at supply frequency and 1500 A the most convenient for tests. Experience has shown that this load is no less exacting than the recommended three half-period load.

Thus an arrester which is intended to limit internal surges must be able to carry the instantaneous flow of current of the recommended three

---

* S.F. Erin, V.A. Filimonov, T.K. Ivanova and A.Ia. Sharlot took part in development work.

** This conclusion has also been confirmed by research at the Direct current Research Institute.

half-period oscillatory discharge or its equivalent at the supply frequency. The puncture and residual voltages of the arrester must not exceed 2.5 U_p during internal surges, and the arc must be quenched for a sinusoidal recovery voltage of at least 1.6 U_p at approx. 50 c/s. Since the arrester itself gives rise to transient phenomena on interrupting the current, the steady state voltage at the point where the arrester is installed must not exceed 1.4 to 1.5 U_p.

The type of sparkgap in the internal surge arrester and their arc-quenching capacity

The sparkgap is one of the main items in an arrester. Those in the arrester under consideration consist of a series of individual gaps. The arc-quenching capacity η of this particular "multiple-gap" design can be defined as the ratio of the puncture voltage U_{punct} to the quenching voltage U_q at which a specific current is reliably interrupted at supply frequency.

In multiple sparkgaps of conventional RVS-type "valve" arresters the arc quenching capacity $\eta = \frac{U_{punct}}{U_q} = 2.0$ to 2.5 for a current of 100 A. This arc-quenching capacity is clearly inadequate for the sparkgaps of internal surge arresters. That of the Institute's magnetic spark gaps with a rotating arc is much higher. Currents up to 250 A can be interrupted in the lightning arresters, whilst the puncture voltage is reduced to 2.5 U_p [2]. Later investigations have shown that their arc-quenching capacity is still high even if currents of 1000 to 1500 A flow through the gaps for 0.01 sec. But the individual magnetic spark gaps of the internal surge arrester have smaller air gaps between the electrodes than the lightning arrester and their puncture voltage is lower accordingly (3 to 4 kV_{max}).

The sparkgap (Fig. 1) is an annular slot between two copper electrodes 1 and 2 which are arranged concentrically in the horizontal plane. The electrodes are accomodated in a chamber formed by upper and lower walls 3 and 4. Double walls are used for the chamber (pressed paper on the inside and micanite on the outside). The walls are 1.5 mm away from the electrodes which prevents them affecting the puncture voltage of the gap. The electrodes are 3 mm thick and their operating surface is polished and carefully de-greased to facilitate the movement of the arc under the effect of the magnetic field produced by the permanent ring magnets 5 and 6.

The gaps are connected together by means of the magnets, one magnet being set between each pair of sparkgaps. In this case the m.m.f.'s of the magnets are summed and the induction in the gap is increased. The strength of the magnetic field in the air gap must be 700 to 800 oersted. Special auxiliary electrodes 7 and 8 are used to activate the sparkgap. In this way the impulse coefficient of an individual sparkgap in maintained at 1.25 for a pre-discharge time of 0.1 μ sec, or 1.1 for 1 μ sec. The scatter (variation) of the puncture voltage has been reduced to a minimum at supply frequency.

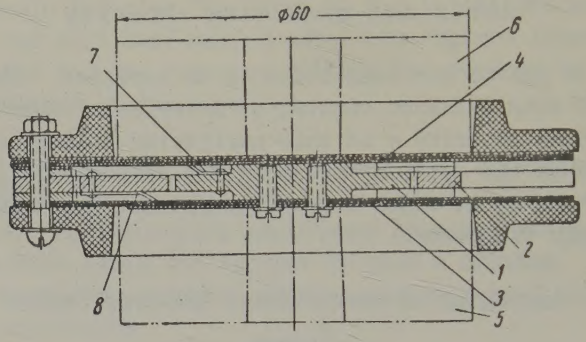

Fig. 1. An individual magnetic sparkgap.

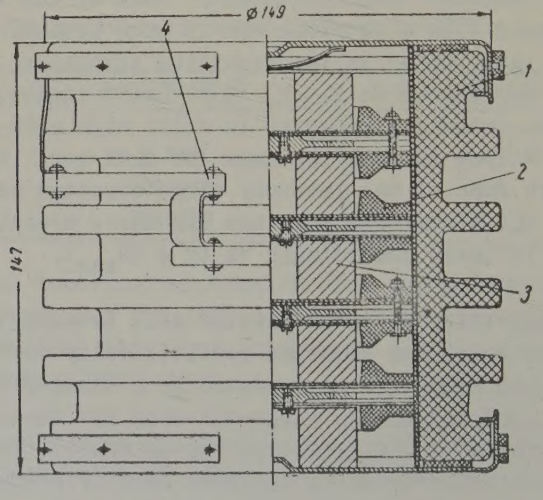

Fig. 2. A set of sparkgaps:

1 – Porcelain covering; 2 – sparkgap; *3* – magnet; *4* – shunting resistance.

Four individual sparkgaps are arranged in a porcelain covering to form one sparkgap sub-unit (Fig. 2). Each such sub-unit is shunted by non-linear carborundum disk-resistors ($\alpha \approx 0.35$) to ensure a uniform distribution of the voltage over the sub-unit. The total conduction current of each sub-unit is 1200 μA at a voltage of 3600 V. Five sub-units and their disk-resistors are then assembled in a standard porcelain jacket to form the complete sparkgap unit. Thus a complete unit consists of twenty sparkgaps and the set of disk-resistors.

The arc-quenching capacity of the arrester mainly depends on the properties of the individual sparkgaps. We will therefore consider their characteristics first.

The arc-quenching properties of an individual sparkgap can be assessed quite conveniently in terms of "relative recovery strength" (the recovery strength calculated as a percentage of the puncture voltage). Fig. 3 shows the results of 100 measurements* of the relative recovery strength of an individual sparkgap after carrying a current of 1500 A for one half-period at 50 c/s. The puncture voltage of the gap is 4 kV_{max}.

It must be borne in mind that the recovery strength of all the individual gaps is not exactly the same and, as can be seen from Fig. 3, the results are quite scattered. A large number of tests are therefore always required before the lower envelope of the recovery strength can be determined.

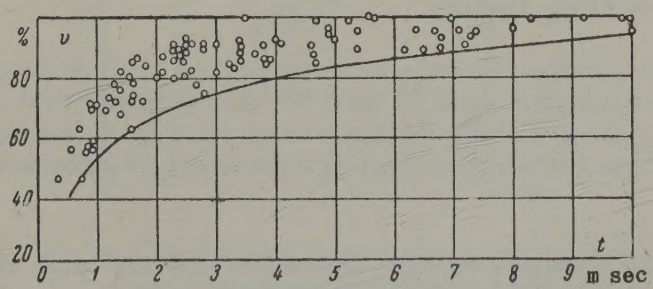

Fig. 3. The recovery strength of an individual magnetic sparkgap as a percentage of the puncture voltage.

Some idea of the arc-quenching properties of the individual sparkgaps under different internal fault conditions was required. Tests were therefore made on the individual sparkgaps at the maximum puncture voltage 4kV using oscillatory decaying discharges of different ampli-

* The method of measurement has already been described [2].

tude and duration (see Table 1).

TABLE 1

Loads as in Fig. 4	Number of half-period	Length of each half-period, msec	Amplitude of the current in each half-period, kA
1	1	10	1.5
2	2	10	1.5; 0.8
3	4	10	1.4; 0.8; 0.5; 0.3
4	3	5.3	1.4; 0.9; 0.5
5	3	3.3	1.5; 0.9; 0.5
6	1	5	1.5

The lower envelopes of the recovery strength in Fig. 4 were obtained by measurements. The following conclusions can be drawn.

An increased number of half-periods of a given duration in one oscillatory discharge notably reduces the recovery strength. On the other hand, a decrease in the duration of the half-periods (below 10 μ sec) has the opposite effect and increases the recovery strength. From the point of view of recovery strength, loads 5 and 6 are "lighter" than the fundamental load 1.

It therefore seems advisable to consider test load 5 for estimates of the recovery strength; this is also the most probable load in practice. On this basis the quenching voltage of the sparkgap is not unjustifiably reduced, as this could otherwise limit the field of application of the arrester.

In multiple sparkgaps we also require to know the total recovery strength of all the individual gaps together.

Given a uniform distribution of the voltage over the individual sparkgaps, one would expect the "absolute" recovery strength to increase in direct proportion to the number of sparkgaps with constant relative recovery strength.

But the distribution of the voltage inside each sub-unit of four sparkgaps is capacitive and the capacitance of the individual sparkgaps is not the same. The puncture voltage of each sub-unit is therefore

about 5 to 10 per cent below the minimum total puncture voltage of the individual gaps. This naturally would not reduce the relative recovery strength if the voltage distribution over the individual gaps were the same after the passage of current as before the breakdown. But the sparkgaps are filled with highly ionized gases immediately after the current has passed through zero and the voltage distribution is markedly changed both by conductance and changes in capacitance*.

The probability of low values of recovery strength must increase as more individual sparkgaps are joined together since the recovery voltage is applied simultaneously to a larger number of gaps and a premature breakdown of any one of them usually leads to a premature breakdown of them all. A reduced recovery strength in multiple sparkgaps must be accepted and estimates which are based on the test results of individual gaps even if a large number of tests have been made should be treated with caution. It is better to use the results of tests on sets of two gaps or on particular sub-units (four gaps together).

For a final assessment of the arc-quenching capacity of the multiple sparkgap of the arrester, the arc-quenching capacity of the complete units had to be checked by the usual service tests.

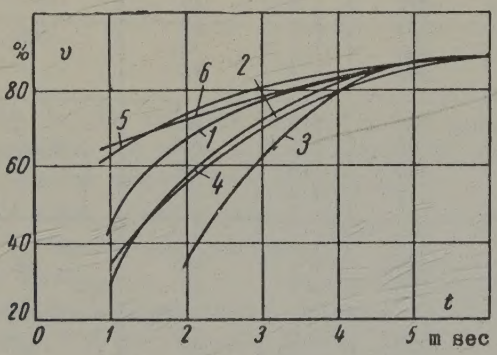

Fig. 4. The recovery strength of an individual magnetic sparkgap under various loads.

It can easily be shown analytically that when testing a finished unit under conditions equivalent to those existing in an actual arrester, it is essential to reduce the voltage of the system, the total resistance and the operating resistance of the arrester in proportion to any decrease in the number of sparkgaps, whereas the capacitances in

* The capacitance of an individual sparkgap is about 50 pF and the capacitive-susceptance current is no more than 5 MkA at supply frequency and the pre-puncture voltage.

parallel with the unit must be correspondingly increased. The short circuit current of the plant will then remain constant as well as the accompanying current (load current).

Equivalent conditions were provided for the rupturing capacity tests carried out on finished units for 500 kV arresters.

The principal results are given in Table 2. Each finished unit consists of five sub-units of four individual sparkgaps with a maximum puncture voltage of 3.4 kV (the 500 kV arresters are made of these sparkgaps). The puncture voltage of the finished units $U_{punct.fu}$ was between 55 and 63 kV. The short-circuit current was between 1800 and 3000 A for the "mean" variable e.m.f. in the various tests.

TABLE 2

No. of unit	Amplitude of interrupted current, A	η	No. of interruptions in one cycle	Total number of interruptions in all the cycles
1	850 770 850 460	1.8 1.5 1.4 1.4	19 19 9 16	103
2	400 1 100 450 740	1.5 1.5 1.6 1.4	20 16 19 18	73
3	630 535 670	1.5 1.4 1.3	21 26 20	67
4	650 800	1.3 1.25	19 16	35
5	650 1 300	1.5 1.4	5 1	6
6	1 000 1 000	1.45 1.28	20 7	27
7	1 000 900	1.46 1.33	21 11	32
8	1 180	1.4	11	11

The load currents were controlled between 450 and 1200 A. In the

majority of the tests η was between 1.4 and 1.5, but in some series of tests it equalled 1.25 to 1.3.

It must be pointed out that each complete unit was tested more than twenty times in almost every case, even though gaps with pressed paper laminations were only designed for up to twenty trials.

It is of interest to compare the re-strike voltage of complete units as measured during the tests with the recovery strength of sets of two gaps under identical loads (Fig. 5).

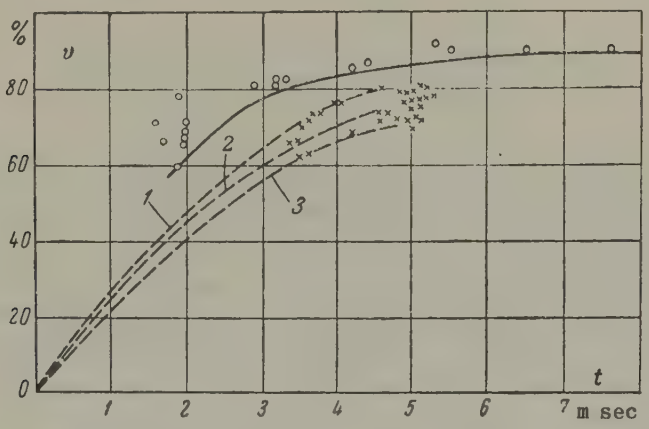

Fig. 5. The recovery strength of the magnetic sparkgaps and units in the combined arrester at a load of 1000 A with H_m = 800 oersted: 0 – a set of two sparkgaps (U_{punct} = 6.8 kV_{max}); X – complete unit (20 sparkgaps, $U_{punct.fu}$ = 55 to 64 kV_{max}.); 1, 2, 3 – sinusoidal recovery voltages with amplitudes respectively 0.8, 0.75 and 0.7 of the puncture voltage of the unit.

This comparison shows that the lowest and least probable re-strike voltage in complete units is 15 to 20 per cent below the recovery strength of sets of two gaps for the lowest sinusoidal recovery voltage $U_{rec} = 0.7\ U_{punct}$.

This decrease in the re-strike voltage is probably due to the ageing of the individual sparkgaps and the possible reduction in the overall recovery strength of the sparkgaps in the complete unit.

The conclusion to be drawn from these results is that a load current

of about 1000 A is quite acceptable for η = 1.4 to 1.5 if the number of trial discharges is twenty or less and there is then every probability of faultless clearance. Incidentally, these tests were made for more exacting conditions than occur in actual service since the operating resistance of the arrester had to be greatly reduced in order to obtain a current of 1000 to 1300 A at a source voltage equal to quenching voltage of the complete unit. The current through the unit is in point of fact about 500 A at the quenching voltage and only reaches 1000 to 1500 A in the transition period when the voltage across the unit is slightly greater than the quenching voltage.

The operating resistance in the internal surge arrester

There is no need to discuss the well-known merits of non-linear resistors. It need only be pointed out that the "vilite" disk-resistor of 150 mm diameter used in the 500 kV lightning arrester was unsuitable for the internal surge arrester because at least five such disks would have been required in parallel. "Vilite" (i.e. the compound of SiC, clay and graphite) will only operate at low current densities and its non-linearity coefficient is only about 0.3 in the range of currents produced by internal voltage surges.

A new non-linear material called "tervite" was therefore specially developed for internal surge arresters. This material has several times more current capacity than vilite [6]. But the coefficient of non-linearity of tervite is somewhat inferior to that of vilite. The current capacity of both vilite and tervite increases with increasing conductivity of the material, but the non-linearity diminishes.

The operating resistor in an internal surge arrester can either be made of disks 125 mm in diameter and 50 mm thick or disks 70 mm in diameter and 20 mm thick. The units using the latter are fitted with three parallel columns of disks. Fig. 6 illustrates the current capacity of an arrester as a function of the properties of disks with the maximum resistance possible for the type of arrester in question.

The number of disks in the internal surge arrester depends on the residual voltage which must not exceed 2.5 U_p for a current of 1500 A on a 10/20 μ sec surge.

Curve 1 in Fig. 7 shows the voltampere characteristic of the internal surge arrester. It must be borne in mind that the residual voltage in an arrester with tervite resistors increases if the steepness of the

current wavefront is reduced for a given current. As an example, the residual voltage increases by 3 per cent if the wavefront is reduced from 10 to 3 μ sec with a current of 10 kA.

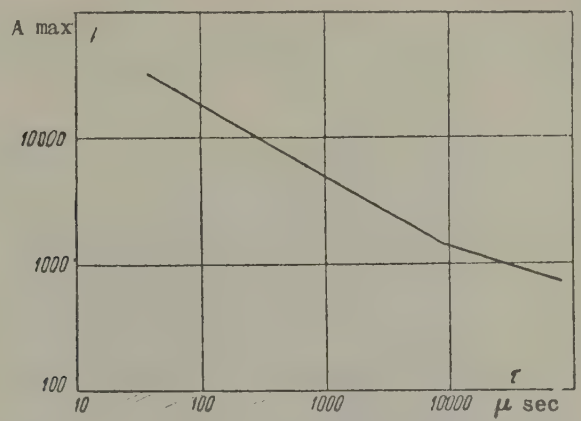

Fig. 6. The carrying capacity of "tervite" resistance in the combined 500 kV arrester after at least 20 discharges:
$\tau < 10{,}000$ μsec – the length of an aperiodic wave of 20/40 μ sec (up to the half-drop point); $\tau > 10{,}000$ μ sec – a periodic wave (frequency 50 c/s).

The combination of the internal surge and lightning arresters

It will be seen from curve 1 in Fig. 7 that the tervite resistor for internal surge protection cannot reduce the overvoltages due to direct lightning strokes to the required level since the calculated impulse current through the arrester is 10 kA.

To permit the use of tervite disks in 500 kV arresters and still limit surges to 1260 kV at currents of 10 kA it would have been necessary to use a resistor which would satisfy curve 2. In actual fact the current through the arrester during internal surges is over 1.5 kA and this is unacceptable both as regards the carrying capacity of the resistor and the arc-quenching capacity of the sparkgaps. With direct lightning strokes internal surges can be ignored and a quenching voltage roughly equal to 1.3 U_p need only be considered. The surge current (curve 3) does not then exceed 800 to 900 A and it can therefore be interrupted quite easily by the sparkgaps. All these considerations

led to the design of the "combined" arrester which protects against internal surges as well as direct lightning strokes.

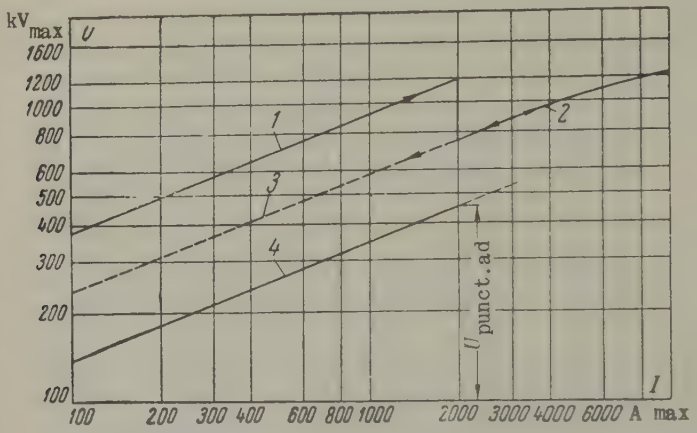

Fig. 7. The voltampere characteristics of the combined 500 kV discharger:
1 – internal surge arrester; *1, 2, 3* (sic) – – lightning arrester; *4* – shunted part of arrester; $U_{punct.ad}$ – puncture voltage of the additional sparkgap.

The "combined" arrester uses the same internal surge arrester, except that a part of its operating resistance is shunted by an additional multiple-sparkgap unit which is composed of individual rotating arc sparkgaps (Fig. 8). The puncture voltage of the shunt sparkgaps is selected so that their breakdown takes place at the moment when the voltage across all the operating resistance reaches the impulse level of protection (1260 kV). The part of this resistance which is shunted is designed to prevent the voltage across the rest of the resistance exceeding 1260 kV at a current of 10 kA (curve 2, Fig. 7). The voltampere characteristic of the shunted part of the resistance is represented by curve 4 in Fig. 7.

During internal surges when the current through the arrester does not exceed 2 kA, the arrester operates like an internal surge arrester and there is no breakdown of the shunt gap.

After a direct lightning stroke when the current increases to 10 kA, there is first a breakdown of the main sparkgap, but the current continues to flow through the operating resistance until the voltage across it reaches 1260 kV. As shown in Fig. 7, this takes place at a current

in excess of 2 kA. At this point there is a breakdown of the additional sparkgap and if the current increases further the voltage across the arrester is determined by the other remaining part of the operating resistance (curve 2 in Fig.7).

The size of the combined arrester is practically the same as the internal surge arrester and there is very little difference in cost.

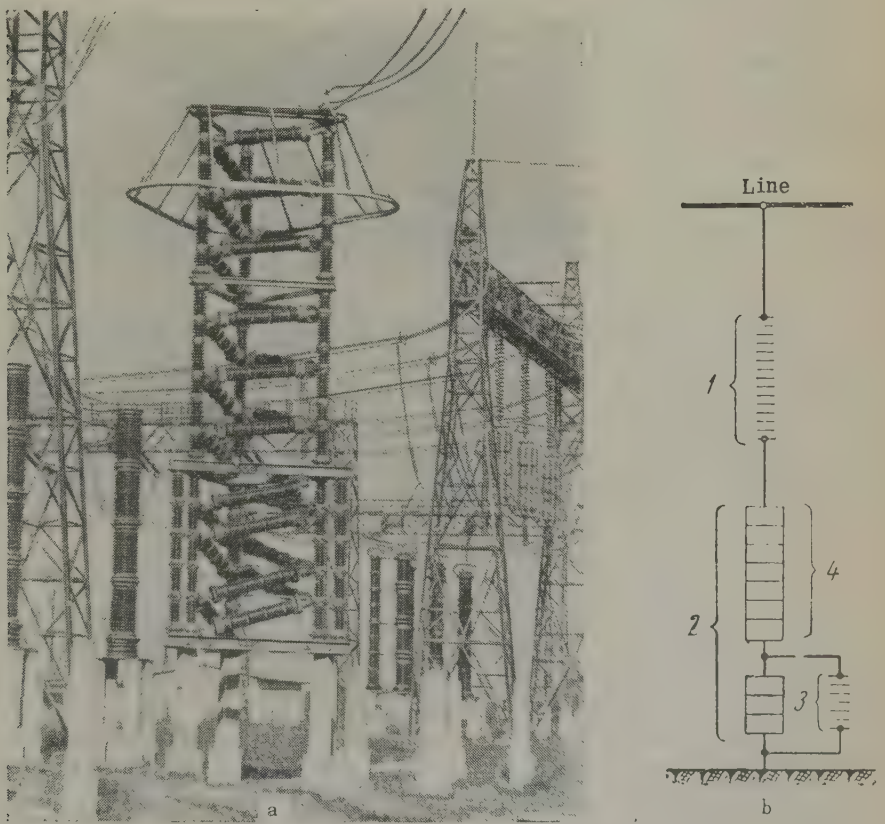

Fig. 8. Side view (a) and main circuit (b) of the combined 500 kV magnetic arrester.
1 - main sparkgaps; *2* - resistances of the internal surge arrester; *3* - additional (shunting) sparkgaps; *4* - the resistance in the lightning part of the arrester.

Before the final characteristics and parameters of the combined arrester could be determined it was necessary to make certain that the

following conditions would be fulfilled:

Impulse puncture and residual voltage	1260 kV
Amplitude of current in internal surges	$\leqslant 2.5\ U_p$
Puncture voltage during internal surges	$2.5\ U_p$
Residual voltage at a current of 10 kA and a wave of 10/20 μ sec	1260 kV

Conditions 2 and 3 determine the number of disks in the operating resistance. Condition 5 defines the proportion of shunt disks in the operating resistance (in our case, 39.6% of the total operating resistance).

It is also necessary to prevent the breakdown of the shunt sparkgaps when the arrester is dealing with an internal surge because at this moment a voltage amounting to 39.6% of the total breakdown (puncture) voltage can be applied to the shunted part of the operating resistance and this can immediately be followed by a similar proportion of the residual voltage at 1.5 kA. It is calculated that this condition can be satisfied by a 5 per cent margin given an impulse coefficient of the shunt sparkgaps equal to one (experimentally determined) and a 5 per cent scatter in the puncture voltages of the gap. It is obvious that the changeover after a direct lightning stroke will then take place with a voltage across the arrester which is no greater in amplitude than

$$U_{\text{punct}} = \frac{1.05 \cdot (1 + 0{,}05)}{(1 - 0.05)}\, 2.5 U_p = 2.9 U_p = 1\,250 \text{ kV},$$

as required by condition 1.

The non-shunted part of the operating resistance in the combined arrester (60.4%) satisfies the fifth condition by ensuring a residual voltage no greater than 1220 kV at a current of 10 kA with a wavefront of 10 μ sec.

The quenching voltage of the combined arrester must be such that the puncture voltage of the discharger does not exceed 2.5 U_p (fourth condition). Given a scatter of $\pm$ 7 per cent, the mean puncture voltage is

$$U_{\text{punct.av}} = (2.34 \pm 0{,}16)\, U_p = (710 \pm 50)\sqrt{2} \text{ kV}_{\text{max}}.$$

Taking the arc quenching capacity η as 1.46 from test results, we get

$$U_q = \frac{U_{\text{punct.av}}}{\eta} = \frac{2{,}34 U_p}{1{,}46} = 1{,}6 U_p.$$

Design of the combined discharger

A side view of the combined arrester is shown in Fig. 8(a). It consists of 27 complete units. These are "spirally" mounted on three pillars of KO-400S, KO-35 and KO-15 type isolators. The arrester is divided into three sections (stories) by triangular metal frames. The bottom section contains 10 units, five with resistors and five with sparkgaps. Each unit with resistors is shunted by its own sparkgap unit. Every unit with a resistor is composed of three parallel columns with 55 disks in each column. Every sparkgap unit consists of 32 individual sparkgaps. The top two sections contain 17 complete units all of the same type. Each of these units comprises 20 sparkgaps and three parallel columns with 25 or 26 disk resistors in each column (the lightning part of the combined arrester). A ring 4.8 m in diameter is provided to balance the voltage distribution in the presence of impulse phenomena. The arrester is 8.5 *m* high and weighs about 9 tons.

Laboratory tests and electrical characteristics

The main characteristics of the arrester were improved as a result of tests on the individual units and the arrester as a whole. The puncture voltage of 17 complete units each composed of individual gaps with a puncture voltage of 3.3 to 3.44 kV was between 60 and 63.5 kV (mean values).

The maximum deviation about the mean puncture voltage was up to $\pm$ 7 per cent on some units. Measurement of the volt-second characteristics showed that the impulse coefficient of the complete units was 1.1 for pre-discharge times $>$ 4 μ sec, 0.9 for 1.5 μ sec and 1.13 for 1 μ sec. Thermal tests on the finished units under a sustained voltage equal to

$$\frac{525}{\sqrt{3 \cdot 17}} = 17.8 \text{ kV}$$

and a corresponding phase voltage across the whole arrester showed that the temperature rise on the surface of the shunt resistance was no more than 18 to 20°C above ambient air temperature.

Rupturing capacity tests showed that the quenching voltage of the arrester can be based on a coefficient of arc quenching capacity η = = 1.46 and if the mean puncture voltage of the arrester equals 2.34 U_p, it is estimated by the quantity 1.6 U_p.

The puncture voltage of the arrester was measured on a laboratory model without the bottom section (i.e. without the additional units with the disks and the sparkgaps to shunt them).

The mean amplitude of the puncture voltage is 1030 kV ± 2.5 per cent at supply frequency.

The volt-second characteristic of the arrester is shown in Fig. 9 for discharges on the front of wedge-shaped waves.

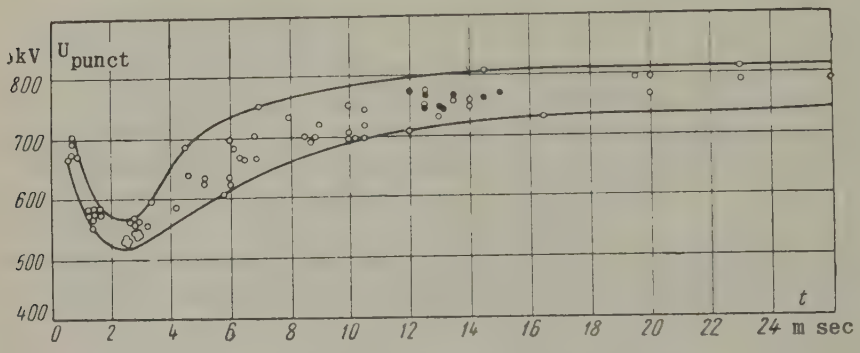

Fig. 9. The impulse puncture voltages of the combined 500 kV arrester with a wedge-shaped wave.
o – negative polarity; • – positive polarity.

The impulse puncture voltage is 800 kV for a pre-discharge time greater than 5 μ sec, up to 700 kV for 1 μ sec, but falls to 550 kV for a pre-discharge time of 2 to 3 μ sec.

The main electrical characteristics are listed below:

Rated voltage, kV	500
Maximum sustained voltage applied to arrester is service, kV	304
Quenching voltage, kV:	
after direct lightning strokes	395
for internal surges	485
Puncture voltage at supply frequency (+7% with 90 per cent probability), kV	710
Impulse puncture voltage for pre-discharge times of 2 to 20 μ sec, kV	1200
Residual voltage at impulse currents of 10 kA and 10/20 μ/sec, kV	1260
The residual voltage passing a current of 1.5 kA for one half-period of supply frequency, kV	1070

Residual instantaneous applied voltage on changing over to the discharge of a lightning stroke from the internal surge conditions, kV_{max} 1250

Number of lightning or internal surge discharges withstood without damage .. .. at least 20

From test results it can therefore be stated that overvoltages in 500 kV lines can be reduced to 2.5 U_p by using the combined arrester if the necessary conditions are fulfilled and certain other measures are taken.

Translated by O.M. Blunn

REFERENCES

1. V.P. Savel'ev; *The 500 kV magnetic arrester, (Magnitnyi razriadnik 500 kv).* Kuibyshev oblastnyi pravleniem nauchno-tekh. obshch. energ. prom., (1957).
2. V.P. Savel'ev and V.V. Shmatovich; *Vest. elektroprom.*, No.1, (1960).
3. M.L. Levinshtein and K.P. Kadomskaia; *Elektrichestvo*, No.8, (1959).
4. V.P. Fotin; *Voltage rises in long distance a.c. transmission lines in the presence of unbalanced earth faults, (Povysheniia napriazhenii v dlinnykh liniiakh peremennogo toka pri nesimmetrichnykh korotkikh zamykaniiakh na zemliu).* Trud. Vsesiuznogo elektrotekh. inst., (1958).
5. A.A. Akopian; *Elektrichestvo*, No. 11, (1957).
6. V.I. Pruzhinina, T.K. Ivanova and L.V. Iamanova; *Elektrichestvo*, No.2 (1958).

THE OPTIMUM OUTPUT OF INDUCTION MOTORS IN REACTOR-CONTROLLED DRIVES*

V.L. ANKHIMIUK (Byelorussian Polytechnical Institute) and
O.P. IL'IN (Middle Asia Polytechnical Institute)

(Received 15 August 1960)

This paper describes a new method of designing induction motors for reactor-controlled drives [1-3] in which the power of the motor is selected in conjunction with the rated slip, as defined by the resistance of the rotor circuit. The rated slip is so calculated that maximum use is made of the motor output over the desired range of speeds for a given load graph. Less power is required. If the initial speed of the motor and, consequently, the speed of the output shaft is reduced the speed can be increased by adjusting the ratio of the reduction gears.

Fig. 1 shows the main circuits of typical electric drives. For the sake of simplicity feedbacks have been omitted and only one control winding (CW) is shown.

In these systems the speed of the induction motor is changed by varying the slip. Additional losses therefore arise during speed control. The changes in the speed of the rotor also affect the cooling of the motor.

The power of the motor must therefore be calculated so as to obtain average losses and average heat dissipation.

The total losses of an induction motor (in relative units) at rated voltage on the stator terminals are:

$$\Delta p = (1 + k_r)(ms + \nu k s_{nom}), \tag{1}$$

* *Elektrichestvo*, 4, 39-42, 1961.

where $\Delta p = \frac{975 \Delta P}{M_{nom} n_0}$ – the ratio of total losses ΔP to rated output;

M_{nom} and n_0 – the rated torque and synchronous speed of the motor;

$k_r = \frac{r_1}{r_2'}$ – the ratio of the stator and rotor resistances;

$m = \frac{M}{M_{nom}}$ – the relative torque on the motor shaft;

s_{nom} – the rated slip;

$k = \frac{\Delta P_c}{\Delta p_{v\,nom}}$ – the loss factor, equal to the ratio of constant losses to variable losses under rated motor conditions;

$\nu = \frac{n}{n_0}$ – the relative speed of the motor.

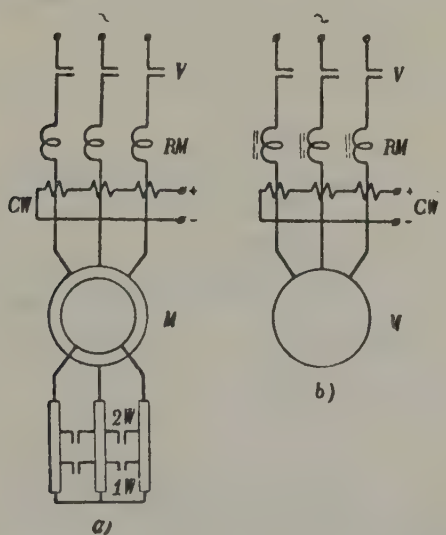

Fig. 1. Main circuits of induction motors in reactor-controlled drives
(*a* – slipping motor; *b* – squirrel cage).

Equation 1 is only an approximation since it is assumed that the constant losses are proportional to speed. In point of fact, the constant losses depend on the motor voltage as well as its speed. To calculate the constant losses in reactor-controlled drives it is there-

fore necessary to divide these losses into those components which depend on speed or voltage and then calculate the magnitude of the magnetizing current at the speed in question in the light of the non-linearity of the no load characteristic. But these are very complicated calculations. Equation (1) is so much simpler and the error is still within five per cent.

If a slipping motor is used, i.e. an induction motor with a wound rotor, the heating losses are

$$\Delta p_h = (1 + k_r)(ms\sigma + \nu k s_{nom}), \tag{2}$$

where $\sigma = \frac{r_2'}{r_2' + r_1'}$ — is the ratio of the rotor resistance to the total resistance of the rotor circuit (but in squirrel-cage motors $\sigma = 1$).

In speed control the required output of the motor depends on its initial speed. It will now be shown that the output of a motor is optimum at a particular initial speed.

The range of speed control is

$$D = \frac{n_1}{n_2} = \frac{\nu_1}{\nu_2} = \frac{1 - s_1}{1 - s_2}, \tag{3}$$

where n_1 and n_2 are the initial and minimum speeds of the motor; and
ν_1 and ν_2 – relative values of the initial and maximum speeds.

Substituting in (2) the value of s_2 from 3 for s and the value of $\frac{\nu_1}{D}$ for ν_2, we get:

$$\Delta p_h = (1 + k_r)\left(m\sigma \frac{D - \nu_1}{D} + \frac{\nu_1}{D} k s_{nom}\right). \tag{4}$$

The relative heat dissipation of the motor can be expressed by the equation

$$a = \frac{a_0 + (1 - a_0)\sqrt{\nu}}{a_0 + (1 - a_0)\sqrt{\nu_{nom}}}, \tag{5}$$

where a is the ratio of the heat dissipation at actual speed to the heat dissipation at rated speed;

a_0 – the ratio of the heat dissipation with rotor locked to the heat dissipation at synchronous speed of the rotor.

Expression (5) for the relationship between heat dissipation and speed gives practically the same results as those obtained by Suiskii's formula [4] for model A and AO motors. The value of a_0 can be calculated from the formulae in Suiskii's book [4]. A considerable amount of research has been devoted to the relationship between the coefficient of heat dissipation and the speed of the air [7, 8] and this justifies the assumption that formula (5) is also applicable to other types of induction motors.

For a motor to satisfy the heating conditions, it is necessary that

$$\Delta p_{\text{h.av}} \leqslant a_{\text{av}} \Delta p_{\text{nom}}, \tag{6}$$

where $\Delta p_{\text{h.av}}$ is the relative mean heating loss in one cycle;

a_{av} – the mean relative heat dissipation;

Δp_{nom} – the relative rated losses of the motor.

Using equations (4) to (6) and assuming that $\sqrt{\nu_{\text{nom}}} = 1$, for a long period of operation:

$$m = \frac{s_{\text{nom}}}{a} \frac{a_0 D + (1 - a_0)\sqrt{D\nu_1} - \gamma\nu_1}{(D - \nu_1)(1 - \gamma)}, \tag{7}$$

where

$$\gamma = \frac{k}{1 + k} = \frac{\Delta P_{\text{av, nom}}}{\Delta P_{\text{nom}}}$$

In speed control when the torque is constant,

$$\frac{s_{\text{nom}}}{a} = \frac{s_1}{k_1 m}. \tag{8}$$

The coefficient k_1 in (8) takes into account the need to ensure a rigid mechanical characteristic by a system of feedback when operating at the initial speed. This coefficient should be 1 to 2 if $s_1 > 0.005$.

Jointly solving equations (7) and (8), we get:

$$m = \sqrt{\frac{(1 - \nu_1)\left[a_0 D + (1 - a_0)\sqrt{D\nu_1} - \gamma\nu_1\right]}{k_1 (D - \nu_1)(1 - \gamma)}}. \tag{9}$$

Equation (9) permits the determination of the optimum output of a wound rotor induction motor from the torque over the desired range of speeds.

At the speed v the relative power is

$$p = mv. \tag{10}$$

The curves in Fig. 2 show the degree of power utilization and the maximum torque for given heating conditions as a function of initial speed.

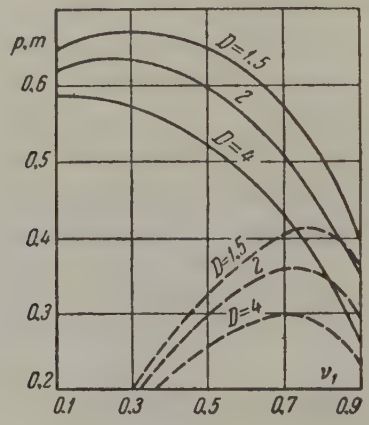

Fig. 2. Maximum torque and power of a phase induction motor as a function of initial speed under given heating conditions.
p – motor power; *m* – max torque; *D* – range of speed control.

The rated slip is even more important in deciding upon the power of a squirrel-cage induction motor. To determine the effect of rated slip on its output, consider a "basic" squirrel-cage induction motor and assume that $P_{nom,b}$, I_{nom}, $\cos \phi_b$, η_b, $k_{r.b}$ and γ_b are given, where the subscript b refers to this *basic* squirrel cage motor. Replacing the rotor of this basic motor by a rotor with a different resistance:

$$r_2' = \frac{r_{2b}'}{\varepsilon},$$

The change of rotor involves changes in the rated slip, its efficiency at rated torque, the rated output and the distribution of the

losses. In this case

$$s_{\text{nom}}=\frac{s_{\text{nom. b}}}{\varepsilon};\quad k_r=k_{rb}\varepsilon;\quad \Delta P_{v2\text{nom}}=\frac{\Delta P_{v2\text{nom. b}}}{\varepsilon};$$
$$\gamma=\frac{\gamma_b\varepsilon(1+k_{rb})}{(1-\gamma_b)(1+k_{2b}\varepsilon)+\gamma_b\varepsilon(1+k_{rb})}.$$

In relative units, the rated losses of the basic motor are:

$$\Delta p_{\text{nom. b}}=s_{\text{nom. b}}\frac{(1+k_{rb})}{1-\gamma_b}. \tag{12}$$

The total losses of this motor at the maximum speed v_2 in relative units are:

$$\Delta p=\frac{m(1+k_{rb}\varepsilon)(1-\gamma_b)(D-\nu_1)+s_{\text{nom. b}}\gamma_b(1+k_{rb})\nu_1}{D(1-\gamma_b)} \tag{13}$$

In this case equation (6) takes the form

$$\Delta p=a\Delta p_{\text{nom. b}} \tag{14}$$

However, the initial speed v_1 is related to the torque m and the value of v by the equation

$$\varepsilon=\frac{k_1 s_{\text{nom. b}}}{1-\nu_1}m. \tag{15}$$

Substituting (12), (13) and (15) in (14) and solving w.r.t. m:

$$m=\frac{1-\nu_1}{2k_1k_{rb}s_{\text{nom. b}}}(\sqrt{1+C}-1), \tag{16}$$

where

$$C=\frac{4s^2_{\text{nom. b}}(1+k_{rb})k_1k_{rb}[a_0D+(1-a_0)\sqrt{D\nu_1}-\gamma_b\nu_1]}{(1-\nu_1)(D-\nu_1)(1-\gamma_b)}. \tag{17}$$

By (16) it is possible to obtain the maximum load torque of a squirrel cage motor for given heating conditions. The relative power of this squirrel cage motor is defined by equation (10).

Fig. 3 shows m and p as a function of v_1 for the squirrel-cage motor.

The efficiency and power factor of the drive can be calculated by Osokin's [5] or Terekhov's [6] formulae. Suppose it is required to compare variations in the energy indices of drives as a function of the speed range and initial speed. To do this use is made of an energy coefficient

$$k_e = \frac{\eta \cos\varphi}{\eta_{nom} \cos\varphi_{nom}} = \frac{P_2 I_{1nom}}{P_{2nom} I_1}, \tag{18}$$

where η is the efficiency and $\cos\phi$ the power factor of the motor-reactor system.

An expression is obtained for the energy coefficient at minimum speed by putting $I_1 = bI'_2$ and $I_{1\,nom} = b_{nom} I'_{2\,nom}$ and expressing the secondary currents in terms of the power and slip in the light of (8):

$$k_e = k_b \frac{\nu_1}{\nu_{nom}} \sqrt{\frac{1-\nu_1}{k_1 D(D-\nu_1)}}, \tag{19}$$

where $k_b = \frac{b_{nom}}{b}$.

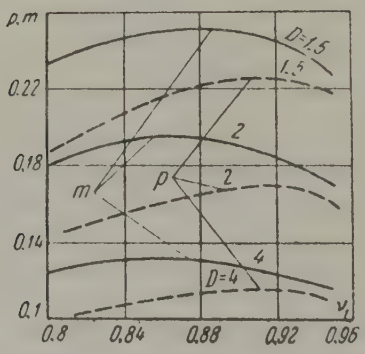

Fig. 3. Maximum torque and power of a squirrel-cage induction motor as a function of initial speed under given heating conditions.

The values of b, b_{nom} and k_b can be found from an equivalent T - network of the induction motor.

Assuming that the phase angle between the currents in the magnetizing branch and the operating circuit of the rotor is approximately 90°:

$$b=\sqrt{1+i_0^2};\quad b_{nom}=\sqrt{1+i_{0nom}^2}$$

where

$$i_0=\frac{I_0}{I_2'}=\frac{\sqrt{\left(\frac{r_2'+r_m'}{s}\right)^2+x_2'^2}}{x_0};\quad i_{0nom}=\frac{I_{0nom}}{I_{2nom}'}.$$

Neglecting the value of x'_2 in the rotor current equation compared with the first term in the radicand:

$$i_0=i_{0nom}\frac{r_2'+r_m'}{r_2'}\frac{s_{nom}}{s}=i_{0nom}\frac{s_{nom}}{\sigma s}=i_{0nom}\frac{s_1}{sk_1m}.$$

Considering 3,

$$k_b=\frac{\sqrt{1+i_{0nom}^2}}{\sqrt{1+i_{0nom}^2\frac{D^2(1-\nu_1)^2}{k_1^2m^2(D-\nu_1)^2}}}. \tag{20}$$

The energy coefficient is a maximum when

$$\nu_1\approx\frac{3D+1-\sqrt{9D^2-10D+1}}{4}. \tag{21}$$

This value has been obtained on the assumption that k_b = const.

This is quite permissible since there is no significant variation in k_b in the region under consideration.

The relative rated speed of the basic motor $\nu_{nom.b}$ has to be substituted for ν_{nom} in formula (19) for the squirrel-cage motor.

Thus the following formulae can be used to assess the required output of

(a) slipring motors

$$\left.\begin{aligned} P_{\text{nom}} &= P_s \frac{D+6}{3} \text{ if } D = (1.5 \text{ to } 5); \\ P_{\text{nom}} &= \frac{P_s}{(2.1 \text{ to } 1.2) D} \text{ if } D < 1.5; \\ P_{\text{nom}} &= \frac{P_s}{(0.31 \text{ to } 0.0024) D} \text{ if } D > 5; \end{aligned}\right\} \quad (22)$$

(b) squirrel-cage motors if D = 1.5 to 5:

$$P_{\text{nom}} = P_s \frac{D+1.25}{0.6}, \quad (23)$$

where P_s is the static power on the motor shaft at the initial speed.

Example

This method will now be illustrated by applying it to the choice of motor for a large mill drive.

1. Details of the AK-52-6 type slipring induction motor: 380 V, 2.8 kW, 920 rev/min, η = 78%, $\cos \phi$ = 0.74. According to reference manuals α_0 = 0.3, k_r = 1.36 and γ = 0.268. It is assumed that k_1 = 1.5.

Fig. 2 shows the maximum motor torque as calculated by equation 9 for the given heating conditions as a function on the initial speed for various ranges of speed control, D. Curves are also given for the motor power p as a function of $m v_1$ at maximum speed. These curves define the degree of power utilization for speed control with constant torque.

It will be seen from Fig. 2 that the utilization of the motor power is a maximum ($p_{\max}$) when the initial speed v_1 = 0.7 to 0.75. Fig. 4 shows how $p_{\max}$ varies with the range of speed control D. This diagram also shows $s_{\text{nom.opt}}$ and $k_{e.\max}$ as functions of D.

The optimum rated slip is

$$s_{\text{nom.opt}} = \frac{s_{\text{nom}}}{\sigma_{\text{opt}}} = \frac{1 - v_{1\text{opt}}}{k_1 m_{1\text{ opt}}},$$

where $v_{1.\text{opt}}$ and $m_{1.\text{opt}}$ are the initial speed and motor torque corresponding to maximum power;

$\sigma_{opt} = \frac{s_{nom}}{s_{nom.opt}}$ – a quantity which defines the resistance of the rotor circuit as required for the maximum utilization of the motor power.

The term $k_{e.max}$ is found from formula (19) for values of v_1 from (21). These values of v_1 coincide with $v_{1.opt}$.

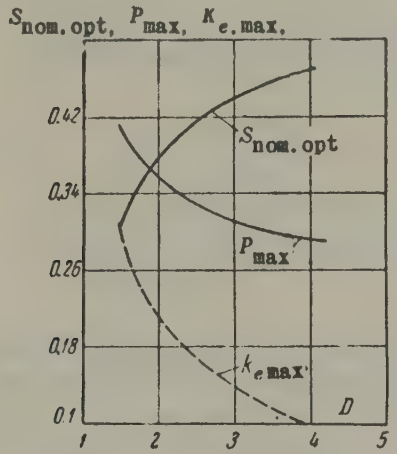

Fig. 4. Characteristics of a slipring induction motor in a reactor-controlled drive.

Thus, for slipring motors the conditions of maximum utilization of motor power are practically the same as those under which the energy coefficient is a maximum.

(2) Consider now an A51-6 type squirrel-cage induction motor of 380 V, 2.8 kW and 950 rev/min with $\eta = 82.5\%$ and $\cos\phi = 0.78$.

It is presupposed that $a_0 = 0.3$, $k_r = 1.77$, $\gamma = 0.317$ and $k_1 = 1.5$. Fig. 3 shows the torque m and power p as a function of the initial speed v_1 as calculated by formulae (16) and (10).

Fig. 5 shows $s_{nom.opt}$, p_{max} and k_e as a function of the range of speed control D. The conditions under which the utilization of the power of a squirrel-cage motor is a maximum are not the same as those which maximize the energy coefficient. Septate curves are therefore shown in Fig. 5 for that value of $k_{e.max}$ and k_e which correspond to maximum utilization of motor power as a function of D.

It will therefore be seen that 1.65 to 2.56 times less power is

required from a slipring motor than from a squirrel-cage motor over the range $D = 1.5$ to 4 and that the energy coefficient of the slipring motor is greater by a factor of 1.33 to 1.54.

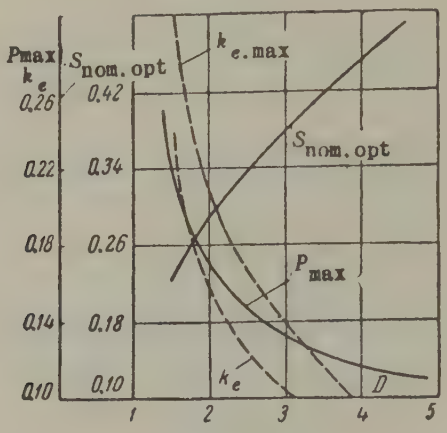

Fig. 5. Characteristics of a squirrel-cage induction motor in a reactor-controlled drive.

Translated by O.M. Blunn

REFERENCES

1. M.M. Sokolov; *The electrical equipment of common industrial plant, (Elektroborudovanie obshchepromyshlennykh mekhanizmov).* Gosenergoizdat, (1959).
2. V.M. Terekhov; *Elektrochestvo,* No.7, (1959).
3. A.G. Ivakhnenko; *Automatic speed control of low-power induction motors, (Avtomaticheskoe regulirovanie skorosti asinkhronnykh dvigatelei nebol'shoi moshchnosti).* Akad. Nauk Ukr.S.S.R. (1953).
4. P.A. Suiskii; *The Automatic electric drive, Collected works, (Avtomatizirovannyi elektroprivod).* Sborn. Gosenergoizdat, (1960).
5. M.N. Osokin; *Elektrichestvo,* No. 12, (1959).
6. V.M. Terekhov; *The scientific and technical problems of the automatic electric drive, Collected works, (Nauchno-tekhnicheskie problemy avtomatizirovannogo elektroprivoda).* Sborn. Akad. Nauk SSSR, (1957).
7. I.M. Postnikov; *The development of electrical machines, (Proektirovanie elektricheskikh mashin).* Gosenergoizdat, (1952).
8. A.E. Alekseev; *The design of electrical machines, (Konstruktsiia elektricheskikh mashin).* Gosenergoizdat, (1949).

A METHOD OF REDUCING TRANSIENT PHENOMENA IN CIRCUITS WITH INDUCTANCE COILS AND SEMICONDUCTOR RECTIFIERS*

B.M. MENSKII

Moscow

(Received 22 August 1960)

The principal feature of the transient phenomena which occur when closing a circuit containing a semiconductor rectifier bridge and inductance coils at the input and output (Fig. 1) is the shorter duration of the phenomena compared with the closing of a d.c. circuit with an output coil r_{out} and L_{out} [1,2].

The duration of the transient phenomena in such a circuit depends upon the relationship between the circuit criteria. The circuit is defined by three items assuming that the rectifiers are ideal:

$$\varphi_{out} = \operatorname{arc\,tan} \frac{\omega L_{out}}{r_{out} + r_a},$$

$$\varphi_{in} = \operatorname{arc\,tan} \frac{\omega L_{in}}{r_{in} + r_a};$$

$$\xi = \frac{\sqrt{(r_{in} + r_a)^2 + (\omega L_{in})^2}}{r_{out} + r_a},$$

where ω is the frequency of the applied alternating voltage and r_a the forward resistance of the rectifier.

The parameters ϕ_{out} and ϕ_{in} show the relationship between the inductive reactance and resistance at the input and output of the circuit. The symbol ξ represents the relationship between the total

* *Elektrichestvo*, 4, 58-61, 1961.

resistance to the alternating current at the input and the resistance to the rectified current at the output. To determine all these items the forward resistance of the rectifier bridge is divided between the input and output.

Consider now the relationship which must exist between these items for the transient phenomena to be reduced to the shortest possible period of time on closing the circuit. It is assumed that the circuit is closed at the commencement of a positive half-wave of alternating voltage. A first period of conduction β_1 commences when the circuit has been closed, i.e. rectifiers I are live ($i_{in} = i_1 = i_{out}$) and rectifiers II are non-conducting ($i_{II} = 0$).

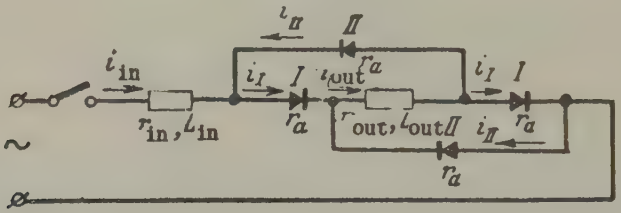

Fig. 1. Circuit containing inductance coils and a rectifier bridge.

If the electrical angle $\vartheta = \omega t$ (where t is time) read from the instant the circuit is closed, the output current in the first period of conduction is described by the expression

$$i_{out} = I_m \sin(\vartheta - \varphi) + I_m \sin\varphi e^{-}$$

where

$$I_m = \frac{U_m}{\sqrt{(r_{in} + 2r_a + r_{out})^2 + (\omega L_{in} + \omega L_{out})^2}}$$

$$\varphi = \operatorname{arctan}\frac{\omega L_{in} + \omega L_{out}}{r_{in} + 2r_a + r_{out}};$$

$$\sigma = \operatorname{cotan}\varphi.$$

and U_m is the amplitude of the applied voltage.

The first period of conduction ends at $\theta = \beta_1$, when the voltage

applied to rectifier II equals

$$U_{II} = (r_{out} + r_a) i_{out} + \omega L_{out} \frac{di_{out}}{d\vartheta} = 0.$$

Hence, by substituting the value of i_{out}, an equation can be written for the first period of conduction β_1:

$$\sin(\beta_1 + \varphi_{out} - \varphi) = \sin(\varphi_{out} - \varphi) e^{-\sigma\beta_1}. \quad (1)$$

The current in the output coil at the end of the first period of conduction is

$$I_{\beta_1} = I_m \frac{\sin\varphi_{out}}{\sin(\varphi_{out} - \varphi)} = \sin\beta_1. \quad (2)$$

The first period of conduction is followed by a period of commutation γ_1 during which all the rectifiers in the bridge are live. For this period of commutation

$$i_{out} = I_{\beta_1} e^{-\sigma_{out}(\vartheta - \beta_1)}$$

and

$$i_{in} = cI_m \sin(\vartheta - \varphi_{in}) + [I_{\beta_1} - cI_m \sin(\beta_1 - \varphi_{in})] e^{-\sigma_{in}(\vartheta - \beta_1)},$$

where

$$\sigma_{out} = \operatorname{cotan}\varphi_{out}$$

$$\sigma_{in} = \operatorname{cotan}\varphi_{in};$$

$$c = \frac{\sqrt{(r_{in} + 2r_a + r_{out})^2 + (\omega L_{in} + \omega L_{out})^2}}{\sqrt{(r_{in} + r_a)^2 + (\omega L_{in})^2}}.$$

This period of commutation ends at $\vartheta = \beta_1 + \gamma_1$, when the current in rectifier I becomes zero:

$$i_1 = \frac{1}{2}(i_{in} + i_{out}) = 0.$$

Hence, by substituting the values i_{in} and i_{out}, an equation for the period of commutation γ_1 is:

$$cI_m \sin(\beta_1 + \gamma_1 - \varphi_{in}) + I_{\beta 1}(e^{-\sigma_{in}\gamma_1} + e^{-\sigma_{out}\gamma_1}) - cI_m \sin(\beta_1 - \varphi_{in}) e^{-\sigma_{in}\gamma_1} = 0. \quad (3)$$

The current in the output coil at the end of the period of commutation is:

$$I_{\gamma_1} = I_{\beta_1} e^{-\sigma_{out}\gamma_1}. \tag{4}$$

A second period of conduction then follows during which rectifiers II are live ($i_{out} = i_{II} = -i_{in}$) but rectifiers I are "off" ($i_I = 0$).

The current in the output coil is defined in this case by the equation

$$i_{out} = -I_m \sin(\vartheta - \varphi) + \\ + [I_{\gamma_1} + I_m \sin(\beta_1 + \gamma_1 - \varphi)]\, e^{-\sigma[\vartheta - (\beta_1 + \gamma_1)]}.$$

The current in the output coil at the end of the second period of conduction is:

$$I_{\beta_2} = -I_m \sin(\beta_1 + \gamma_1 + \beta_2 - \varphi) + \\ + [I_{\gamma_1} + I_m \sin(\beta_1 + \gamma_1 - \varphi)]\, e^{-\sigma\beta_2}, \tag{5}$$

where β_2 is the second period of conduction.

If the current in the output coil is the same in value at the end of the first period of conduction as at the end of the steady state period of conduction, and if steady state conditions follow the first period of conduction, then

$$I_{\beta_2} = I_{\beta_1}$$

and

$$\gamma_1 + \beta_2 = \pi.$$

Equating the value of $I\beta_1$ from equation (2) to the value of $I\beta_2$ from (5) and substituting $\beta_1 = \pi - \gamma_1$, as well as the value of $I\gamma_1$ from (4):

$$\sin(\varphi_{out} - \varphi)\sin(\beta_1 + \gamma_1 - \varphi) + \sin\varphi_{out} \times \\ \times \sin\beta_1 e^{-\sigma_{out}\gamma_1} - \sin\varphi \sin(\beta_1 + \varphi_{out} - \varphi)\, e^{-\sigma(\gamma_1 - \pi)} = 0. \tag{6}$$

Equation (6) provides a relationship between the parameters which satisfies the requirement, i.e. steady state conditions will follow the first period of conduction if the circuit is closed when the voltage passes through zero.

Exactly the same factors affect the transient phenomena during the first period of conduction (i.e. the configuration of the circuit and the variation in applied voltage) when $\beta_1 - \beta \leqslant \vartheta \leqslant \beta_1$, as in the steady state period of conduction (Fig. 2a). Therefore the current in the output coil when $\vartheta = \beta_1 - \beta = \psi$ has exactly the same value as at the commencement of the steady state period of conduction.

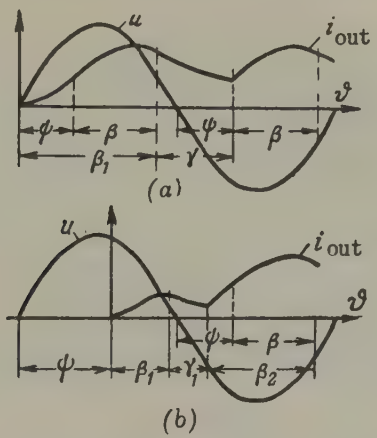

Fig. 2. Transient behaviour in a circuit with the optimum relationship between its criteria:

a) $\psi_1 = 0$; *b)* $\psi_1 \neq 0$.

Thus, if the relationship between the circuit criteria corresponds to equation (6), and if the circuit is closed at the moment the mains voltage passes through zero, the duration of the transient phenomena is then defined by the expression

$$t' = \frac{\psi}{\omega},$$

where ψ is the angle between the steady state period of conduction and the mains voltage ($\psi < \pi$).

Obviously, if the circuit is closed at any other moment of time (Fig. 2b), the duration of the transient phenomena is:

$$t'' = \frac{\pi + \psi - \psi_1}{\omega},$$

where ψ_1 is the initial angle.

Hence, if the relationship between the circuit criteria corresponds to equation (6), the duration of the transient phenomena on closing this circuit is less than one full wave and varies between the following limits depending on the exact instant at which the circuit is closed:

$$\frac{\psi}{\omega} \leqslant t < \frac{\pi + \psi}{\omega}.$$

Equation (6) contains the angles β_1 and γ_1 as well as the circuit items. This entails the use of equations (1) and (3). Equation (6) also contains another symbol ϕ which is a function of the fundamental circuit items ϕ_{out}, ϕ_{in} and ξ. The relationship between these items is expressed by the equation

$$\xi = \frac{\sin(\varphi_{out} - \varphi)}{\cos\varphi_{out}\sin(\varphi - \varphi_{in})}. \tag{7}$$

It is convenient to transform equations 1, 3, 6 and 7 into:

$$\operatorname{cotan}(\varphi_{out} - \varphi)\sin\beta_1 + \cos\beta_1 = e^{-\sigma\beta_1}; \tag{8}$$

$$\begin{aligned}&[\cos(\beta_1 + \gamma_1 - \varphi_{out}) - \cos(\beta_1 + \gamma_1 + \varphi_{out} - 2\varphi_{in})] + \\ &+ [\cos(\beta_1 - \varphi_{out}) - \cos(\beta_1 + \varphi_{out})]\, e^{-\sigma_{out}\gamma_1} + \\ &+ [\cos(\beta_1 + \varphi_{out} - 2\varphi_{in}) - \cos(\beta_1 + \varphi_{out})]\, e^{-\sigma_{in}\gamma_1} = 0;\end{aligned} \tag{9}$$

$$\begin{aligned}&[\cos(\beta_1 + \gamma_1 - \varphi_{out}) - \cos(\beta_1 + \gamma_1 + \varphi_{out} - 2\varphi)] + \\ &+ [\cos(\beta_1 - \varphi_{out}) - \cos(\beta_1 + \varphi_{out})]\, e^{-\sigma_{out}\gamma_1} - \\ &- [\cos(\beta_1 + \varphi_{out} - 2\varphi) - \cos(\beta_1 + \varphi_{out})]\, e^{\sigma(\pi - \gamma_1)} = 0;\end{aligned} \tag{10}$$

$$\xi = \frac{2\sin(\varphi_{out} - \varphi)}{\sin(\varphi + \varphi_{out} - \varphi_{in}) + \sin(\varphi - \varphi_{out} - \varphi_{in})}. \tag{11}$$

This set of equations allows those values of ϕ_{in} and ξ to be found which reduce the transient phenomena in question to the shortest possible period of time for the given value of ϕ_{out}.

The actual method of calculation is as follows. Given the value of ϕ, find the first period of conduction from equation (8), the period

of commutation from (10), the value of ϕ_{in} from (9) and that of ξ from (11). Given several values of ϕ, the relationship between ϕ_{in} and ξ for the given value of ϕ_{out} can be plotted.

This set of equations is however indeterminate if $\phi_{out} = \phi_{in} = \phi$. The circuit criteria of minimum transient phenomena are in this case defined by the equation

$$\xi \cos \varphi = 1, \tag{12}$$

whence it follows that $r_{in} = r_{out}$ and $L_{in} = L_{out}$.

The results obtained by this set of equations or (12) are given in Fig. 3. Using these curves that value of ξ for ϕ_{out} and ϕ_{in} can be found which minimizes the duration of the transient phenomena on closing the circuit. Graphical interpolation can be employed for intermediate values of ϕ_{out}. For example, if $\phi_{out} = 80^\circ$ and $\phi_{in} = 75^\circ$, an auxiliary curve $\xi = f(\phi_{out})$ for $\phi_{in} = 75^\circ$ can be plotted as in Fig. 4 and it is then apparent that $\xi = 6.3$ for the specified values of ϕ_{out} and ϕ_{in}.

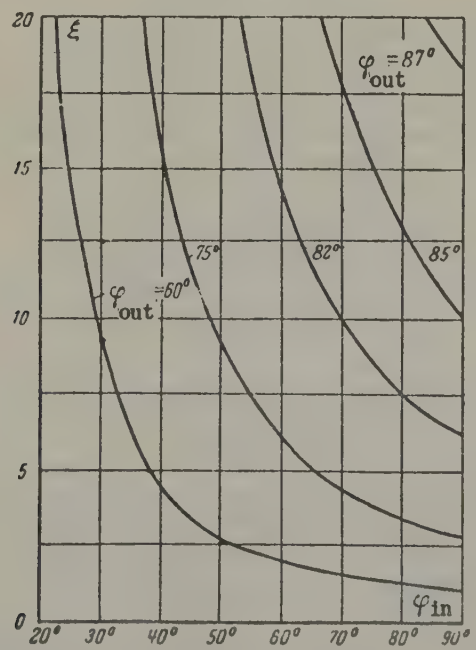

Fig. 3. Curves for determining the optimum relationship between the circuit criteria.

Fig. 5 shows an oscillogram of transient phenomena which occur on closing a circuit whose parameters correspond to equation (12). The rectifier bridge consists of DGTs – 24 type germanium rectifiers (two rectifiers in parallel in each arm). Coils with an inductance of 0.17 H and resistances of 0.54 ohms were connected at the input and output. The frequency of the applied voltage was 50 c/s.

The early end to transient conditions in this circuit is due to the dynamic redistribution of the voltages [2]. During the transient conditions a much larger proportion of the applied voltage influences the output coil than during steady state conditions. Rather a large margin of voltage is therefore required if transient phenomena are to be minimized, i.e. the inductance of the input coil must be quite large. The precise relationship between the circuit items is defined by equations (8) to (11) (or (12) if $\phi_{out} = \phi_{in}$).

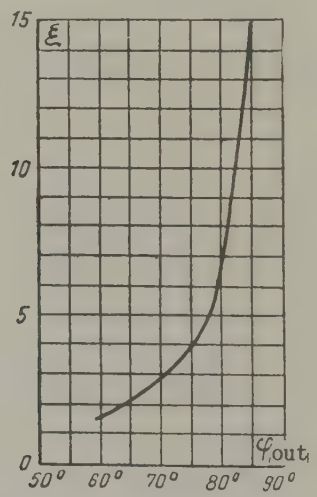

Fig. 4. Auxiliary curve for graphical interpolation.

If ϕ_{out} or ξ is allowed to be less than the value indicated by these equations, the transient conditions will be prolonged, and if $\xi = 0$, the duration of the transient conditions will be the same as when closing a d.c. circuit with an output coil.

Transient phenomena will also persist for a longer period of time if ϕ_{out} or ξ are greater than the value indicated by the equations. In this event the current in the first half-wave may be greater than in the steady state, and if $\xi \to \infty$, the duration of the transient con-

ditions will be the same as when closing an a.c. circuit with an input coil.

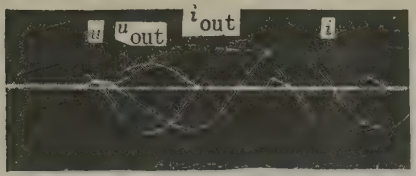

Fig. 5. Oscillogram of the transient on closing a circuit with optimum criteria: u – applied alternating voltage; u_{out} – voltage of output coil; i_{out} – current of output coil; i – current of input coil.

Translated by O.M. Blunn

REFERENCES

1. V.E. Bogoliubov; *Transient phenomena in ferroresonant circuits with magnetization, (Perekhodnye protsessy v ferrorezonansnykh tsepiakh s podmagnichivaniem).* Thesis for the degree of doctor, ME' I, (1954).
2. L.A. Bessonov; *Dynamic phenomena in circuits with semiconductor rectifiers, (Dinamicheskie iavleniia v tsepiakh a poluprovodnikovymi ventiliami).* Trud. Vsesoiuz. zaochnogo energet. inst., No. 7, (1957).

A NEW METHOD OF TESTING THE BRUSHES OF ELECTRICAL MACHINES*

A.M. TRUSHKOV

Tomsk

(Received 9 November 1960)

The brushgear tests specified in the State Standards (GOST) do not reveal the conditions under which a particular type of brush will give the best service. This shortcoming is felt quite acutely at the present time because of the particularly arduous conditions which have to be satisfied in modern high speed machines at 5000 to 6000 rev/min and high commutator voltages. No criterion is available by which to select the appropriate type of brush for particular operating conditions.

In this paper it is proposed to take the magnitude of the minimum voltage for sparking at the end of commutation (the sparking voltage) as an extra criterion by which to estimate the electrical properties of brushes. When the commutation conditions are so unfavourable that sparking is unavoidable, the erosion of the contact surfaces can best be reduced by using brushes with a low sparking voltage since in this case the arc will discharge with less energy.

The sparking voltage of various types of brushes can be established by the test circuit illustrated in Fig. 1. This system uses a "collector-interrupter" which periodically discharges an electrical circuit which is supplied from a battery. The voltage drop in the contact can be measured by a voltmeter and an EO-7 type cathode-ray oscillograph. As the voltage gradually increases, the appearance of sparking is marked by a luminous spot on the oscillograph (see point *a* in Fig. 2). If the time scale is increased, a "line of arc combustion" at a constant voltage will correspond to this spot.

It is well-known that the interruption of a commutation circuit is

* *Elektrichestvo*, No.4, p.84, 1961.

greatly affected by its inductance. To keep the latter constant as an increasingly large voltage is applied to the slip contact, the voltage supply has to be varied by connecting different numbers of cells. The minimum sparking voltage is found from the relationship between Oa' and Ob in the oscillograms. The test results of brushes 4 x 4 mm are as follows:

Type of brush	Minimum arcing voltage, V
MG	9.0
MG – 1	9.56
Г – 3	11.3
EG – 2a	12.16
EG – 4	12.96

The average of ten measurements was taken for each type of brush. The speed of the interrupter was 1500 rev/min and the current interrupted was 10-11 A.

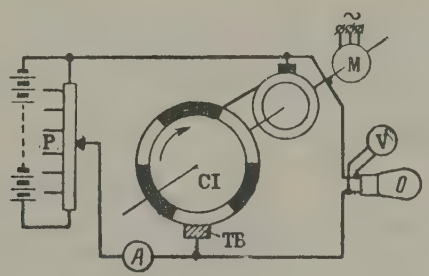

Fig. 1. The test circuit:

TB – Test brush; *CI* – contact interrupter; *M* – motor; *P* – potentiometer; *A* – ammeter; *V* – voltmeter; *O* – oscillograph.

From test results, EG – 4 type brushes had the maximum sparking voltage and MG the minimum.

There is a different minimum sparking voltage for each type of brush and this difference is as much as 25 to 30 per cent. The relationships between sparking voltages correspond qualitatively to the relationships between the actual commutation capacity (i.e. a low sparking voltage implies good commutation).

It is worthwhile using brushes with the minimum sparking voltage from the point of view of reducing the erosion of the contact materials.

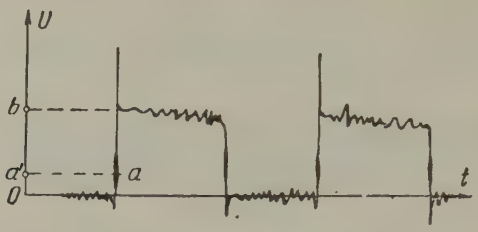

Fig. 2. Oscillogram of the contact voltage.

On the basis of this data, the minimum sparking voltage at the end of commutation can be recommended as an extra criterion of the electrical properties of brushes.

Translated by O.M. Blunn

ABSTRACTS FROM PAPERS PUBLISHED IN ELEKTRICHESTVO No. 4, 1961

Computer mathematics

A computer study of transient phenomena in synchronous machines using differential equations with periodic coefficients. B.M. Kagan et al., (pp. 43-48).

The authors illustrate the way computers can be used to solve differential equations with periodic coefficients. A network containing synchronous machines under transient conditions is used as an example.

Control engineering

A contribution to the theory of linear circuits with variable parameters. V.S. Davydov, (pp. 51-58).

Relationships are derived for the steady state in a linear parametric system under the influence of an external harmonic voltage. These relationships take a form which is as near as possible to the usual relationships used in the theory of alternating currents.

High frequency engineering

The design of reactive frequency converters for 100 to 500 c/s. M.M. Tarashchanskii, (pp. 73-75).

A short account is given of the main problems involved in the design of "reactive frequency converters" as used to convert alternating currents of 50 c/s into high frequency currents of 100 to 500 c/s for machine tools. Particular attention is paid to the dimensions of the stator.

Insulation

The use of life curves and other methods for determining the corona resistance of high voltage insulation. N.V. Aleksandrov, (pp. 61-68).

An account is given of the methods and some of the equipment used in the Lenin Electrical Engineering Institute to determine the corona resistance of varnishes, mica products and other insulation. The

steepness of the "life curves" and sustained electrical strength are used as criteria for a comparative analysis of the materials.

Aluminium windings with enamel, fibre and oxide insulation. V.A. Privezentsev, (pp. 68-73).

The increase in demand in the U.S.S.R. for low-cost aluminium winding conductors is considered together with the methods of production and properties of aluminium conductors with enamel, paper, glassfibre, oxide and glassfibre-oxide insulation.

Power systems

The propagation of surges in networks with twin-circuit transmission lines. A.S. Dadunashvili, (pp. 5-13).

An analysis is made of the phenomena associated with the propagation of surges in twin-circuit transmission lines. This is a special application of an already known method of breaking down surge waves into their components. Test results are given.

The lightning performance of 275-500 kV transmission lines. M.V. Kostenko, et al., (pp. 20-26).

A theoretical analysis is made of the effect of the tower inductance, lightning arc and supply voltage on the lightning performance of transmission lines and an estimate made of the probability of strikes. Statistical data of lightning strikes in the U.S.S.R. and the western world are given. This approach to the problem stresses the importance of the height of the towers and the effect of lightning strikes which by-pass the earth wires to the conductors.

The electrical characteristics of the ground and their effect on the design of outdoor foundations. L.E. E'bin et al., (pp. 26-30).

The authors propose a method of designing foundations for electrical equipment which allows for local and seasonal changes in the electrical characteristics of the earth. It is assumed that the electrical conductivity of the ground is a function of curvilinear coordinates of the electrical field.

A simple method of calculating short circuit currents in networks with steel conductors. L.M. Perhsina, (pp.30-34).

A simple and quite accurate method is proposed for calculating the the short circuit currents in networks with steel conductors where the impedance of the conductors is a function of the current. Use

is made of linearized voltampere characteristics.

Rotating machines

The mis-use of circuit transformations in the mathematical analysis of electrical machines. I.I. Talalov, (pp.34-38).

A study is made of the fundamental principles and relationships involved in mathematical transformations as applied to the design of the circuits and windings of electrical machines. The author has in mind certain mistaken modifications of these methods which have been used on computers.

A new electrostatic current generator using dielectric friction. N.G. Drozdov et al., (pp. 48-50).

A description is given of a small climatically-stable 800 V electrostatic generator with a plexiglass and teflon stator and a plexiglass-metal rotor. The internal surface of the stator is charged by polyethylene brushes on the rotor. Alternating or direct current can be produced. A 500 pF capacitor can be charged to 200 V in 20 to 25 revolutions of the rotor.

Progress in the electric drives of excavators. Iu.Ia. Vul', (pp. 81-83).

An account is given of operating experience with two amplidyne-type motor-generator sets for the lifting and traction drives on large excavators.

Statistical methods

A statistical and graphical method of designing equipment for a given reliability. Ia.A. Rips, (pp. 76-81).

An example is given of a way to design an electromagnetic relay for a given reliability and production cost. The method makes it possible to establish the necessary margin of safety and to estimate the effect of parameters on the reliability and durability of the device. The method is of general application.

Traction

The use of 25 kV on a.c. electrified railways. A.V. Voronin et al., (pp. 1-5).

Proposals have in the past been made for a general changeover to 35 kV on heavily loaded sections of the three-phase a.c. electrified

railway system of 50 c/s in the U.S.S.R. This paper explains why it has been decided to retain 25 kV. However, further cost analysis is to be undertaken to see whether it is advisable to use 35 kV on systems supplied from 220 kV power lines.

A NEW METHOD OF STUDYING LARGE COMPLEX POWER SYSTEMS ON ANALOGUE COMPUTERS*

N.I. SOKOLOV, Yu.E. GUREVICH and Z.G. KHVOSHCHINSKAYA

(Moscow)

(Received 25 July 1960)

Analogue computers are now extensively used to study the transient behaviour, control and stability of synchronous generators and it is quite natural to try and apply them to more complicated systems containing several generators, loads as well as other line elements.

Several methods have been proposed for this purpose:

1. An analogue may be formed of each machine in its own co-ordinates and then all reduced to a common system of co-ordinates [1,3];

2. The equations of the generators may be written in a synchronously rotating system of co-ordinates [2];

3. The equations of the generators may be written in terms of self- and mutual impedances and analogues formed by these equations [3].

However, method 1 leads to very cumbersome and impracticable computing schemes and methods 2 and 3 are apparently only possible if it is assumed, *inter alia*, that the impedances in the direct and quadrature axes are equal and if there is no (active) resistance. Methods 1 and 2 are very complicated, whilst in 1 and 3 the amount of computing apparatus increases out of proportion to the number of stations, and intermediate results are not at all readily appreciated, being expressed in coordinates α_c, β_c, etc.

---

* *Elektrichestvo*, 5, 1-8, 1961.

In this paper a method is proposed which permits the study of power systems of any degree of complexity on analogue computers on the usual assumptions. The number of computing amplifiers increases in proportion to the number of stations, loads and lines studied. The individual elements of a power system can be studied with different degrees of approximation. As far as the authors know, nobody has ever used the proposed method previously.

The main feature of the proposed method is that each element and its adjacent section of the line can be studied separately from all the other elements by the equations describing it.

The means of constructing the scheme depends on whether or not there is a point in the system which can be regarded as an infinite bus-bar. If such a point is present, the complete scheme consists of two types of element, namely:

1. Elements which link the infinite bus-bar with the network nodes and lines which interconnect the individual nodes;

2. Elements for the stations and loads.

The equations of line elements (type 1) contain the known input quantities of each element, i.e. the voltage at the sending end of the line, definable by the modulus and phase relative to the voltage of the infinite bus-bar, and the active and reactive power at the receiving end of the line, defined by the power balance at the node. The output quantities are the modulus and phase of the voltage at the receiving end of the line and, if necessary, the active and reactive power at the beginning of the line. The infinite bus is the beginning of the first line and the nearest points to the infinte bus are the beginning of the other lines. Thus, elements of type 1 permit successive determination of the modulus and phase of the voltages at the nodes.

For station and load elements (type 2) the input quantities are the modulus and phase of the voltages at the respective nodes.

The active and reactive power reaching them constitutes the output.

The principle is illustrated in Fig. 1.

The method can be modified if there is no infinite bus-bar and one of the generator stations is adopted as "reference". The angles of the rotor at all the other stations are read off from the axis of the rotor at the reference generator station. The analogue of the network is also

begun from the bus-bars of this station. It is also necessary to control the speed of the prime movers and consequently their torque, for otherwise it is impossible to balance the active power.

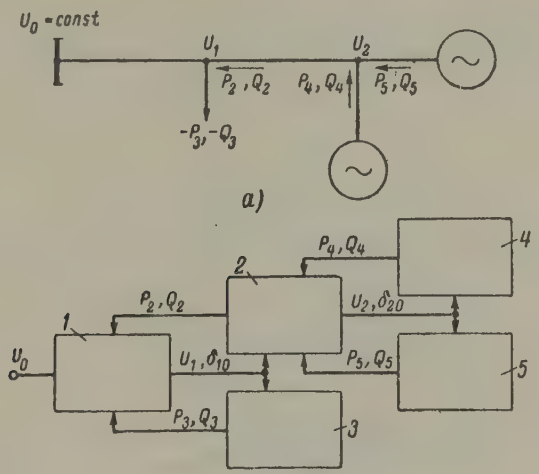

Fig. 1. Circuit (a) and block-diagram (b).
1 – line; *2* – line; *3* – load; *4* – alternator; *5* – alternator; *P* – active power; *Q* – reactive power.

The computing schemes are therefore analogous to the circuits of actual networks and there is therefore no difficulty in excluding some elements, including others, or clearing short circuits, etc. The number of elements must naturally be restricted for the study; but all elements in operational units can be covered. A larger number of amplifiers has to be used to study complex systems, but this cannot lead to self-excitation if the individual groups of elements are stable. In practice, four to five stations can be studied.

The proposed method allows special analogues of generators and line sections, etc. to be formed, which can then be combined to solve particular problems.

Analogues of elements

Line sections. Consider the transmission of power P from the node m to the node n via the impedance z_{mn} (Fig. 2a). It can be assumed that the active and reactive power into the line from the node m and the voltage

at node n are known. It is required to find the angle between the vector voltages at the nodes δ_{mn}, the voltage U_m and in certain cases active and reactive power at the other end of the line. The fundamental case of power transmission without loss is considered when $r_{mn} = x_{mn}$ and $P_m = -P_n$.

Suppose that the voltage U_m is also known. The angle δ_{mn} is then found from the equation

$$P_m = \frac{U_m U_n}{x_{mn}} \sin \delta_{mn}. \tag{1}$$

Alternatively, given δ_{mn}, the voltage can be found from the expressions

$$Q_m = \frac{U_m^2}{x_{mn}} - \frac{U_m U_n}{x_{mn}} \cos \delta_{mn}; \tag{2}$$

$$Q_n = \frac{U_n^2}{x_{mn}} - \frac{U_m U_n}{x_{mn}} \cos \delta_{mn}. \tag{3}$$

where Q is the reactive power.

The circuit in Fig. 2b, which refers to equation (1), contains an operational amplifier, a function generator* which gives the sine of the input, and a multiplier.

Putting α for the output voltage of the operational amplifier, the amplifier receives the difference between P_m and $\frac{U_m U_n}{x_{mn}} \sin \alpha$ at its input. This difference must be very small since an operational amplifier has no self-feedback and its amplification factor is very high. If P_m or $\frac{U_m U_n}{x_{mn}} \sin \alpha$ change, the difference between these quantities will increase and change sign at the input to the amplifier on passing through the sine unit. The value of α changes so that the difference becomes negligible. It is obvious that this will occur when $\alpha = \delta_{mn}$.

Such methods are extensively used in mathematical simulation to

* In our case we used sin and cos function generators made in the power system laboratory of the All-Union Electrical Energy Research Institute using tyrite (fergusonite) resistors. These generators can produce functions of an argument lying between the limits -2π and $+2\pi$.

obtain inverse functions. For example, a circuit with no multiplier ensures that $U_{out} = \sin^{-1} U_{in}$.

The circuit in Fig. 2b is stable if $\delta_{mn} < 90°$, since negative feedback becomes positive if δ_{mn} is large. But in the case under consideration the circuit is linked with the computing scheme of the generator which always has negative feedback, thereby ensuring the correct production of any value of the angle δ_{mn}.

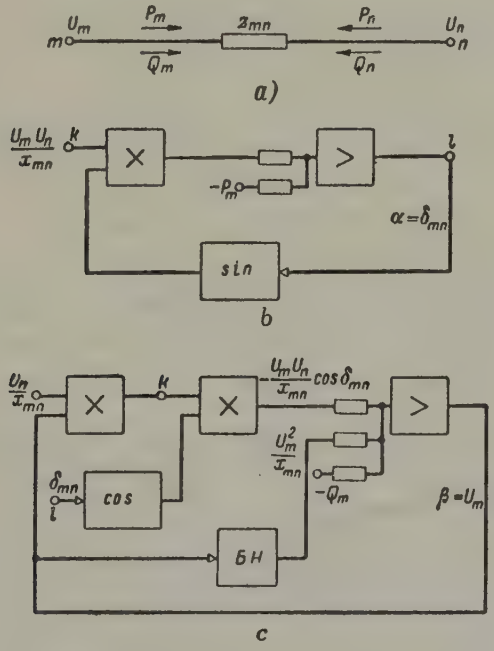

Fig. 2. A section of the line.
a – line section; *b* – circuit producing angle δ_{mn}; *c* – circuit producing nodal voltages.

The voltage U_n is found in a similar way. The corresponding circuit contains an amplifier without self-feedback, so that the following expression is obtained:

$$-\beta \frac{U_n}{x_{mn}} \cos\delta_{mn} - Q_m + \frac{\beta^2}{x_{mn}} = 0,$$

where β is the output voltage of the amplifier.

Comparing this expression with expression (2), it will be seen that

$\beta = U_m$.

The circuit also contains a multiplier and a cos function generator (a "quadrator"), which ensures that $U_{out} = U_{in}^2$.

The circuits in Fig. 2a and 2b are combined by joining the points k and l in each circuit. The inputs are then P_m, Q_m and U_n, and the outputs U_m and δ_{mn}. If necessary, Q_n can easily be obtained in accordance with equation (3). This requires one extra cos function generator for the voltage U_n *sic*. It should be pointed out, however, that only one cos function generator is normally required for each node, regardless of the number of outgoing lines from each node.

In a closed network the inter-nodal links are analysed by expressions (1)-(3). The active and reactive power flows are determined from the known nodal voltages and angle δ_{mn}, and they are then introduced into the power adders.

When the resistance of the line is included, the following expressions are used to determine the active and reactive power at the ends of the line with positive directions from the node into the line:

$$P_n = \frac{U_n^2}{z_{mn}^2} r_{mn} - \frac{U_m U_n}{z_{mn}^2} (x_{mn} \sin \delta_{mn} + r_{mn} \cos \delta_{mn}); \tag{4}$$

$$P_m = \frac{U_m^2}{z_{mn}^2} r_{mn} + \frac{U_m U_n}{z_{mn}^2} \times \times (x_{mn} \sin \delta_{mn} - r_{mn} \cos \delta_{mn}); \tag{5}$$

$$Q_n = \frac{U_n^2}{z_{mn}^2} x_{mn} + \frac{U_m U_n}{z_{mn}^2} \times \times (r_{mn} \sin \delta_{mn} - x_{mn} \cos \delta_{mn}); \tag{6}$$

$$Q_m = \frac{U_n^2}{z_{mn}^2} x_{mn} - \frac{U_m U_n}{z_{mn}^2} \times \times (r_{mn} \sin \delta_{mn} + x_{mn} \cos \delta_{mn}), \tag{7}$$

where

$$z_{mn}^2 = x_{mn}^2 + r_{mn}^2.$$

The inclusion of line resistance presents no difficulty, and a section of the line can be studied in the same way by equations (4)-(7). The only difference is that quantities which are proportional to $\sin \delta_{mn}$

and cos δ_{mn} are introduced into the circuits by summators and integrators to obtain δ_{mn} as well as U_m.

Generators. It is best to study generators in the direct (d) and quadrature (q) axes associated with the rotor. The analysis is particularly graphic since all the quantities have physical significance.

Generators can either be studied by the Gorev-Park equations [3] or by the equivalent networks proposed by the Gorodskii [4, 5]. The former method has been used for a number of years in the dynamic control laboratory of the power-station department at the Moscow Power Institute (MEI). The second method is more convenient, since fewer operational amplifiers are required, the criteria of the machines can easily be varied and any number of rotor circuits on a synchronous machine can be included.

Gorodskii's equivalent networks (see Fig. 3) have certain similarities with the conventional equivalent networks of synchronous machines. In them, ohmic resistances are substituted for inductances, and capacitances for (active) resistances, whilst the input impedances of the circuits for the direct (d) and transverse (q) axes correspond to the reactances $x_d(p)$ and $x_q(p)$ in transient and steady states.

Gorodskii's equivalent networks were proposed previously and took no account of the variation of the exciter voltage due to the action of the regulator. To include this factor correctly in the network corresponding to the direct axis of the machine, it is necessary to introduce a current I at point b in Fig. 3a proportional to the voltage U_f and independent of U_q (see appendix I). The current I is the "forced" component of the excitation current I_f flowing through the reactance x_{of}. Under transient conditions the current I_f is the sum of the "forced" current $I_{fe} = I \equiv u_f$ and the force (transient) component due to the variation of the voltage u_q or u_f.

This requires a special "current source" with an infinite output resistance. The magnitude of the introduced current should be proportional to the control voltage and independent of the external resistance within definite limits. This special "current source" is obtained by using two operational amplifiers (see appendix II and Fig. 4).

When using Gorodskii's equivalent circuits on the computer, points a and a_1 (see Fig. 3) are connected to the outputs of the operational amplifiers which produce the voltages u_q and u_d. It is convenient to include the transformer resistance and the inductive reactance of the line up to the node in the leakage reactance x_a of the equivalent network. It is

Undesirable for the capacitances in the branches of the equivalent network to be in excess of 10 μF. This requirement determines the magnitude of the ohmic resistances and currents in the branches. The resistances should not be too small, for otherwise the amplifiers may be overloaded.

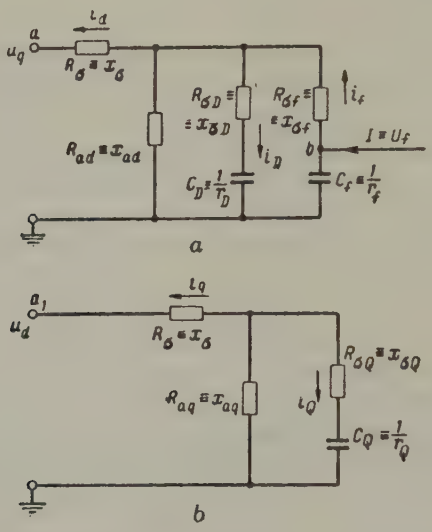

Fig. 3. Equivalent circuit of generator.
a – along direct axis; *b* – along quadrature axis.

Instruments and oscillograph loops can be connected in series in the circuits to measure the currents. It must however be borne in mind that the currents do not usually exceed 1 mA and so the currents are usually converted into voltages by other amplifiers for further study and measurement. For the sake of convenience in taking measurements, the "current source" (see Fig. 4) is connected to a slightly different equivalent network of the generator (Fig. 5c). This new network is practically the same as the original one, since the resistances of the u_q and u_d are close to zero.

The stator currents i_d and i_q can be estimated from the voltage drop in the leakage reactance x_σ. The input impedance r_2 of amplifier *10* is connected in parallel with r_1. The latter must be made such that

$$\frac{r_1 r_2}{r_1 + r_2} \equiv x_\sigma.$$

The excitation current i_f can be estimated from the difference in voltage to earth at points *b* (the position of the "current source")

and c (position of amplifier *10*). Since the output voltage of amplifier *9* is equal to the voltage at point b, but opposite in sign, it is therefore sufficient to add the voltages after amplifier *9* and at point c. In calculating the impedance r_1 it is necessary to take the input impedance r_3 of amplifier *11* into account.

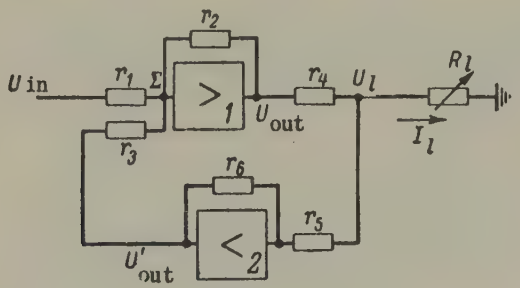

Fig. 4. Equivalent circuit of "current source".

The currents in the damping winding are usually difficult to measure, but this can be done by adding another amplifier (see Fig. 5c).

The voltages u_q and u_d at the terminals of the equivalent relay are obtained by "projecting" the voltage at the node where the generator is connected along the axis of the machine (see Fig. 5b).

Use is made of multipliers and adders to determine the active and reactive power from the generator to the node:

$$\left.\begin{aligned} P &= u_d i_d + u_q i_q; \\ Q &= u_q i_q - u_d i_d, \end{aligned}\right\} \qquad (8)$$

It is presupposed that $P \approx m$.

Variation in rotor angle are found by twice integrating the equations of motion of the rotor about a certain reference axis which rotates at the synchronous speed.

$$T_j p^2 \delta = P_{\text{mech}} - P_{\text{el}}. \qquad (9)$$

The reference axis is the voltage vector at the infinite bus-bars. The angle between the quadrature axis of the generator and the nodal voltage is obtained by subtracting the angle of the node-bus-bar from the equation of motion.

It is assumed that the turbine torque is constant. Alternatively, a

speed-controlled turbine may be studied separately [3]. The generator can be provided with any excitation regulator and exciter. No special explanation is required to study these elements [6]. The authors of this article have adopted the circuit shown in Fig. 5.

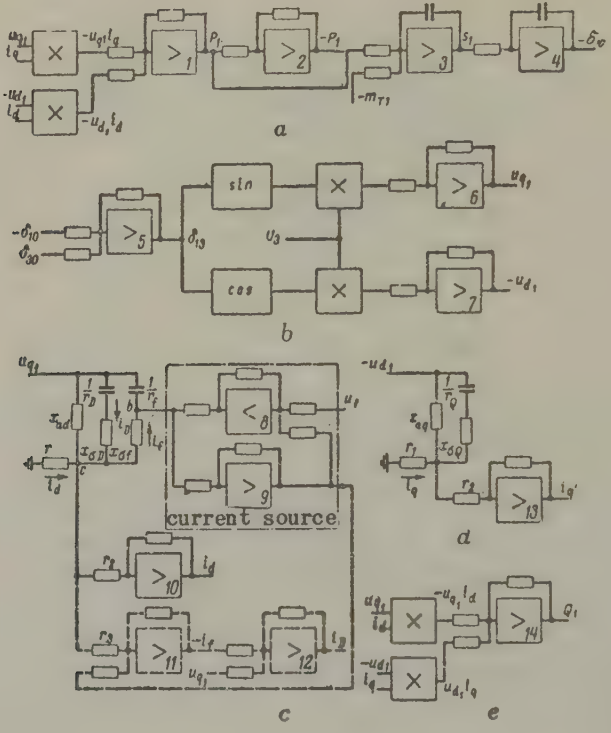

Fig. 5. Computing scheme of generator.
a – active power and the equation of motion of the generator; *b* – projection of the nodal voltages along the axes of the generator; *c* – direct-axis of the generator; *d* – quadrature axis of the generator; *e* – reactive power.

In many cases it is possible to simplify the study of generators by substituting constant impedances and a constant e.m.f. for the "contact" resistance found from the preceding conditions. The equation of motion remains unchanged. The electromagnetic power is obtained from the equation

$$P \approx \frac{E'_d U}{x'_d + x_{gn}} \sin \delta, \qquad (10)$$

where U is the nodal voltage; x_{gn} is the impedance from the generator terminals up to the node; δ is the angle of the generator e.m.f. in relation to the node.

The reactive power is found by a similar formula to (2).

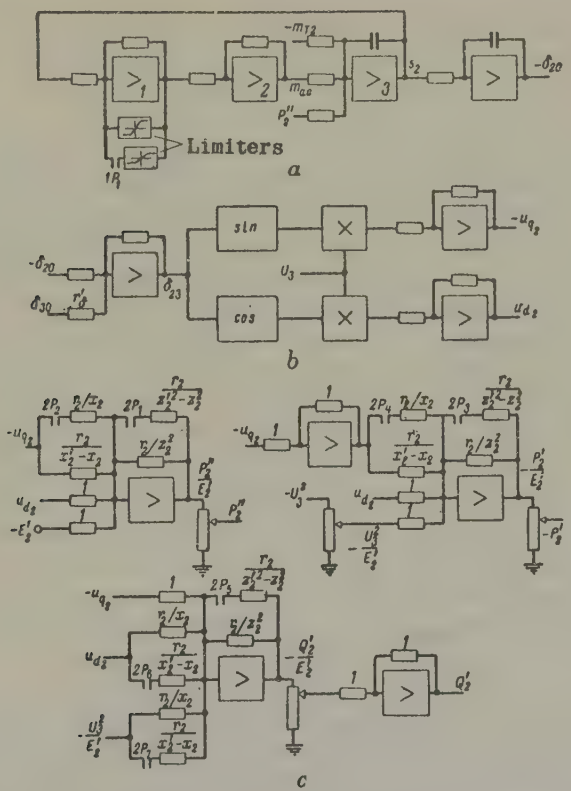

Fig. 6. Simplified computing circuit of generator.

$z'_2=\sqrt{z_2^2+x_2'^2}$ – line resistance in post-fault conditions;

a – equation of motion of the generator; *b* – projection of the nodal voltages along the axes of the generator; *c* – the active and reactive power.

Given that E'_d is constant, the asynchronous torque m_{as}, which exists if $s \neq 0$, can be ignored. However, asynchronous torque can be included approximately in the way illustrated by Fig. 6, where a value of m_{as}, which is proportional to the slip s, is passed into amplifier 3. If the slip is in excess of its critical value the torque remains constant. Provision is made for altering the amount of asynchronous torque during

short circuits.

Loads and static elements at the nodes. Loads and their dynamic properties can be studied by a similar circuit to that used for the generators by making certain assumptions.

Static loads are simulated in accordance with the equations

$$P = U^2 G_l, \quad Q = U^2 B_l. \tag{11}$$

The term U^2 is usually known; if G_l and B_l are constants, they can be included when calculating the input impedances of the amplifiers for adding the active and reactive power. Such loads can therefore be studied without additional amplifiers. There is no difficulty in studying loads in the light of their steady-state functions $P_l = f_1(U)$ and $Q_l = f_2(U)$. This requires non-linear elements. Neither is there any difficulty in studying shunt reactors, line capacitances or parallel load resistances for restraint under transient conditions, etc.

Short-circuits and post-fault conditions. A short circuit is effected at a node by introducing a shunt $x_{s/c}$ into the node at the time of the fault. This shunt is connected in the same way as a reactive load. By selecting the magnitude of the input impedance at the input to the amplifier adding the reactive power, it is an easy matter to produce a short circuit of any type at any remote point. By taking the minimum possible input impedance ($x_{s/c} \approx 0$), it is possible in practice to obtain an exact three-phase short circuit at the node.

In the study of post-fault conditions it is usually necessary to provide for a change in the impedance of one of the links between the nodes (disconnexion of one of the parallel lines). This is done by automatically changing the input impedances after the short circuit has been cleared.

Example

The proposed method has been applied to the circuit shown in Fig.7 which contains the station *1*, a single generator with a bus-bar load *L*, and the receiving systems *0* and *2*. The bus-bars of receiving systems *0* are assumed to be infinite.

The transformer e.m.f.'s of the generators and variations in the reactance of the generators and lines during generator rotor oscillation are ignored; it is assumed that the generators are unsaturated; the

line resistance is ignored wherever it has no appreciable effect. The method is equally applicable if these simplifications are not adopted, but the circuit is a little more complicated as a result. Only the transformer e.m.f. present any difficulties, but these can be ignored in the majority of cases.

The block-diagrams and circuit-diagrams are given in Figs. 5, 6, 8 and 9. The excitation control has been omitted from the generator circuit in Fig.5 and torque is assumed to be constant. The receiving system 2 (Fig. 7) is simulated by an equivalent generator with a constant e.m.f. after the contact resistance (see Fig.6). The line resistance is included in the study of the lines linking stations 1 and 2, and provision is made for a system of relays to change the line resistance after faults. Receiving system 2 was studied by the equations of motion and expressions (4), (6) and (7).

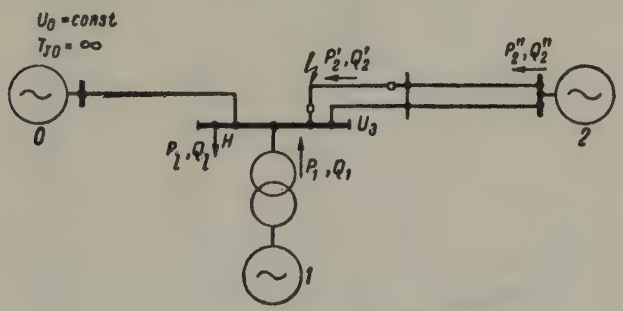

Fig. 7. The simulated network.

The broken lines in Figs. 5 and 9 indicate elements which were later found necessary during the adjustment of the circuit, as well as elements which were included to measure the rotor currents. A system of relays was used to study short circuits. Relay *1P* was live during the short circuit and *2P* afterwards.

By way of example, Fig. 10 shows one of the oscillograms taken during a two-phase earth fault at a node with a high-response excitation regulator.

Circuit adjustment

The proposed method allows the adjustment and verification of each individual circuit element, which simplifies and speeds up the preparations for the study and the study itself. For example, to adjust the

generator circuit it is sufficient to supply the voltage U_3 from an independent source and the generator is, as it were, connected to the infinite bus-bar. To adjust the circuit of a section of the line and a node it is convenient to substitute independent voltages for the active and reactive power of the generators and the loads.

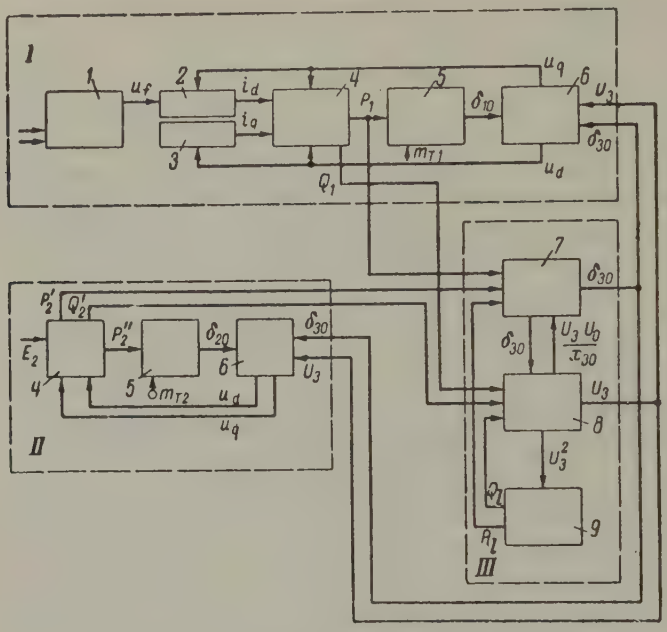

Fig. 8. Simulation block-diagram.

I – first generator; *II* – second generator; *III* – line and node. *1* – automatic voltage regulator; *2* – the *d*-axis; *3* – the *q*-axis; *4* – active and reactive power; *5* – equation of motion; *6* – projection of nodal voltages; *7* – determination of δ_{20}; *8* – determination of U_3; *9* – nodal load.

Gorodskii's equivalent circuits are first adjusted in the direct and quadrature axes. The resistances and capacitances must be correct to three significant digits. It is convenient to adjust the "current source" (Fig. 4) by varying the resistance r_3 (see appendix II) in such a way that the load current measured by the micro-ammeter is independent of the load impedance. Impedances r_1 and r_2 are set to an appropriate scale, and r_4 is such that amplifier *1* of the "current source" is not overloaded under any operating conditions of the generator.

In the node and line circuit (Fig. 9) special attention must be paid to the operational amplifiers which produce the angle δ_{30} and voltage U_3. The amplifiers must have no self-feedback under any circumstances. However, it has been shown by circuit tests that generation* occurs in the circuit in connexion with the weaking of the total negative feedback at angles in excess of 90°. This requires the inclusion of a capacitance C_δ in the feedback of the amplifier producing the angle δ_{30}. Self-excitation was thereby eliminated completely. A capacitance of 0.07 μ F was in fact used. Tests showed that no marked error resulted in the size of the angles.

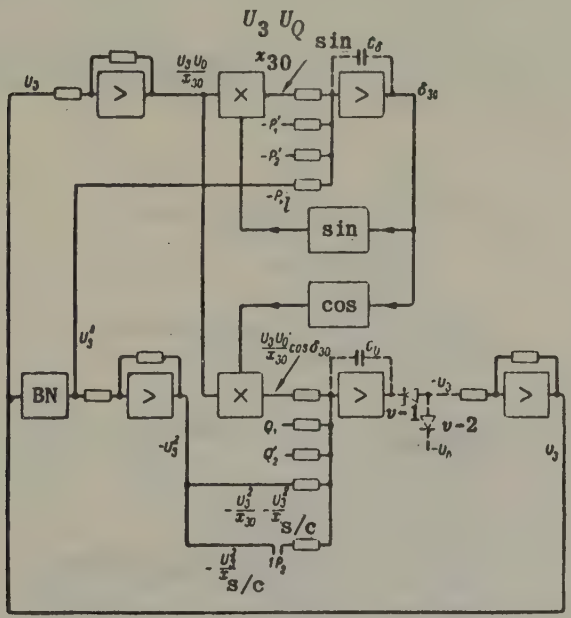

Fig. 9. Computing circuit of node and line section.

More favourable conditions exist in the line-node circuit in which the voltage was produced. It is sufficient for C_U to be about 0.02 μ F. This figure has very little effect even if the voltage varies widely.

Any error due to the capacitances C_δ or C_U can be eliminated by using a "retarded time scale", in which case there is no increase in C_δ or C_U.

---

* Use was made of UPT-4-type amplifiers.

There remains one further aspect of the method (see Fig. 9) which requires special comment. The impedance of the transformer and the leakage reactance of the generator were combined in the simulation of the generator. In the operation of the circuit the reactive power flowing to the node was proportional to its voltage. At the moment the circuit is started (triggered), or when a three-phase short circuit is cleared at the node, all the operational amplifiers producing U_3 receive zero potentials and U_3 remains zero. Although this is an unstable state of equilibrium, the circuit reverts to its operating state after a lapse of time. This random delay can be eliminated by introducing a low starting voltage U_S (Fig. 9), which removes the circuit from its unstable state almost instantaneously, and the source of the starting voltage ceases to have any further effect on the system owing to the valves V-1 and V-2. The voltage U_S can be used to define a residual positive sequence voltage at the node as required for studying non-symmetrical faults and remote short circuits.

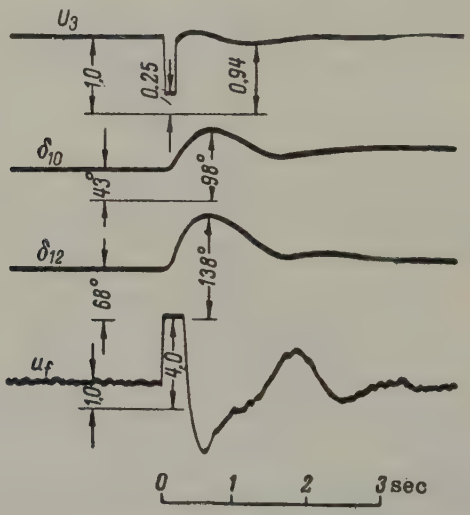

Fig. 10. Oscillogram of a two-phase earth fault at a node.

The proposed method is also applicable to out-of-step conditions. The amplifiers producing the angles δ_{10}, δ_{20} and δ_{30} are fitted with switching devices which shunt the feedback capacitances when the angle becomes 360°. When the slip becomes large (over 3 per cent) an error begins to creep in if C_s is large and a "natural" time scale adopted. This error can be practically eliminated by using a "retarded time scale".

Appendix I.
Equivalent network of a generator

The equivalent network used in this paper differs from that proposed by Gorodskii [4] in that a variable "current source" is introduced to include excitation control. Other methods of including excitation control have been published. For instance, a similar method to Gorodskii's was described in [7], in which a correctional circuit was added to adjust for changes in excitation.

It will now be shown that the "current-source" method describes the behaviour of the generator correctly.

Ignoring the transformer e.m.f. and stator resistances, the generator performance can be described by the equations*

$$u_d = + x_q i_q;$$
$$u_q = x_{ad} i_f - x_d i_d;$$
$$u_f = p(x_f i_f - x_{ad} i_d) + r_f i_f.$$

Hence the current in the direct axis is

$$i_d(p) = \frac{u_q(p)}{x_d(p)} - \frac{G(p)\,u_f(p)}{x_d(p)}. \qquad \text{(I-1)}$$

The first term on the right of equation (I-1) describes the effects due to the external voltage $u_q(p)$, whilst the second fully defines the excitation and can be written in the form

$$i_f(p)\frac{G(p)\,r_f}{x_d(p)}, \qquad \text{(I-2)}$$

where $i_f(p)G(p)r_f$ is the equivalent voltage at the terminals of direct axis definable by the "forced" excitation current $i_{f.f}(p)$.

The equivalence of the generator performance and equivalent network will now be shown for the simplest case of no damping windings.

It is well known that for the generator

$$x_d(p) = \frac{x_d + x'_d T_{f0} p}{1 + T_{f0} p}; \qquad \text{(I-3)}$$

$$G(p) = \frac{x_{ad}}{r_f(1 + T_{f0} p)}, \qquad \text{(I-4)}$$

* The q-axis leads the d-axis.

where u_f is the slip-ring voltage; i_f is the rotor current; T_{f0} is the time constant of the excitation winding if all the other circuits are broken.

For the equivalent network in Fig. 5 the addition of x_{ad} with $x_{\sigma f} + \frac{r_f}{p}$ in parallel and with x_σ in series gives

$$x_d(p) = \frac{x_\sigma + x_{ad} + x_\sigma T_{f0} p + x_{\sigma f} x_{ad} \frac{p}{r_f}}{1 + T_{f0} p} = \\ = \frac{x_d + x'_d T_{f0} p}{1 + T_{f0} p}. \qquad \text{(I-5)}$$

The voltage at the terminals of the open network when carrying the "forced" current $i_{f.f}(p)$

$$u(p) = i_{f\,f}(p) \frac{\frac{r_f}{p} x_{ad}}{x_{\sigma f} + x_{ad} + \frac{r_f}{p}} = \\ = \frac{x_{ad}}{1 + T_{f0} p} i_{f\,f}(p). \qquad \text{(I-6)}$$

With the stator closed, the current component due to the excitation (i.e. due to the current $i_{f.f}(p)$) can be expressed as follows:

$$\frac{1}{x_d(p)} \frac{x_{ad}}{1 + T_{f0} p} i_{f\,f}(p) = \\ = \frac{x_{ad} i_{f\,f}(p) r_f}{x_d(p) r_f (1 + T_{f0} p)} = \frac{G(p)}{x_d(p)} u_f(p). \qquad \text{(I-7)}$$

Thus the operator expressions for the generator currents fully agree with the equivalent networks.

Appendix II.
The current source

The load current I_l in Fig. 4 is made independent of the load impedance R_l by a positive feedback which increases the output voltage of amplifier l with increasing U and, consequently, R_l.

It will now be shown that I_l is independent of R_l if the impedances are correctly chosen.

It is well known that the potential at the summation point Σ of an amplifier is negligibly small. Suppose, therefore, that $\Sigma = 0$. The sum of the currents at the point Σ then takes the form

$$\frac{U_{in}}{r_1} + \frac{U_{out}}{r_2} + \frac{U'_{out}}{r_3} = 0. \qquad \text{(II-1)}$$

Since

$$r_5 = r_6$$
$$U'_{out} = -U_l$$
$$U_{out} = U_l\left(1 + r_4\frac{r_5 + R_l}{r_5 R_l}\right),$$

it follows that expression (II-1) can be re-written in the form

$$\frac{U_{in}}{r_1} + \frac{U_l}{r_2}\left(1 + r_4\frac{r_5 + R_l}{r_5 R_l}\right) - \frac{U_l}{r_3} = 0, \qquad \text{(II-2)}$$

whence

$$I_l = \frac{U_l}{R_l} = -\frac{U_{in}}{r_1}\,\frac{r_2 r_3 r_5}{R_l(r_3 r_4 + r_3 r_5 - r_2 r_5) + r_3 r_4 r_5} \qquad \text{(II-3)}$$

Suppose that in expression (II-3)

$$r_3 r_4 + r_3 r_5 = r_2 r_5, \qquad \text{(II-4)}$$

The current I_l will then be independent of the load

$$I_l = -U_{in}\frac{r_2}{r_1 r_4}.$$

Thus, the "current source" functions correctly if condition (II-4) is fulfilled, whence it follows that

$$r_3 = \frac{r_2 r_5}{r_4 + r_5}. \qquad \text{(II-5)}$$

Translated by O.M. Blunn

1. S.V. Strakhov; *Elektrichestvo*, 7 (1957).
2. V.S. Tarasov, A.I. Vazhnov, Iu.V. Rakitskii, V.V. Popov and L.N. Semenova; *Elektrichestvo*, 4 (1960).
3. Ya.N. Luginskii and M.G. Portnoi; *The application of mathematical analogues to the study of electro-mechanical behaviour in electrical systems (Primeneniye matematicheskikh modelei dlia issledovaniya elektro-mekhanicheskikh perekhodnykh protsessov v elektricheskikh sistemakh). Trud. VNIIE*, IX (1959).
4. D.A. Gorodskii; *Elektrichestvo*, 15 (1934).
5. D.A. Gorodskii; *Elektrichestvo*, 18 (1934).
6. V.I. Pishchikov and N.I. Sokolov; *The effect of high-response excitation control on the stability of synchronous generators operating in parallel (Vlyanye sil'nogo regulirovaniya vozbuzhdeniya na ustoichivost' parallel'noi raboty sinkhronnykh generatorov). Trud. VNIIE*, IX (1959).
7. H. Buhler; *Bull. Oerlikon*, 330, Oct. (1958).

THE SELF-EXCITATION OF INDUCTION MOTORS WITH SERIES CAPACITORS*

V.G. BAUMAN, O.V. IVANOV and B.I. KOMAROV

(Leningrad Mining Institute)

(Received 14 November 1960)

The self-excitation of induction motors [1-7] is one of the main obstacles to the use of series capacitors for the compensation of the voltages drop in local distribution networks. Its effect is to limit the maximum stable output of the motors supplied from high-voltage transmission lines [8].

The self-excitation of an induction motor can be regarded as parametric resonance in an oscillatory system in which the equivalent inductance periodically varies with the mutual induction between the circuits of the system. Under definite conditions the "free" oscillations in such a system may decay, increase or even remain constant depending on the relationship between the energy introduced into the system when a parameter changes and the energy loss during this period of time.

The emergence of parametric resonance expresses itself mathematically in an unstable solution of the differential equation of the system. However, at the boundary of stability there exist free oscillations which do not decay and it is therefore possible to determine the boundary conditions of self-excitation by the methods of steady state analysis usually applied to induction motors.

The simplest way to determine the boundary conditions is to use Wagner's equivalent circuit [2].

---

* *Elektrichestvo*, 5, 38-44, 1961.

Fig. 1 shows an equivalent circuit for the "free" currents of an induction motor with series capacitors. All the reactances of the circuit are defined at 50 c/s. The frequency of the free oscillations at the boundary of stability ω_0 is proportional to the supply frequency. The rotor slip relative to the field of free currents at the boundary of stability is

$$s_0 = \frac{\omega_0 - \omega_r}{\omega_0}, \tag{1}$$

where ω_r is the angular velocity of rotation of the rotor as a proportion of synchronous speed at 50 c/s.

The conditions for the existence of non-decaying free oscillations in the circuit in Fig. 1 can easily be found by Kirchhoff's laws

$$\dot{I}_1 + \dot{I}_2 + \dot{I}_3 = 0;$$

$$\dot{I}_1 Z_1 - \dot{I}_3 Z_3 = 0; \quad \dot{I}_2 Z_2 - \dot{I}_3 Z_3 = 0,$$

where

$$Z_1 = r_1 + j\left(\omega_0 x_{1s} - \frac{x_c}{\omega_0}\right);$$

$$Z_2 = \frac{r_2'}{s_0} + j\omega_0 x_{2s}';$$

$$Z_3 = j\omega_0 x_M.$$

Solving this set of equations with respect to the current I_2:

$$\dot{I}_2\left(Z_2 + \frac{Z_1 Z_3}{Z_1 + Z_3}\right) = 0.$$

It follows from this expression that if $I_2 \neq 0$, then the equivalent impedance of the circuit $Z_2 + \frac{Z_1 Z_3}{Z_1 + Z_3}$ must equal zero. (Points above symbols indicate complex quantities).

The conditions for the existence of non-decaying oscillations in the circuit in Fig. 1 can thus be written in the form

$$Z_2 + \frac{Z_1 Z_3}{Z_1 + Z_3} = 0$$

or

$$\frac{r_2'}{s_0}+j\omega_0 x_{2s}'+\frac{j\omega_0 x_M\left[r_1+j\left(\omega_0 x_{1s}-\frac{x_c}{\omega_0}\right)\right]}{r_1+j\left[\omega_0(x_M+x_{1s})-\frac{x_c}{\omega_0}\right]}=0. \qquad (2)$$

The real and imaginary parts of equation (1) are then equated to zero separately and for the sake of simplicity

$$x_{1s}+x_M=x_1 \text{ и } x_{1s}+\frac{x_{2s}'x_M}{x_{2s}'+x_M}=x',$$

Hence

$$\left.\begin{aligned} r_1^2&=-\left(\omega_0 x_1-\frac{x_c}{\omega_0}\right)\left(\omega_0 x'-\frac{x_c}{\omega_0}\right)\\ \text{and}\qquad \frac{s_0}{r_2'}&=-\frac{r_1^2+\left(\omega_0 x_1-\frac{x_c}{\omega_0}\right)^2}{\omega_0^2 x_M^2 r_1}. \end{aligned}\right\} \qquad (3)$$

It follows from this equation that the slip s_0 can only be negative in the presence of self-excitation, i.e. the velocity ω_r of the rotor of an induction motor during self-excitation must be greater than the frequency of the free oscillations ω_0 (operating as a generator at the frequency of the free currents).

When considered with equation (2), the second equation in (3) can be written in the form:

$$\left(\frac{s_0}{r_2'}\right)^2=-\frac{\left(\omega_0 x_1-\frac{x_c}{\omega_0}\right)}{\omega_0^2 x_2'^2\left(\omega_0 x'-\frac{x_c}{\omega_0}\right)}, \qquad (4)$$

where

$$x_2'=x_M+x_{2s}'.$$

and x_c is the capacitive reactance.

Using equations (1), (3) and (4) it is possible to find the frequencies ω_{01} and ω_{02} of those free oscillations at the boundary of stability which correspond to the values of the slip s_{01} and s_{02} and,

consequently, the velocity bounds of the zone of self-excitation ω_{r1} and ω_{r2} can also be determined.

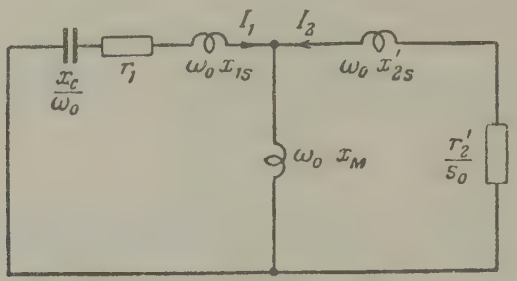

Fig. 1. Equivalent circuit.

It has been shown by calculations and tests that the boundary frequencies ω_{01} and ω_{02} in systems in which self-excitation has been specially eliminated are usually very little different from the respective frequencies ω'_{01} and ω'_{02} in systems without losses ($r_1 = 0$), which are equal to

$$\omega'_{01} = \sqrt{\frac{x_c}{x_1}} \text{ and } \omega'_{02} = \sqrt{\frac{x_c}{x'}}.$$

The self-excitation of induction motors occurs at rotor speeds

$$\omega_{r2} > \omega_r > \omega_{r1}.$$

Over this range one of the roots of the characteristic equation of the system will have a positive real part [1, 2, 4, 6] and, consequently, increasing free oscillations will occur in the system.

At speeds ω_{r1} and ω_{r2} the real part of this root is zero and constant free oscillations will continue in the system (boundary of the zone of self-excitation). At speeds $\omega_{r1} > \omega_r > \omega_{r2}$ the free oscillations will decay.

In voltage control systems using series capacitors the theoretical limits ω_{r1} and ω_{r2} are usually below synchronous speed at 50 c/s. If the resistance r_1 is increased there is a corresponding narrowing of the velocity bounds of the self-excitation zone, as follows from equations (3) and (4), but at the critical value of $r_1 (r_1 = r_{1cr})$ these bounds merge and if $r_1 > r_{1cr}$ self-excitation is impossible. An expression can easily be obtained for r_{1cr} from equation (3) by determin-

ing the maximum of the function defined by this equation [2,6]:

$$r_{1cr}=\sqrt{x_c}(\sqrt{x_1}-\sqrt{x'}). \quad (5)$$

It will be seen from an analysis of this expression that r_{1cr} decreases in value with a decreasing percentage modulation of the equivalent inductance of the motor:

$$m=\frac{x_1-x'}{x_1+x'}$$

In deriving the propositions underlying the theory of self-excitation in induction motors it is assumed that all the criteria of the system are linear or else dependent solely on the magnitude of the free currents [5].

It is also assumed that the speed of the rotor is constant. Such assumptions are only permissible in the study of asynchronous generators. Previous papers [1,3,4,5,7,8], have not dealt with asynchronous generators operating as motors for this reason. It has been shown by tests that the special features of the motor state have a decisive effect on the nature of the development of self-excitation in asynchronous machines under these conditions.

The authors have undertaken research which now makes it possible to form a qualitative estimate of the effect of individual factors on the nature of the development of self-excitation in induction motors.

There are a number of distinctive features of the development of self-excitation in asynchronous generators operating as motors:

1. The criteria of the machine depend on the magnitude of the voltages and currents of the "forced" process, in which the supply source defines the frequency, as well as on the currents and voltages in the free process;

2. The self-excitation of the motor at speeds below normal is only possible during acceleration of the rotor within the resonant zone. The possibility of the rotor crawling in the zone of self-excitation is determined by the time taken to pass through this zone and the time taken for free oscillations to develop; i.e. it depends on the moment of static and dynamic (mechanical) resistance, the magnitude of the supply voltage and the numerical values of the circuit criteria.

3. The performance of an excited motor can only be stable at the

lower velocity limit of the self-excitation zone [2].

The magnitude of the input voltage has the most important effect on the development self-excitation in a motor. It has been established by tests on AOL and A type motors with series capacitors at supply voltages from 60 to 500 V that the self-excitation of a motor can be divided into five distinct stages in which the excitation develops in different forms.

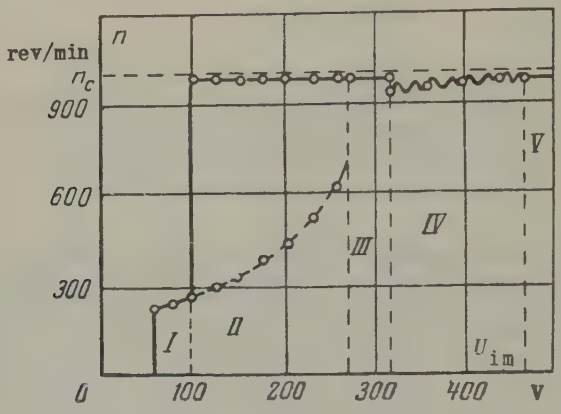

Fig. 2. Speed n as a function of the input voltage U_{in} for A-41-6 type motors (capacitive reactance x_c = 6.6 ohms; line resistance r_l = 0; GD^2_M (flywheel effect) = 0.

The curve for $n = f(U_{in})$ in Fig. 2 is divided into five sections by the vertical broken lines. The continuous line represents the speeds attainable by the motor on starting from a standstill. The broken line in region II shows the running speeds of a motor which is repeatedly switched on and off but not allowed to stop rotating. The broken line at the end of this region shows the speeds which are attained by a continuous increase in the supply voltage of the excited motor.

The motor does not gain speed in the first region. It crawls at a lower speed corresponding to the reduced resonant frequency of the system. In this region the self-excitation of the motor develops as follows (Fig. 3a). On starting, the rotor accelerates according to its mechanical characteristic (Fig. 3a) to the lower boundary of the self-excitation zone under the influence of an excess torque equal to the difference between the driving torque and the moment of static resistance.

As soon as the speed of the rotor passes beyond the lower limit of

the self-excitation zone, self-excitation of the motor sets in and the machine begins to function as a generator at the frequency of the free currents. When the rotor is in the zone of self-excitation, the braking torque created by the field of free currents succeeds in increasing so much that the resulting torque of the machine becomes less than the moment of static resistance. The speed of the rotor therefore drops and the motor leaves the zone of self-excitation. The rotor now starts to accelerate all over again and crosses the lower boundary, but this time there is a much less excess torque so that the rotor now decelerates much more quickly under the influence of the free currents and it stabilises at point A (Fig. 3a) where its speed corresponds to the lower boundary of the self-excitation zone. In this case the amplitude of the free oscillations is restricted by the change in speed of the rotor,

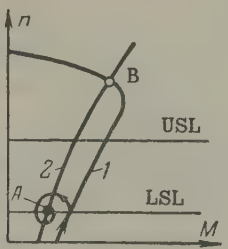

a

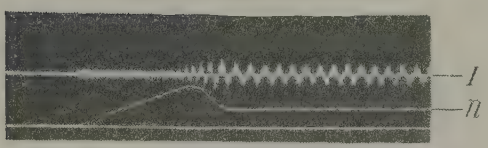

b

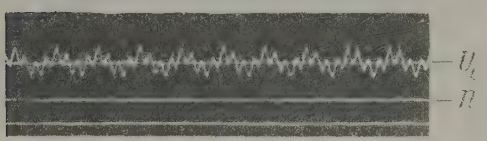

c

Fig. 3. The starting of induction motors in region I(a), oscillograms (b,c). *1* – torque speed characteristic of a non-excited induction motor; *2* – characteristic of the load torque; *B* – point of normal operation; *LSL* and *USL* - lower and upper speed limits of the self-excitation zones; U_C – capacitor voltage.

which is the typical feature of the development of self-excitation in generators operating as motors*.

The currents and voltages during the self-excitation of a motor are distorted in zone I by the appearance of considerable low frequency components. Fig. 3(b) and (c) shows oscillograms which illustrate the variation in the speed of the motor when self-excited and the shape of the typical curve of steady state oscillations in region I.

It should be pointed out that use is made of a curve representing the voltage drop of capacitors U_c for which the typical distortions present in self-excitation are more pronounced.

In region II (Fig. 2) the motor, on starting from a complete standstill, accelerates to its rated speed and, crossing the resonant zone, is self-excited, only locking at lower speeds if switched on and off without being allowed to stop rotating.

At the end of region II self-excitation can only be maintained by a continuous increase in the supply voltage to the already excited motor.

It will be seen from the curve in Fig. 2 that a self-excited motor will lock at a higher speed depending on the extent to which the supply voltage is increased. This is explained by the saturation of the machine steel owing to the appearance of low frequency components in the voltage at the terminals of the motor and the associated reduction in the no-load inductive reactance of the machine x_1 [2]. The starting diagrams and oscillograms appropriate to this region are shown in Fig. 4.

The reason why the self-excitation zone is crossed when starting after a complete standstill is that the rotor in region II manages to pass through the zone before free oscillations can develop which are capable of creating a generator moment sufficient to decelerate the rotor (Fig. 4) [2, 6].

If the input voltage is increased still further, self-excitation cannot be maintained even by continuously increasing the voltage applied to the already excited motor, i.e. there is no self-excitation in region III (Fig. 2). This is explained by the narrowing of the self-excitation zone owing to the considerable reduction in the no-load inductive reactance x_1 and the decreased percentage modulation of the parameter (equivalent inductance).

---

* In the self-excitation of generators the amplitude of the free oscillations is usually limited by the saturation of the steel.

In region IV the motor again begins to be self-excited with a continuous increase in the input voltage whether the motor is started from standstill or repeatedly switched on and off). The explanation is that the types of machine under consideration have a lower equivalent inductive reactance x' approximately equal to the short circuit inductive reactance which fixes the position of the upper speed boundary of the zone. Furthermore, it is not a constant quantity but diminishes as the input voltage is increased. If the short circuit inductance is reduced the upper speed boundary of the zone is moved upwards and at the beginning of the fourth region it is raised above the normal operating point of the motor (Fig. 5). The normal operating point then comes within the self-excitation zone and the motor is perpetually self-excited in this region.

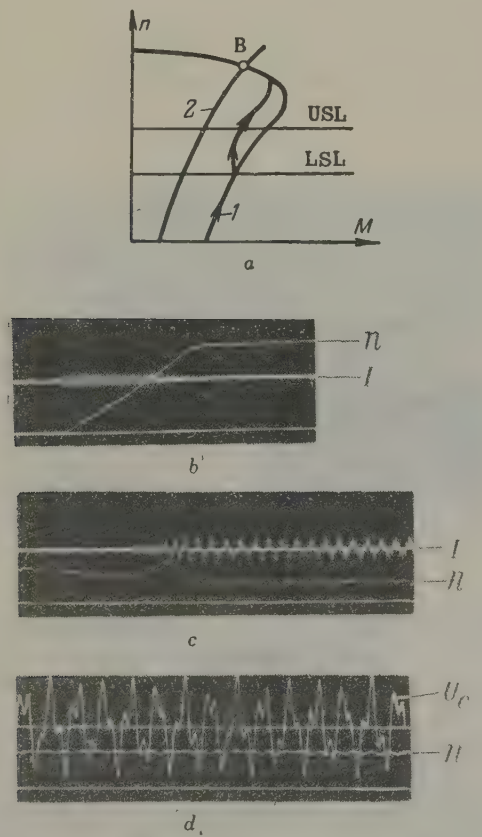

Fig. 4. The starting of induction motors in region II.
(Symbols as in Fig. 3)

Accordingly, there are grounds to suppose that motors with open shallow rotor slots (for which the short-circuit inductance is practically independent of the magnitude of the input voltage) will not have a region IV. Tests have been made which corroborate this idea [2].

Numerous tests have also shown that region IV generally covers a range of voltages quite close to the voltage of the motor (see Fig. 2).

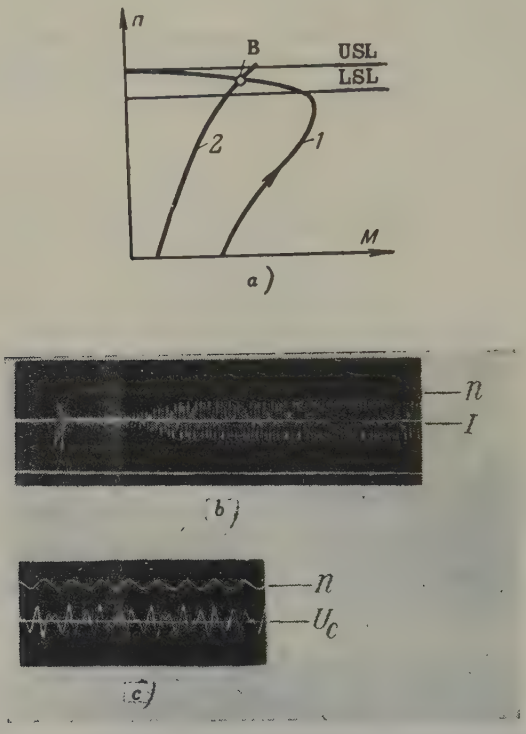

Fig. 5. The starting of an induction motors in region IV.
(Symbols as in Fig. 3)

It has been found that in this region self-excitation proceeds at speeds close to the normal speed of the rotor at comparatively low values of capacitive reactance (roughly up to 50 per cent of the short circuit inductive reactance of the machine). But the rotor speed of a self-excited machine tends to fall in this region to the extent that the capacitive reactance is increased.

The self-excitation of a motor in region IV is always accompanied by

stable oscillations in the torque and speed of the rotor.

It will be seen from the oscillograms in Fig. 5 that the voltage (current) curves are distorted in this region on account of the speed variations of the rotor and the saturation of the steel. Thus, the nature of the self-excitation of an induction motor near rated voltages is substantially different from that considered in the published literature.

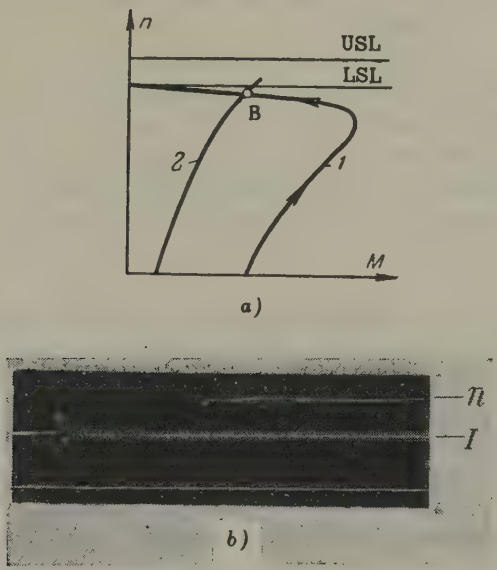

Fig. 6. The starting of induction motors in region V.
(Symbols as in Fig. 3)

In the solution of practical problems connected with the use of series capacitors to compensate voltage drops in distribution networks, attention must be concentrated on the behaviour of induction motors at voltages close to rated voltage, i.e. in region IV.

If the input voltage is increased still further, the self-excitation of the motor again ceases (region V in Fig. 2). The explanation is that the lower boundary of the excitation zone rises above the normal operating point at such high voltages. Typical starting curves and oscillograms of region V are shown in Fig. 6.

Region V begins to narrow and vanish as capacitive reactance is

increased and subsequently the same happens to region II.

If a resistance (the line resistance r_1) is connected in series with the capacitors region III and V widen and then I and IV narrow and disappear altogether.

This is explained by the narrowing of the self-excitation zone when a resistance is included. This agrees well with the theory of parametric excitation. It should however be pointed out that greatly improved results are obtainable by calculating the value of the resistance which will eliminate self-excitation.

However, it should be mentioned that the inclusion of a resistance which is calculated to ensure the desired degree of compensation of the voltage drop τ [7], can only eliminate the self-excitation of a motor at voltages near nominal if the capacitive reactance x_c is no more than about 30 per cent above the short-circuit inductive reactance of the machine $x_{s/c}$.

The flywheel effect of the rotating parts also has an appreciable effect on the nature of self-excitation, particularly in region IV.

Region I is much wider when motors with a fly-wheel are started and region II is pushed up to higher voltages since the flywheel considerably increases the time taken to pass through the self-excitation zone.

A particularly valuable result of increasing the flywheel effect of the rotating parts of a machine is the widening of regions III and V through the narrowing and final disappearance of region IV. The combined effect of a flywheel and resistance is to eliminate self-excitation over a very wide range of input voltages including rated voltage.

By using a flywheel, self-excitation has been eliminated in tests at voltages near nominal for $\tau = 1$ and $x_c = x_{s/c}$, i.e. with complete compensation of the short circuit inductive reactance of the machine. Without a flywheel such a large resistance is required to eliminate self-excitation at voltages near nominal that even with $x_c \approx 0.35\ x_{s/c}$ (see, for example, Fig. 7a) the use of series capacitors was still ineffective when only partial compensation of voltage drop was accepted.

Other methods of calculation have implied that the resistance must be made even larger to eliminate self-excitation.

Fig. 7a shows curves $T_j = f(r_1)$ for two values of x_c in reference to

an A-41-6 type motor where

$T_j = \frac{2.74 GD_e^2 n_{nom}^2 \cdot 10^{-6}}{P_{nom}}$ – equivalent inertia content of a motor with a flywheel, sec;

GD_e^2 – the flywheel torque of a rotor with a flywheel, kg.m^2;

n_{nom} – rated speed of motor, rev/min;

P_{nom} – rated motor output, kW.

These curves define the requisite line resistance r_l for a given inertia constant and vice versa.

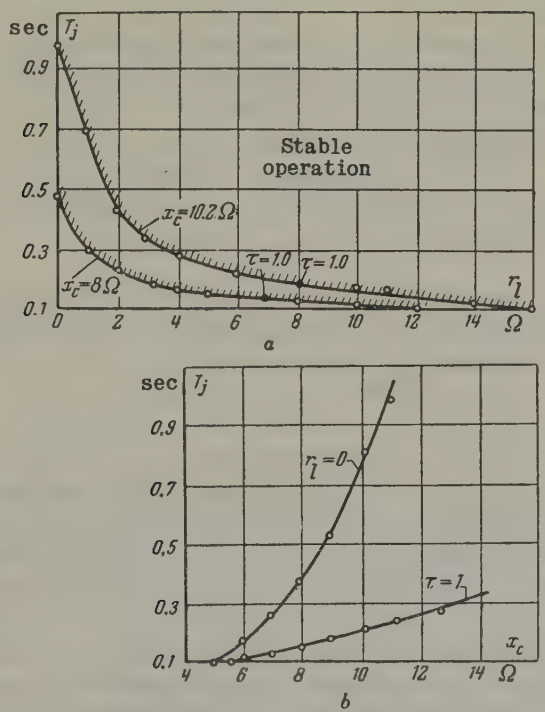

Fig. 7. The inertia constant T_j as function of line resistance r_l (a) and capacitive reactance x_c (b) for A-41-6 type induction motors. Inertia constant of motor T_{jn} = 0.1 sec.

It should be seen from Fig. 7(a) that the elimination of self-excitation is influenced especially and to a considerable extent by a

small additional increase in the inertia constant (relative to the natural inertia constant of the motor). Thus, if $x_c = 0.57\ x_{s/c}$, the elimination of self-excitation is particularly influenced by an increase in the inertia constant within the limits of 0.1 to 0.3 sec. In the case in question it is enough to increase it to 0.2 sec in order to eliminate self-excitation (with complete compensation of the voltage drop).

There are therefore grounds to suppose that in using series capacitors under real conditions there will be no self-excitation of loaded motors at voltages near nominal, even if the capacitive reactance x_c is comparatively large and that the voltage drop will be fully compensated.

Fig. 7(b) shows the inertia constant T_j as a function of x_c for two values of r_l, namely, zero and that corresponding to complete compensation of voltage losses ($\tau = 1$). The regions lying above each curve correspond to normal operation of the motor (no self-excitation). It follows from Fig. 7(b) that an increase in the inertia constant of the machine has a particularly marked effect on the elimination of self-excitation in the presence of line resistance.

The curves in Fig. 7 were obtained for a constant input voltage equal to the rated voltage of the motor $U_{nom} = 380$ V.

Research into the performance of induction motors supplied via capacitive line equipment [8] has also shown that flywheel mass improves the stability of motors.

Conclusions

1. The special features of the self excitation which occurs when a generator is used as a motor have a considerable influence on the nature of the development of self-excitation in asynchronous machines.

The input voltage has the most important effect. Five regions can be discerned in which the development of self-excitation takes a different form depending on the magnitude of the input voltage.

2. The self-excitation of induction motors of the type under consideration is substantially different from what it is generally considered to be in the published literature at rated voltage (region IV in Fig. 2).

Stable oscillation in speed and torque is typical of motors operating

in this region. The resonant speed in this region is very little different from the normal speed of the motor. If the capacitive reactance x_c is increased there is an accompanying reduction of the resonant speed in this region. The current and voltage curves are greatly distorted by oscillation in speed and saturation of the steel.

3. A line resistance r_l assists the elimination of self-excitation by narrowing the fourth region of self-excitation.

But if $x_c > 0.3\ x_{s/c}$, the requisite value of r_1 to eliminate self-excitation is still inadequate to compensate fully the voltage drop in the line.

4. An additional flywheel effect also helps to narrow the fourth region, i.e. to eliminate self-excitation at rated voltage.

Unloaded induction motors are more inclined to self-excitation at the rated input voltage than loaded motors.

The influence of the additional flywheel effect is particularly significant if a line resistance is included.

Translated by O. Blunn

REFERENCES

1. J.W. Butler and C. Concordia; *El. Eng.* No.8 (1937).
2. C.F. Wagner; *Trans. Amer. Inst. elect. engrs.* Vol. 60 (1941).
3. P. Satche; *Bull. Soc. franc. Electr.*, 7 (1951).
4. N. Knudsen; *ASEA J.*, 5-6 (1954).
5. A.I. Dolginov; *Resonance in electrical circuits and systems, (Rezonans v elektricheskikh tsepiakh i sistemakh).* Gosenergoizdat, (1957).
6. V. Laion; *Analysis of transient phenomena in electrical s.c. machines, Analiz perekhodnykh protsessov v elektricheskikh mashinakh peremennogo toka).* Gosenergoizdat (1958).
7. V.G. Bauman, O.V. Ivanov and B.I. Komarov; *Nauch. dokl. vyssh. shol.*, (ser. Gornoe delo), No.4, (1958).
8. D.N. Bulashevich and V.D. Yurenkov; *Capacitive off-take of power from transmission lines, (Emkostnyi otbor moshchnosti ot linii elektroperedachi).* Gosenergoizdat (1959).

DIRECT TESTING OF CIRCUIT BREAKERS BY THE JOINT USE OF SURGE GENERATORS AND GOREV OSCILLATORY CIRCUITS*

Ya.N. SHERMAN

(All-Union Electrical Engineering Institute, Leningrad)

(Received 18 November 1961)

In recent years Gorev oscillatory circuits have come to be used on a large scale in the U.S.S.R. as the short circuit power source for rupturing capacity tests on high-duty circuit breakers. In these oscillatory circuits the necessary energy for the tests is stored in a large bank of static capacitors.

Experience has shown that high-voltage test laboratories require two or three synchronous surge generators with an equivalent three phase short circuit power of 2.5 to 3.5 thousand MVA and a Gorev oscillatory circuit with an equivalent three phase short circuit power of 2 to 2.5 thousand MVA. This equipment is used for synthetic tests in which the surge generators are the current source and the oscillatory circuit the recovery voltage source.

It is also possible to make direct tests in which the power of the surge generator and that of the oscillatory circuit are used separately. It would however be very useful to combine their individual powers in direct tests.

The only combined systems [1] which have as yet been proposed for direct tests use the active power of the surge generator circuit. No provision has been made for adding the reactive power of the two source

---

* *Elektrichestvo*, 5, 52-57, 1961.

However, research at the Leningrad branch of the All-Union Electrical Engineering Institute since 1956 has solved this problem by connecting the surge generator either in series [2] or in parallel [3] with the oscillatory circuit. It will be shown that the decay of the test current can be compensated either by the active power of the generator or by a method of "pulsation".

The special switchgear which has been developed in the U.S.S.R. in recent years has now made it possible to combine a surge generator with a Gorev oscillatory circuit for direct tests. The new switchgear includes a controlled spherical discharger (U.Sh.R), an automatic test control device (PAU) and a synchronous switch VA-12.

Connexion in series

Fig. 1 illustrates the main test circuit with the generator connected in series with the oscillatory circuit.

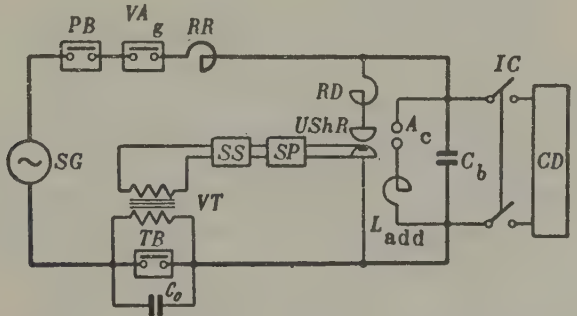

Fig. 1. Main test circuit for combined use of surge generator and Gorev oscillatory circuit connected in series:

SG – synchronous surge generator; C_b – main capacitor bank of oscillatory circuit; *RR* – reactor; *TB* – test breaker; *PB* – protective breaker; *VA* – synchronous switch (*g* – generator); *IC* – interrupter for charge circuit; *CD* – charging device of oscillatory circuit; A_c protective gap (arrester); L_{add} – additional protective inductance; *RD* – reactor which is connected to capacitor bank; *SS* – electronic synchronization system; *USHR* – new controlled spherical discharger; *SP* – ?; *VT* – voltage transformer

The circuit in Fig. 1 is similar to the circuit published previously in this journal [4], but it includes an extra reactor *RD* which is connected to the capacitor bank by means of the controlled spherical discharger (U.Sh.R) and the electronic synchronization system *SS* (immediately after the arc has been quenched in the circuit breaker on test. The inductance of the reactor *RD* is such that a current of supply frequency (50 c/s) flows in the circuit C_b – *RD* on closure of the spherical discharger (C_b - bank capacitance). Consequently, after the arc has been quenched in the test breaker *TB*, the capacitor voltage is cosinusoidal in shape and, in view of this, the recovery voltage at the terminals of the test breaker, equal to the sum of the generator e.m.f. and the voltage at the capacitor bank C_b, will also have the conventional cosinusoidal shape.

Best use is made of the equipment by connecting the capacitor bank, surge generator and test breaker in the test circuit through power transformers.

To achieve maximum test power the system must operate normally and this requires initially that the amplitude of the free oscillations should vanish completely (provided compensation is not used for damping the test current). It will be seen from expressions A1 and A2 in the appendix that this condition is satisfied if the initial capacitor voltage (U^*_{C0}) equals the amplitude of the voltage drop on the capacitance from the forced component of the current and if the phase of the connexion ψ^*_e equals the phase angle between the forced current component and the generator e.m.f., i.e. if (including the change in sign)

$$U^*_{C0} = -U_{C\ \max} \tag{1}$$

and

$$\psi^*_e = -\beta. \tag{2}$$

But if the attenuation of the test current is to be compensated, the initial conditions have to be slightly different from 1 and 2. They are selected in such a way that the decay of the test current is reduced owing to the presence of a transient component of frequency reduction.

The series method of connexion also allows an increase in test current when the self-reactance of the bus-bars or the dynamic stability of the generator are the limiting factors. The self-reactance of bus-bars can be compensated by the capacitor bank C_b.

Overvoltages can occur at the capacitor bank if conditions 1 and 2

are not satisfied at the beginning of the test. Protection is provided by arranging a gap (an "arrester") $A_{s/c}$ in parallel with the bank which shorts the bank, or else, (to reduce the discharge current), closes it through an additional inductance L_{add}, which produces a high frequency current in the discharge circuit. It has been shown by calculations and tests that the fault current is no larger than the maximum short-circuit current of the surge generator.

Trial rupturing capacity tests have been carried out on VMG-133 type circuit breakers at breaking currents of 10 and 20 kA and a voltage of 10 kV in order to assess the merits of the system and to check the design formulae.

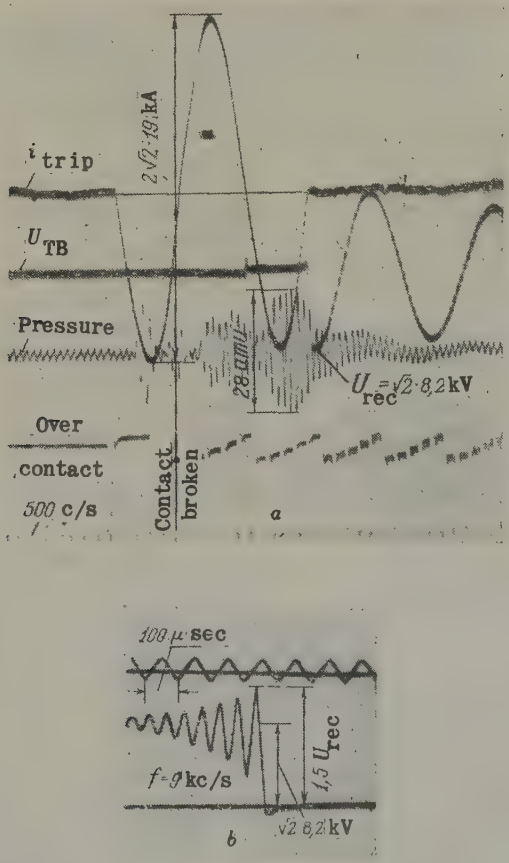

Fig. 2. Magnetic (a) and cathode-ray (b) oscillograms of direct test on a VMG-133 type circuit breaker with the surge generator and oscillatory circuit connected in series. i_{trip} – tripping current; U_{TB} – voltage at the terminals of the test breaker.

A TI-12 type generator was excited to 6 kV for the tests. The capacitor bank was connected to the test system via an intermediate transformer. The voltage across the secondary winding of the transformer was 4 kV (20 kV on the capacitor side). The bank incorporated 32 capacitors (type KM-30-19) for test currents of 20 kA and 16 capacitors of the same type for 10 kA.

Fig. 2 shows oscillograms taken during tests at 20 kA.

The tests showed that the proposed method is only slightly more complicated than the conventional system and that good agreement exists between test and calculated data.

Not only does the series system allow the summation of power, the compensation of stray inductance and the damping of the short-circuit current, but it also makes the best possible use of the available test equipment, thereby providing additional power for testing.

Connexion in parallel

Fig. 3 illustrates the parallel method of connexion. The test plant includes a surge generator, a Gorev oscillatory circuit and the breaker test. The test method is as follows. First the surge generator is excited to the required voltage $e_g = E_{max} \cos(\omega t + \psi_e)$. At the same time the capacitor bank is charged to the voltage $U_{C0} = E_{max}$. Then, with the test breaker connected and the phase of the generator voltage ψ_e^* equal to $-\tan^{-1}\frac{R_{e.g.}}{\omega L_g}$ (so that there will be no aperiodic component in the generator current), the generator circuit is closed by the new synchronous switch VA_g for the generator. At the same or a slightly later time an oscillatory circuit switch X_{oc} makes the oscillatory circuit and the extreme branches of the scheme begin to carry the generator current i_g and the oscillatory circuit current i_{oc}, and the branch of the test breaker TB carries the total current i. To achieve complete equivalence in the tests it is necessary for the oscillatory circuit current to attain its zero value slightly after the generator current in the half-period when the arc is quenched in the test breaker*. The total current i then attains zero slightly after the generator current (at the moment

* This can be achieved by slightly reducing the frequency of the oscillatory circuit current compared with that of the generator current or by switching on the oscillatory circuit current slightly after the generator current. Both methods can also be used at the same time.

when the instantaneous values of i_g and i_{oc} are compared).

After the arc has been quenched in the test breaker, the series-connected (sic) generator and oscillatory circuit from a single closed circuit which carries a small balancing current i_b. This current i_b attains zero a few hundred microsec after the arc has been quenched in the test breaker and at this point is interrupted by the "tripping device" TD_{oc} of the oscillatory circuit which is arranged to operate at the precise moment when this will ensure the quenching of the arc in the corresponding half-period of current. In the tests this "tripping device" was either a special breaker or the second pole of the test breaker.

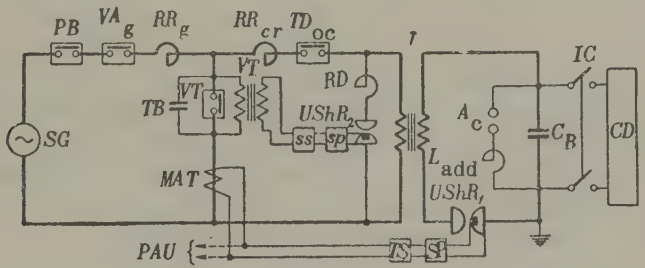

Fig. 3. Main circuit for combined use of surge generator and Gorev oscillatory circuit connected in parallel.

Legend as in Fig. 1 plus *MAT* – master air-cored transformer; *TS* – trigger scheme; *TD* – tripping device (oc = oscillatory circuit): *T* – transformer; *PAU* – new automatic test control device.

When the arc has been quenched in the test breaker, the voltage begins to recover at its terminals at a rate determined by the equivalent inductance of the whole scheme and the capacitance of the bank C_b. Before the arc is quenched in the oscillatory circuit tripping device TD_{oc}, the recovery voltage has an intermediate value between the generator e.m.f. and the voltage on the main capacitor bank; after the arc has been quenched in TD_{oc}, it becomes equal to the generator e.m.f. Since the system has been tuned so that e_g and u_c are close to each other in value, it can be assumed that the recovery voltage is equal to the generator e.m.f. Here the test power of the plant equals:

$$P_{s/c} = I_{trip}U_{rec} = (I_g + I_{oc})U_{rec} = P_g + P_{oc}.$$

Thus, the power of the oscillatory circuit and generator are also

added if the parallel system is used.

The current is controlled by means of the reactors RR_g and RR_{oc}. Since both branches operate independently in a given system when the test breaker is connected, the maximum total current depends on the power of the sources at the given voltages.

The "tripping device" TD_{oc} can either be the second pole of the test breaker or a special breaker. It should be mentioned that another function of the oscillatory circuit tripping device is to serve as a protective breaker to interrupt the oscillatory circuit current in the event of "disruption" of the test breaker (or failure in quenching), its main function of course being to disconnect the balancing current i_b.

The system just described can be regarded as the basic circuit. Direct tests may also be carried out under other conditions with the generator current reaching zero *before* the oscillatory circuit current in the half-period when the arc is quenched in the test breaker. In this case a generator tripping device should be included TD_g for which the laboratory protective breaker *PB* may be used.

After the arc has been quenched in the test breaker and then in the generator tripping device TD_g, the recovery voltage at the terminals of the test breaker is equal to the voltage of the main capacitor bank. To impart the same sinusoidal shape to it as in the series system, the capacitance C_b is connected to the shunt reactor *RD* by the controlled spherical discharger U.Sh.R. directly after the interruption by the generator tripping device TD_g.

However, a detailed theoretical and experimental study of the conditions of the first passage of the balancing current i_b through zero has shown that this modification is not so stable in operation as the fundamental system. Extra equipment (the shunt reactor, the new controlled spherical discharger etc) is also required. The basic system is therefore to be preferred.

The following factors should be considered when adjusting (tuning) the circuit. The instant the arc is quenched in the test breaker, the current in the branch where the "tripping device" is installed must only pass through zero after the total current has done so. Otherwise the branch containing the tripping device can be disconnected before the total current i attains zero and a kink will therefore occur in the curve for the total current immediately before it passes through zero. Moreover, since one of the branches will be disconnected before

the total current i passes through zero, the rate of voltage recovery will depend solely upon the inductance of a single branch and not on the equivalent inductance of the whole scheme.

The capacitors are protected from the surges which may arise if the tripping device fails to quench the arc, by a protective gap (arrester) A_c which connects the bank C_b to the reactance L_{add}.

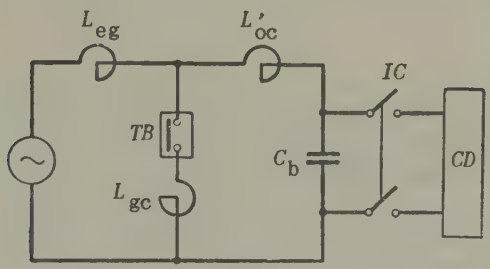

Fig. 4. Main circuit of generator and oscillatory circuit in parallel with an inductance to compensate current attenuation.

L_{gc} – coupling inductance; TB – test breaker; C_b – capacitor bank; CD – charging device; IC – interrupter for charge circuit; L_{eg} – inductance of generator; L'_{oc} – inductance of oscillatory circuit part.

For tests on 6-10 kV breakers, the capacitors of the oscillatory circuit may be connected via step-down transformers T (Fig.3). For tests on breakers over 10 kV the generator, or generator and oscillatory circuit, are connected to the test breaker via transformers. The oscillatory circuit is then connected by the controlled spherical discharger which is operated by a special control system consisting of a master air-cored transformer MAT and a trigger scheme TS which operates the controlled spherical discharger almost immediately after the current begins to flow through the test breaker (after 100 to 500 μ sec). It is not possible to use the same conventional spherical discharger for the parallel system as for the series system [4] since the voltage of the capacitor bank U_{CO} is applied to this discharger both before and after the new synchronous switch VA_g has operated.

Compensation of the test current

When testing circuit breakers with long arcing times, the efficiency

of the proposed method is adversely affected by the decay of the test current. In the proposed parallel system this is aggravated by the increased attenuation of the current in the oscillatory circuit. The decay of the test current can be reduced by pulsation (the "beat" method) or by compensating power losses.

The "pulsation" method is based on the addition of two sinusoidal oscillations at close frequencies. Since the test current i is the sum of two sinusoidal currents (i_g and i_{oc}), it follows that the frequency of the current in the oscillatory circuit can be so selected and the connexion of the oscillatory circuit to the test circuit so timed that a non-decaying or even increasing test current can be produced in part of the test breaker circuit [5,6]. The best possible use is obtained from the equipment if the current in the oscillatory circuit is greater than 50 c/s. This involves no alteration in the test plant because the command from the controlled spherical discharger can be delayed as required by the new automatic test control device *PAU* or by installing an electronic time relay between the trigger scheme *TS* and the *SP* device.

In the other method of compensation a small coupling inductance $L_{g.c.}$ (Fig. 4) is connected in the test breaker circuit which compensates the losses in the oscillatory circuit by the active power of the generator in the same way as in tuned circuits described by Lugovoi [1]. The best result is obtained by adjusting the system so that both methods of compensation can be used.

The system has been proved in the high-voltage test laboratory at the All-Union Electrical Institute in Leningrad.

The second pole of the VMG-133 circuit breaker on test was used as the tripping device TD_{oc} to study the basic circuit, and the laboratory protective breaker to study the modified circuit. Figs. 5 and 6 show magnetic and cathode oscillograms which illustrate the performance of the system for basic and modified connexions.

The tests confirmed the theoretical conclusions and showed that there is practically no difference between the tuning of the parallel system and the tuning of conventional systems with a generator.

Appendix 1.
Formulae for series system of connexion

In the analysis the real generator is replaced by an equivalent generator with an e.m.f. e_g, which decays with a time constant

$\frac{1}{\alpha}$, and a super-contact reactance (literally, a super-transfer resistance) x''_d. The generator e.m.f. is re-written in the form:

$$e_g = E_{max} \cos(\omega t + \psi_e) e^{-\alpha t},$$

where α is a coefficient which is found experimentally from the attenuation of the symmetrical component of the short circuit current in a conventional inductive circuit.

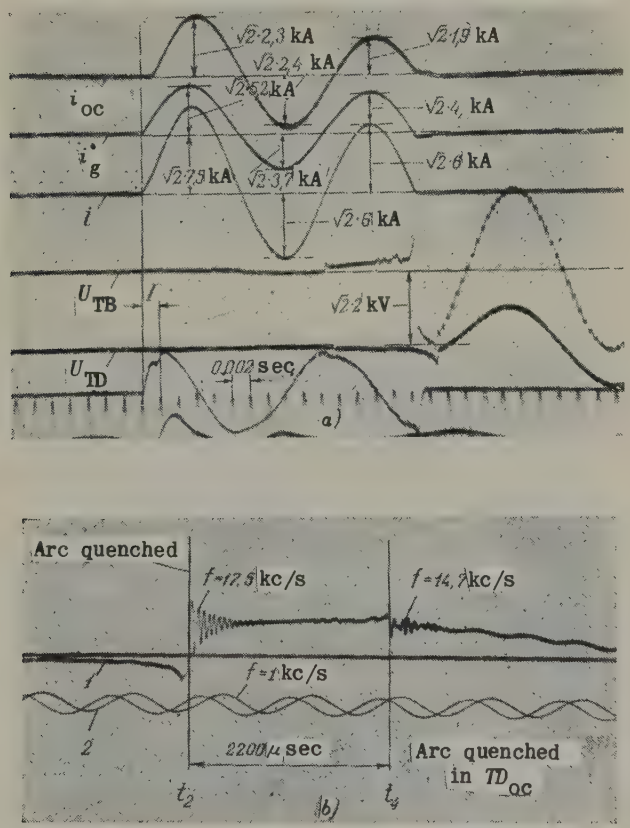

Fig. 5. Magnetic (a) and cathode-ray (b) oscillograms of direct tests on a *VMG*-133 type circuit breaker in the basic parallel system.
i_{oc} – oscillatory circuit current; i_g – generator current; i – test current; U_{TB} – voltage at terminals of test breaker; U_{TD} – voltage at terminals of test breaker *TB*; 2 – graduated frequency.

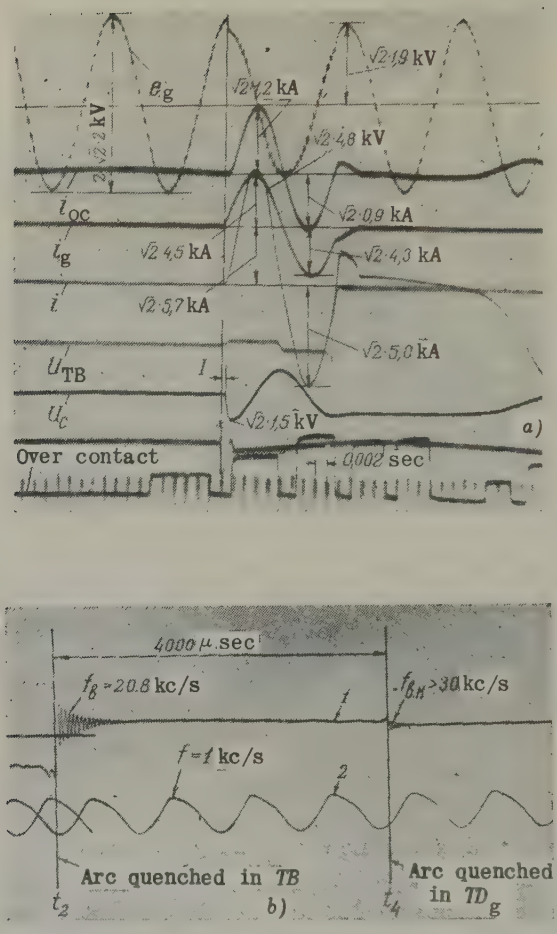

Fig. 6. Oscillograms of tests on a VMG-133 circuit breaker in the modified system (Notation as in Fig. 5)

On the stated assumption, the total current i in the test circuit, the voltage drop in U_C at the capacitor bank, and the recovery voltage U_{rec} can be found from the following expressions:

$$i = I_{max} \sin(\omega t + \psi_e + \beta) e^{-\alpha t} + \\ + I_{max} \sqrt{\frac{k}{k+1}} N \cos(\omega_0 t + \theta) e^{-\delta t}; \quad \text{(A1)}$$

$$u_C = U_{C\ \max} \cos(\omega t + \psi_e + \beta)\, e^{-\alpha t} - \\ - U_{C\ \max}\, N \sin(\omega_0 t + \theta)\, e^{-\delta t}; \tag{A2}$$

$$u_{\text{rec}} = [E_{\max}\, e^{-\alpha \tau_k} \cos(\omega t + \beta) + \\ + U_{C0}\, e^{-\alpha \tau_k} e^{-\delta' k t_v} \cos \omega t](1 - e^{-\delta_{hf} t_v} \cos \omega_v t), \tag{A3}$$

where

$$k = \frac{P_{oc}}{P_g};\quad I_{\max} = \frac{E_{\max}}{\omega L_{e.g}};\quad U_{C\ \max} = \frac{I_{\max}}{C_{oc}} = \\ = kE_{\max};\quad L_{e.g} = \frac{x_g + x_{sh}}{\omega};$$

$$N = \sqrt{\frac{k+1}{k} \sin^2(\psi_e + \beta) + \left[\frac{U_{C0}}{U_{C\ \max}} + \cos(\psi_e + \beta)\right]^2};$$

$$\beta = \arctan \frac{2(\delta - \alpha)(1 + k)}{\omega};$$

$$\theta = \arctan \frac{\dfrac{U_{C0}}{U_{C\ \max}} + \cos(\psi_e + \beta)}{\sqrt{\dfrac{k+1}{k}} \sin(\psi_e + \beta)};$$

$$\omega_0 = \frac{1}{\sqrt{(L_{oc} + L_{eg})\, C_{oc}}} = \sqrt{\frac{k}{k+1}}\, \omega;$$

$$L_{oc} = \frac{1}{\omega^2 C_{oc}};$$

$$\delta = \frac{R_l}{2(L_{e.g} + L_{oc})};$$

$$\omega_v = \frac{1}{\sqrt{(L_{oc} + L_{e.g})\, C_0}};$$

δ_{hf} – the decrement in attenuation of the high frequency component;

τ_k – the length of time that the test current flows;

δ'_k – the decrement in attentuation of the current in the capacitor bank – reactor circuit ($C_b - RD$);

t_v – time from the moment the arc is quenched;

L_{eg} – inductance of the surge generator part;

L_{oc} – inductance of the oscillatory circuit part;

Formula for the parallel system. The generator current i_g and

oscillatory circuit current i_{oc} can be found from the formulae

$$i_g = \frac{E_{max}}{\omega L_{eg}} \sin(\omega t + \psi_e + \varphi)\, e^{-\alpha t}; \tag{A4}$$

$$i_{oc} = \frac{U_{C0}}{\omega L_{oc}} \sin \omega t\, e^{-\delta_k t}. \tag{A5}$$

The recovery voltage, without including power losses, can be found from the expression:

$$u_{rec} = \left[U_{C0} + (E_{max} - U_{C0}) \frac{L_{oc}}{L_{eg} + L_{oc}}\right](1 - \cos \omega_v t). \tag{A6}$$

The balancing current i_b and capacitor voltage U_C can be found by transforming expressions A1 and A2 to suit the parallel system:

$$u_C = -\frac{E_{max}}{n} \cos(\omega t + \xi)\, e^{-\alpha t} + \\ + E_{max}\left(1 + \frac{\cos \xi}{n}\right) \cos \omega_0 t\, e^{-\delta t}; \tag{A7}$$

$$i_b = I_{max.g} \sin(\omega t + \xi)\, e^{-\alpha t} - \\ - \frac{1}{\sqrt{1+n}}\left(1 + \frac{\cos \xi}{n}\right) \sin \omega_0 t\, e^{-\delta t}, \tag{A8}$$

where $I_{max.g} = \dfrac{E_{max}}{\omega L_{eg}}$;

$n = \dfrac{P_{oc}}{P_g}$

$\xi = \sin^{-1} \dfrac{i_{b.0}}{I_{max.g}}$ – the phase angle between i_g and i;

i_{b0} – the initial value of the balancing current which is equal to the instantaneous value of i_g at the moment the arc is quenched in the test breaker.

Translated by O. Blunn

REFERENCES

1. V.S. Lugovoi; *Tuned circuits with loss compensation, (Rezonansnye kontury s mompensatsiei poter')*. Izvest. Akad. Nauk Kirgiz. SSR,

No. 1, (1955).
2. V.V. Kaplan and Ia.N. Sherman; *Method of testing high-voltage circuit breakers, (Sposob ispytaniia vysokovol'tnykh vykliuchatelei).* Soviet Patent No. 122546, 10 June 1959).
3. Ia.N. Sherman; *Method of testing the rupturing capacity of high duty switchgear, (Sposob ispytaniia apparatov vysokogo napriazheniia na otkliuchaiushchuiu sposobnost').* Soviet Patent No. 133523, 14 December(1959).
4. Ia.N. Sherman; *Elektrichestvo,* 7, (1959).
5. V.V. Kaplan and V.M. Nashatyr'; *Elektrichestvo,* No.7, (1957).
6. Ya.N. Sherman; *Device for testing the rupturing capacity of high duty switchgear, (Ustroistvo dlia ispytaniia kommutatsionnykh apparatov vysokogo napriazheniia na otkliuchaiushchuiu sposobnost').* Soviet Patent No. 673091/24, 14 July 1960.

THE NEW NINE-VALVE SIX-PHASE RECTIFIER UNITS*

L.S. FLEISHMAN

(Uralelektroapparat)

(Received 31 January 1961)

Some time ago the electrical works "Uralektroapparat" in the U.S.S.R. made a large 3300 V 12-valve rectifier unit for Soviet railways which was quite original in that two valves were connected in series in each phase. Its rated output was 10,000 kW and this compared very favourably with foreign 24-valve units with rated outputs of up to 8000 kW. Furthermore, it was as efficient as any other existing unit, it saved material (5.3 kg per kW instead of 7 to 13 kg per kW) by the greater output of the individual valves, and only one TMR U-6200 type transformer was required instead of three of four TMRU – 1600 type transformers [2].

One of these units has been in service for two and a half years at a traction sub-station on the Omsk railways and no arcbacks have occurred. The average daily output was 8350 kW and the peak output 16,000kW. The average output over five-hour periods of continuous operation was 12,000 kW. More than a hundred such units are now in use on the railways and arcbacks have been almost completely absent.

However, experience has shown that these units have excess capacity as regards valve strength and current. This could be used to increase rated outputs up to 15,000 and 20,000 kW, but there is no demand for such large units. It is therefore proposed to take advantage of the increase in power and improved reliability and produce low cost rectifier units which can also be used in other branches of industry [1]. The results of tests on the new nine-valve unit [3] are given below.

---

* *Elektrichestvo*, 5, 58-62, 1961.

The main circuit of the nine-valve unit is shown in Fig. 1(a). It will be seen from a comparison of this circuit with that of the original twelve-valve unit in Fig. 1(b) that each valve of the cathode group in the twelve-valve unit is supplied from two valves in the anode group. The performance of the valves is illustrated in Fig. 2, from which it will be seen that the valves of the cathode group conduct current twice in each period so that the mean value of the current in these valves is twice that in the valves of the anode group. The reverse voltage is also applied to each valve in the anode group twice in each period for a time defined by the angle $(60-\gamma)^{\circ}$.

The reliability of the two systems will now be considered.

If a cathode spot occurs on the anode of a valve in the cathode group, an arcback current can only flow if the cathode spot arises simultaneously (more exactly, within the limits of the time of the existence of the cathode spot) on one of the anodes of two valves in the anode group connected to it. Consequently, the probability of arcbacks in the twelve-valve or nine-valve unit is definable as the product of the probabilities of cathode spots occurring on series-connected valves [4].

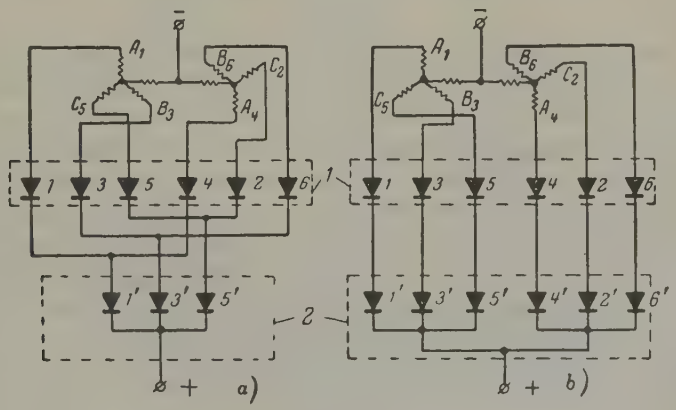

Fig. 1. The nine-valve (a) and twelve-valve (b) rectifier systems. *1* – anode group of valves; *2* – cathode group of valves.

However, other things being equal, arcbacks are only half as likely in the nine-valve unit because an arcback will occur in the twelve-valve unit if a cathode spot should occur say on the anode of valve *1'* and simultaneously on valve *1*, whereas in the nine-valve unit the

cathode spot must occur on the anodes of valves *1* and *4**.

If the cathode spot first arises on the anode of a valve in the anode group, say the anode of valve *1*, then the other valves except *4*, which is in counter-phase with it, can only take part in the arcback if a cathode spot also arises on the anode of the valve *1'*. Consequently, even in this case, the probability of an arcback is definable by the product of the probabilities of cathode spots on the anodes of series-connected valves. But valve *4* is a different matter which must be considered in more detail.

Suppose a cathode spot occurs on the anode of valve *1* at the instant t_1. Valve *4* cannot feed the anode of valve *1* before the moment t_2 since its anode still has a negative potential (Fig. 2a). After the instant t_2 valve *4* cannot feed valve *1* if a control pulse is fed to the grid of anode *4* at the instant t_3 at a slightly advanced angle relative to the natural angle of ignition. This condition has to be satisfied by an appropriate phasing of the pulses relative to the anode voltage with the angle advanced between 3 and 5°, as read from the instant t_3. Partial arcbacks will only occur if the cathode spot on the anode of valve *1* occurs after the anode of the counter-phase valve has fired, or if the cathode spot precedes the firing of the counter-phase valve.

In rectifiers with controlled grids, by far the largest majority of arcbacks occur on the "front" of the reverse voltage [5]. Some experts consider that arcbacks other than on the front of the reverse voltage are only possible if the vacuum is bad [6]. The commutation angle is about 45° for actual commutating inductances and overloads of 4500 A so that the angle is behind about 15° up to the moment the counter-phase valve is ignited. However, there is very little time for cathode spots to exist if there is no supply of energy. Consequently, there is practically no difference in reliability between the twelve-and nine-valve units if the cathode spot occurs on the front of the reverse voltage**. Only in relatively rare cases when cathode spots occur with the "amplitudinal" value of the reverse voltage across the valves in the anode groups will partial arcbacks take place.

---

* It is assumed that the probability of arcbacks on the three valves of the cathode group in the nine-valve unit is equal to that on the six valves of the cathode group in the twelve-valve unit, for the valve current is the same in value in both units.

** In principle the probability of an arcback in twelve-valve units is 1.5 to 2 times less, but this difference has no practical importance in series-connected systems.

The full and partial arcback currents will now be compared.

Utevskii has shown that the arcback currents of three-phase rectification systems can be determined by the following differential equation which holds good if the anode on which the cathode spot arises is only supplied by one valve:

$$\sqrt{3}U_{max}+2L_a\frac{di}{dt}+2r_a i=0,$$

where U_{max} is the maximum value of the phase voltage, L_a the inductance of the phase, and r_a the resistance of the phase.

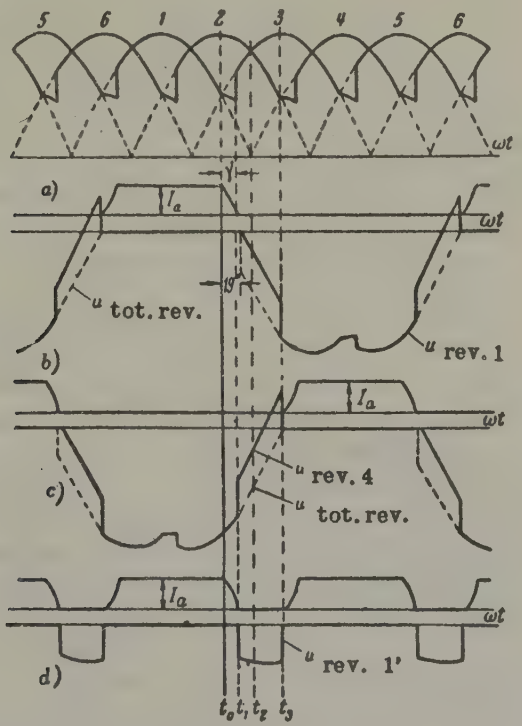

Fig. 2. Curves of the rectified voltage (a) and the anode currents and reverse voltages of valve *1(b)*, valve *4(c)* and valve *1'* in the cathode group (*d*).

With a partial arcback, the arcback current is found from the equation

$$2U_{max}+4L_a\frac{di}{dt}+2r_a i=0.$$

The impedance of balancing reactors and the arc voltage of the valves can be ignored. The four fold value of the circuit inductance is explained by the fact that the partial arcback current flows through transformer windings which are disposed on the common core of a magneti circuit and, consequently, their total reactance is proportional to the square of the number of turns*.

Full arcback currents may be calculated by Utroskii's equations [7].

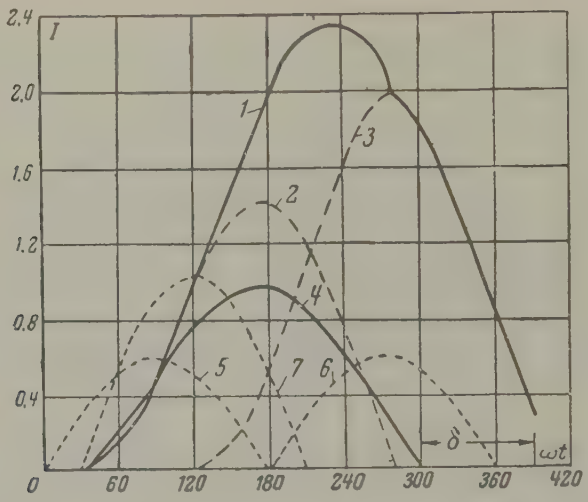

Fig. 3. Full and partial arcback currents.

1 – full arc-back current; *2* and *3* – components of the full arc-back current; *4* – partial arc-back current; *5* and *6* – anode phase voltages determining the partial arc-back current; *7* – line voltage determining the first component of the full arc-back current.

The relative values of full and partial arcback currents are shown in Fig. 3. It will be seen that the current of a partial arcback is about 40 per cent that of a full arcback and, consequently, the e.m.f.' acting on the transformer windings are reduced to about 16 per cent.

It should also be mentioned that with partial arcbacks the current and e.m.f.'s are also substantially reduced by the zero sequence impedance which appears due to the current flowing through the transform

* Secondary windings of transformers are made so that their leakage fluxes can be ignored.

windings on a single core when the primary windings are star-connected.

The curves in Fig. 3 also show that the current of a partial arcback is maintained for about 270° under the most unfavourable conditions for which arcbacks can occur. The intermittent nature of the current must be due to the automatic-elimination of partial arcbacks during a time less than one "period" which prevents breaks in the supply of energy.

It is worthwhile studying the distribution of the total reverse voltage between the series-connected valves in the nine-valve system. Fig. 2 shows the reverse voltages as calculated by formulae obtained from the equivalent network in Fig. 4 for the condition when all the valve impedances are equal. In the calculation it has to be borne in mind that the valve cannot sustain the forward voltage for a period of time equal to that taken for the control capacity of the grids to recover. Therefore, as will be seen from Fig. 2, the reverse voltage on valves in the anode group at commutation angles less than 19° appears gradually and even with a slight delay. The curves have been corroborated by oscillograms taken on a scale model using T-235 type thyratrons. In water-cooled mercury arc rectifier systems the cathode valves are shunted by the resistance of the water and, as a result, the reverse voltage diminishes and slightly alters the shape of the reverse voltage on the anode and cathode valves.

It is already known that each cathode valve conducts current twice in each period and therefore two triggering pulses are also required in each period. Fig. 5(a) shows how this can be done by a grid circuit with a peaking generator. Two impules are supplied in each period by connecting the counter-phase windings of the peaking generator in parallel via semiconductor rectifiers which suppress the negative impulse. The grids of the valves in the anode group are supplied in the conventional way. Fig. 5(b) shows a simplified system using a grid transformer (the control impulses are sinusoidal).

The circuit impedances must be made such that the arcing of the grid extends about 120° for each half-wave of voltage.

In addition to tests on scale models, tests have also been carried out in the works laboratory and by the Omsk and October railways jointly with the MPS Central Research Institute on the automatic elimination of artificial partial arcbacks. Ordinary service tests have also been made.

The artificial partial arcbacks were produced by firing a valve which was connected "counter-parallel" to one of the anode valves. The tests

showed that no partial arcback current flowed when firing the counter-parallel valve in the period of time t_2-t_0. On applying a triggering impulse to the grid of the counter-parallel valve, a partial arcback current only began to flow after the instant t_2. Its maximum value reached about 8350A. The partial arcback current roughly corresponded to an angle of 270°. Under the same conditions, full arcback currents were about 22,000 A. In these tests the rectifier was supplied from two TMRU-6200 type transformers with delta primary windings.

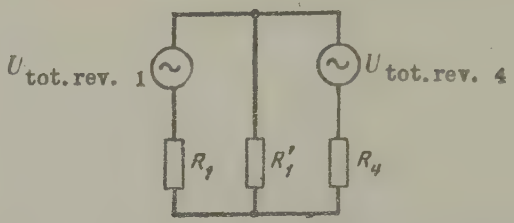

Fig. 4. Equivalent circuit for the distribution of the reverse voltages.

In a second series of tests the partial arcback currents reached 4200 A with the rectifier again supplied from the same transformers with delta windings. The large difference in the partial arcback currents can be explained by the fact that the TMRU-6200 transformer in the second test was supplied through a TDNG-15,000/110 step-down transformer the reactance of which further reduced the current.

As soon as the partial arcback current began to flow, the total reverse voltage was applied to one of the valves in the cathode group when it was conducting. When such units are used on electric railways the valve receives a reverse voltage of 7500 V at currents of 2000 A or more. If the conditions are so severe that the valve cannot sustain them even for one period, the partial arcbacks will change into full arcbacks and the multiplication rule for the probabilities will no longer be valid. The capacity of cathode valves to sustain such conditions was tested by artificial partial arcbacks in a "contact network" (with overhead wires?) at loads up to 3000 A. Fig. 6 shows one of the oscillograms of artificial partial arcbacks caused at the instant when the reverse voltage was initially a maximum.

Several dozen artifical partial arcbacks were produced in all, and in every case they were automatically eliminated, i.e. they took place without causing any of the protective gear to operate and without disconnecting the unit.

The service tests on the reliability of the unit were carried out in April 1960. The test unit was composed of two ARMNV-750 x 6-P rectifiers assembled according to the nine-valve system. The unit was tested for 140 hrs. Its mean output was 5,700 kW, and its peak hourly output 10,000 kW. The largest current reached 3600 A.

During the tests 15 partial arcbacks were registered and all were automatically eliminated. There were no full arcbacks.

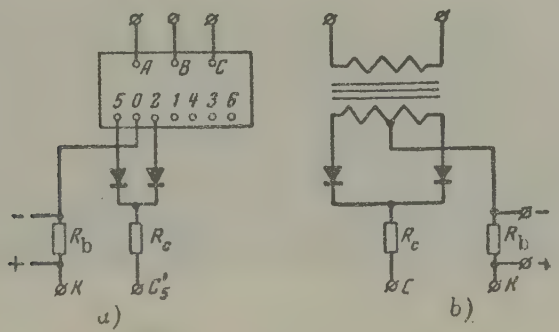

Fig. 5. System of supplying control pulses to valves in the cathode group.

The same unit was subjected to another series of tests in July 1960 in order to check whether the probability of partial arcbacks could be reduced further and to accumulate more experience of service conditions. On this occasion the angle of advance of the grids in the anode group of valves was reduced by about 15° to roughly 5°. The mean output of the unit rose slightly to 5860 kW. A lengthy period of service (over 900 hrs) showed that its overload capacity was high. The peak rectified current reached 4500 A and the hourly output 12,000 kW. The temperature was held at 30 to 45° C during service. Five full arcbacks occurred at intervals of a few hours during the service tests. In every case it was found that the flow of water had ceased through some of the valves owing to air locks but there were no full arcbacks after changing over to different heat exchangers. There were also five partial arcbacks and three were automatically eliminated. In the other two cases the partial arcbacks were accompanied by the tripping of the oil circuit-breaker; the high-speed cathode breaker, polarized to the reverse current, remained connected. These two cases can apparently be explained by the re-occurrence of partial arcbacks in two adjacent periods on the same or other anodes of valves in the anode group.

It is important to point out that no full or partial arcbacks

occurred during maximum loads, which is further evidence of the high overload capacity of the unit. The service tests showed that a reduction in the angle of advance from about 20 to 5° reduced the frequency of arcbacks by more than an order of one.

Fig. 6. Oscillogram of an artificial partial arc-back:

1 – impulse triggering the counter-parallel valve; 2 – the partial arc-back current; *3* – the total reverse voltage.

Conclusions

1. The nine-valve rectifying system permits the development of rectifier units on the basis of the existing RMNV-type valves with a rated output of 10,000 kW and a voltage of 3300 V which are capable of operating at hourly outputs of 12,000 kW with peak outputs of 15,000 kW. The majority of traction sub-stations may therefore be equipped with one large unit which considerably reduces costs.

2. Compared with the twelve-valve units, the new system saves about 25 per cent on the weight of the rectification plant and control cabinet without affecting the rated output or overload capacity of the unit. The efficiency of the nine-valve unit when operating with TMRU-type transformers is hardly inferior to that of the twelve-valve unit and at loads of 0.75 or less its efficiency is higher than that of units without valves connected in series.

3. The rated mean output of each valve in the nine-valve unit is

1100 kW compared with 825 kW for the twelve-valve system and 333-412 kW for foreign units.

The new unit is also more reliable than foreign units.

4. There is no real disadvantage involved in designing the valves in cathode group for currents double those in the anode group, at least as far as voltages of the order of 3000 V are concerned, since valves are only required for mean currents of approximately 1000 A. It will be appreciated that there is no great difficulty involved in producing such valves if it is borne in mind that the effective anode current in the nine-valve system is less than that in the original system by a factor of $\sqrt{2}$ and that its amplitude is only half as much.

The stated test results show that the valves produced by "Uralelektroapparat" satisfy these requirements. Valves of 1000 A are also produced abroad. Furthermore, the series connexion of these valves means that means that they need only satisfy requirements as regards thermal stability. Their strength need not be nearly so high, for they only have to sustain the total reverse voltage and take overvoltages into account.

5. It is expedient to use nine-valve units in those applications of mercury arc rectifiers where (1) it is more economical to use plant with the two reverse star system (人Y) and a balancing reactor than gear with the three phase bridge system; (2) where the production of double-current cathode valves presents no difficult technical problems; (3) where it is otherwise impossible to obtain the required power in one compact unit without series connexion.

Translated by O.M. Blunn

REFERENCES

1. *The report of the interim commission on rectifier engineering (Reshenie Vremennoi Komissii GNTK Soveta Ministrov SSSR po preobrazovotel'noi tekhnike).* Elektroprom. i priborostr., 2, (1960).
2. L.S. Fleishman; *Elektrichestvo,* No.9, (1959).
3. L.S. Fleishman; *Ionic rectifier, (Ionnyi preobrazovotel').* Soviet Patent No.124022, dated 12 July (1957).
4. J. Slepian and W.E. Pakala; *El. Eng.* No.6, (1941).
5. Th. Wasserrab; *BB Mitt.*, 4/5, (1955).
6. M. Danders; *AEG Mitt.*, 11/12 (1958).

7. A.M. Utevskii; *Electromagnetic processes under fault conditions in rectifier units, (Elektromagnitnye protsessy pri avariinykh rezhimakh vypriamitel'nykh agregatov)*. Akad. Nauk SSSR, No.2 (1949).

ABSTRACTS FROM PAPERS PUBLISHED IN ELEKTRICHESTVO No. 5, 1961

Control engineering

The motor drive of a rolling mill reeling machine with an astatic regulator for strip tension. F.F. Olefir, *et al.*, (pp. 23-30).

A description is given of the motor, reeler and regulator which have been developed for a five-stand mill for the continuous rolling of cold-rolled strip. The new system features constant strip tension whent he mill is at rest, tension is maintained at low speeds, motor current is constant from starting to stopping of the reeler and the speed of the roller is adjusted to the diameter of the roll.

The motor drive of the flying shears in continuous billet mills. M.Ya. Pistrak *et al.*, (pp. 31-38).

The gearing and special cutting devices used in the flying shears on Russian billet mills are described. It is claimed that this system is superior to Western electrically speed-balanced shears when billets are standardized to one or two lengths. A study is also made of the system of synchronization.

Insulation

The maximum electrical field strength of the paper-oil insulation of gear used in d.c. transmission. G.S. Kuchinskii, *et al.*, (pp. 64-68).

A study is made of the electrical insulation of current transformers and isolators on 400 kV d.c. transmission lines with particular reference to the sharp edges of electrodes and ionization.

The e.m.f. induced by the radiation of dielectrics. N.G. Drozdov, *et al.*, (pp. 68-69).

An account is given of the measurements which have been taken to establish the magnitude of the e.m.f. which can be caused by low-energy X-ray radiation of dielectrics. It is claimed to be of the order of 0.1 V. The mechanism whereby much larger e.m.f. have been measured is explained in terms of the effect of a high voltage in which the specimen is regarded as part of the dielectric surrounding the X-ray tube.

The electrical strength of mica in impulse tests in vacuum. V.A. Dubinskii, (pp. 71-73).

Various tests which have been carried out to determine the electric strength of mica splittings in vacuum are described. In one test the splittings were boiled in carbon tetrachloride, in another the surface of the splitting was roughened by applying a processed coating of anhydrous MgO and in another test the splittings were subjected to intense ultra-violet radiation. The effect of annealing in hydrogen is also considered.

Power systems

The optimum spacing of supports for overhead aluminium-sheathed cables. V.V. Bolotin *et al.*, (pp. 9-12).

Tests and a mathematical analysis show that the best results are obtained by spacing the brackets of overhead aluminium-sheathed cables 4 to 7 m apart.

The conductivity of reinforced concrete piles for the pylons of 154-500 kV transmission lines. N.P. Katigrob, (pp. 13-15).

An account is given of research into the footing resistance of reinforced concrete piles for the pylons of 154-500 kV transmission lines. In clayey and clayey-sandy soil the resistance has been found to be somewhat less than 10 ohms.

Rectifiers

The steady state electromagnetic phenomena in a full-wave rectifier with a centre-tapped transformer. A.M. Utevskii *et al.*, (pp. 16-23).

A graphical-analytical study is made of the relationship between the operating conditions, operating characteristics and rating of

rectifiers and the type of load and supply scheme.

A semiconductor power relay. V.I. Grinshtein, (p. 70).

A prototype power relay is described consisting of a phase comparison circuit and an executive device in the form of a two-stage transistor amplifier with a polarized relay at the output. Its performance is claimed to be superior to inductance relays. The relay is light in weight and compact in design.

Rotating machines

A method of determining optimum frequency for small induction motors. I.P. Fil', (pp. 44-47).

A mathematical method of determining the optimum frequency is proposed and close agreement is obtained with test results. The implications for small enclosed motors and motors for manually-operated mining drills are considered.

The geometric loci of induction motor currents when the frequency is variable. G.M. Kirichek, (pp. 48-52).

A graphical-analytical method is proposed for plotting the geometric loci of induction motor currents for the general case when the voltage is proportional to the frequency.

The conditions under which three-phase windings of electrical machines will set up a circular rotating magnetic field. E'.G. Fainshtein, (pp. 62-63).

The author shows that there exists a number of combinations of three-phase winding systems and currents which will form a rotating field. Expressions are also obtained for an elliptical field.

CRITERIA OF ELECTRIC ORE-SMELTING FURNACES*

A.S. MIKULINSKII

(Institute of Metallurgy, Urals' Branch of the
U.S.S.R. Academy of Science)

(Received 20 March 1961)

One of the main problems in the development of electrical ore smelting furnaces is that of increasing the output of the individual unit. This would make it possible to reduce the capacital outlay and running costs so much that it would be economical to produce even pig iron in certain parts of the U.S.S.R. The solution of this problem depends to a large extent on the development of methods of determining the optimum parameters of furnaces.

It has been established in previous papers [1, 2, 3] that the geometric and electrical magnitudes of electric furnaces should be fixed so as to ensure a particular energy distribution in the furnace. It is an urgent problem to determine those criteria of the furnace which would ensure the same energy distribution in actual furnaces as in "specimen" furnaces with the best possible operating indices. This requires geometric and electrical similarity between actual furnaces and the "specimen" furnace.

Furnace dimensions

In two previous papers [1,2] it was proposed to use the diameter of the electrode as the determinative quantity for furnaces with circular electrodes. Geometric similarity is attained by observing the following

---

* *Elektrichestvo*, 6, 33-38, 1961.

criteria:

$$\frac{f}{d}=f' \text{ (1a)}; \quad \frac{b}{d}=b' \text{ (1b)}; \quad \frac{l}{d}=l' \text{ (1c)},$$

where f is the distance from the centre of the electrode to the internal wall of the furnace, b the distance between the electrode centres, l the distance from the lower face of the electrode to the zone of comparatively low specific electrical resistance (see diagram), and d the diameter of the electrode.

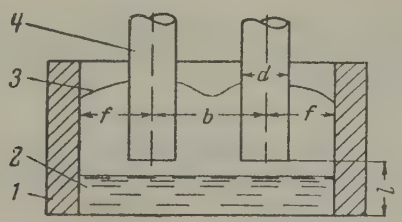

Fig. 1. 1 - brickwork of furnace; 2 - melt; 3 - level of charge; 4 - electrode.

It has been established (4) by an analysis of the electrical field in a 2-electrode furnace that an increase in b' is accompanied by an increase in the current between the electrode I_3. At values of $b' <$ 2.25 to 2.75 the value of I_3 remains practically constant. It therefore follows that it is inadvisable to increase b' above 2.25 to 2.75 in order to reduce the current I_3.

The same conclusion was reached by Sergeev [5] and Platonov after measuring the electrical resistance on a model where the slag was imitated by water solutions and the molten metal by a metallic plate.

For furnaces with square electrodes

$$l = k_0' \sqrt{a_0^2 n_0} = k_0' a_0 n^{1/2}. \qquad (2)$$

where $a_0^2 n_0$ is the section of the electrode and $\frac{b_0}{a_0}=n_0$ is the ratio between the largest and smallest sides of the electrode.

Analysis of electrical fields [1,2]

The secondary voltages in the furnaces can be determined by analysing

the electrical fields. The electrical conductance of the carbon lining of the furnace and live electrodes is taken to be many times greater than that of the charge. Thus the surfaces of its carbon parts are isopotential.

It is known that the coefficients of the charge conductance are a function of pressure and temperature. In order to include them in the analysis it is assumed that they are constant in the horizontal section, whilst with changes in height they vary according to the equation

$$\lambda = \lambda_0 e^{-2hz},$$

where λ and λ_0 are the conductance coefficients of the charge over a height z and if $z = 0$ and h is a coefficient which includes the change in conductance with height.

As a result of solving the Laplace differential equation, the current has been found as a function of the diameter of the electrode d and the extent of the sub-electrode space l.

We require to find a formula for determining the furnace voltage. Suppose that the voltage U_0 of the furnace at a current of 100 A with a uniform specific electrical resistance of the charge is equal to unity. With a specific electrical resistance of the charge in the lower part of the furnace $\rho' = 1$, a radius $r = 1$ and a current $I = 100$ A, we get:

$$100 = k'U_0, \tag{3}$$

where k' is a coefficient which includes the geometric shape of the electrical field (shape factor).

The ratio of the specific resistances in the upper and lower parts of the electrode are:

$$\frac{\rho_1}{\rho_0} = e^{2Hh} = k,$$

where H is the depth to which the electrode is immersed.

The current I is found from the expression

$$I = k'm\frac{U}{R} = k'm\frac{Ud}{\rho_0}, \tag{4}$$

where U is the voltage between the electrodes and the hearth, m a

coefficient which includes the effective specific resistance of all the charge, and R the total resistance.

From expression 4 [2]:

$$U = kI\frac{U_0\rho_1}{kmd} = k'I\frac{U_0\rho_0}{kmd}, \tag{5}$$

or, putting

$$\frac{\rho_0}{km} = \rho$$

and bearing in mind that U = const, it is found that

$$U = k\frac{I\rho}{d}.$$

Equation 5 was found earlier [1, 2] as well as in the paper by Morkramer [6].

Since,

$$I = \frac{P}{\sqrt{3}U} \text{ and } d^2 = \frac{4I}{\pi j} \quad \text{or} \quad d = k''\left(\frac{I}{j}\right)^{1/2}, \tag{6}$$

and putting A for all the constants, the following expression was obtained [1,2]:

$$U = AU_{\text{I}}\left(\frac{\rho_0}{mk}\right)^{2/3}\rho^{1/3}j^{1/3}. \tag{7}$$

To calculate the value of m it is useful to consider a linear conductor of length l_0 with a specific resistance ρ [7]. It is assumed that the electrical field is solely defined by one coordinate z over the height of the furnace.

First case: $\rho = \rho_0$ (uniform conductor). The differential equation for the potential will be:

$$\frac{d^2U}{dz^2} = 0.$$

The boundary conditions are $U = 0$ if $z = 0$, and $U = 1$ if $z = 1$.

The solution of the equation is

$$U = \frac{z}{l}.$$

The current density is

$$j = \frac{1}{\rho_0} \cdot \frac{dU}{dz} = \frac{1}{\rho_0 l}.$$

Second case: $\rho = \rho_0 e^{2hz}$ (non-uniform conductor). The differential equation for the potential is

$$\frac{d^2U}{dz^2} - 2h \frac{dU}{dz} = 0.$$

The boundary conditions will be the same as before. The solution of the equation has the form:

$$U_1 = \frac{e^{2hz} - 1}{e^{2hl} - 1}.$$

The current density is

$$j_1 = \frac{dU}{\rho_0 dz} = \frac{2h}{\rho_0 e^{2h} - 1}.$$

Comparing the values of the current density in the two cases,

$$j_1 = \frac{2hl}{e^{2hl} - 1} j,$$

or, putting

$$\frac{2hl}{e^{2hl}} = m; \quad j_1 = mj; \quad e^{2hl} = k,$$

we get:

$$m = \frac{\ln k}{k - 1}. \tag{8}$$

The criterion E.S. of electrical similarity [2,3]

To ensure a given distribution of energy it is necessary to have a definite value l'. To calculate the optimum value of l' it is necessary to include its functional relationship with some dimension. The diameter of the electrode will be used as such a quantity.

The value of E.S. for furnaces with circular electrodes. The expression for the current density in differential form is

$$j = \frac{1}{\rho} \operatorname{grad} U_h.$$

The left hand side of the equation corresponds to a stepped simplex P_1:

$$j = \frac{I}{F} = \frac{I}{k_1 d^2}; \quad \frac{I}{d^2} = P_1. \tag{9}$$

The right hand side of the equation corresponds to the stepped simplex P_2:

$$\frac{U_h}{\rho l} = \frac{U_h}{\rho l' d}; \quad \frac{U_h}{\rho d} = P_2. \tag{10}$$

The similarity criterion is equal to the ratio between the simplexes of equations (9) and (10) [1,7]

$$ES = \frac{P_2}{P_1} = \frac{U_h d}{\rho I}, \tag{11}$$

or

$$ES = \frac{U_h}{I^{1/2} j^{1/2} \rho}. \tag{12}$$

(11) only contains the specific electrical resistance of the charge materials or semi-products in the vicinity of the lower end of the electrode, since it was shown in a previous paper [3] that the value of this resistance was near to the effective specific resistance of the arc

$$\rho_{\text{eff.a}} = \frac{US}{Il}, \tag{13}$$

where S and l are the section and length of the sub-electrode space.

The flow of current through the arc differs from that through the melt and in particular this manifests itself in a cathode and anode potential drop on the electrode surfaces adjacent to the arc.

Expression (11) for the criterion *E.S.* only holds for a furnace with one electrode. For furnaces with two or three electrodes it is necessary to put MI in the quantity *E.S.* instead of I in view of the branching of part of the current between the electrodes. But since,

$$U_f = \frac{U_l}{\sqrt{3}} \eta_e \cos\varphi,$$

it is found that

$$ES = \frac{U_h d}{MI\rho} = \frac{U_l \eta_e d \cos\varphi}{\sqrt{3} MI\rho} = \frac{U_l \eta_e \cos\varphi}{I^{1/2} j^{1/2} \rho}, \tag{14}$$

where U_f and U_l are the phase and line voltages of the transformer.

For a furnace with one electrode $M = 1$, but for furnaces with two or three electrodes M is somewhat less than unity.

Since under normal operating conditions between 4 and 6 per cent of the total current [3] is branched between the electrodes, it is necessary to take $M = 0.95$.

The value of E.S. for furnaces with square electrodes. For such furnaces the value of l is defined by the equation (1c). The expressions for the other quantities have the following form:

$$R = \rho \frac{k_0'' a_0 n_0^{1/2}}{a_0^2 n_0} = \frac{\rho k_0''}{a_0 n^{1/2}}; \tag{15}$$

$$ES = \frac{U_h a_0 n_0^{1/2}}{l\rho}; \tag{16}$$

$$j = \frac{I}{a_0^2 n_0}. \tag{17}$$

Thus, if it is assumed that the value of the multiplier $a_0 n_0^{1/2}$ is equivalent to d, then the rest of the above conclusions remain unchanged.

From equation 17:

$$a_0^2 n_0 = \frac{I}{j}$$

and, consequently, for furnaces with square electrodes the expression for the criterion

$$ES = \frac{U_h}{I^{1/2} j^{1/2} \rho} = A$$

coincides with (12) for furnaces with circular electrodes and is more general than equation (11).

The relationship between current and output [3]

To determine the quantitative link between the stated quantities it is merely necessary to establish the voltage which would ensure an electrical field similar to the "specimen" field in the actual furnace.

To establish the link between U or I and P use is made of equation (14) and the formula

$$P = \sqrt{3} U_l I \cos\varphi = k' U_l I \cos\varphi.$$

Here

$$U_l = A \frac{M I^{1/2} j^{1/2} \rho}{\eta_e \cos\varphi} = \frac{A'' M^{2/3} P^{1/3} \rho^{2/3} j^{1/3}}{\eta_e^{2/3} \cos\varphi}. \qquad (18)$$

The quantities M and A are constant in furnaces of different power if the same product is being produced. Therefore

$$U_l = A' \frac{\rho^{2/3} (Pj)^{1/3}}{\eta_e^{2/3} \cos\varphi}. \qquad (19)$$

If it is assumed that η_e and $\cos\varphi$ are constant, then equation (19) will assume the form

$$U_h = c_{0I} j^{1/3} P^{1/3} \rho^{2/3}. \qquad (20)$$

Finally, if it is assumed that ρ is also constant, then

$$U_h = c_{0II} j^{1/3} P^{1/3}. \qquad (21)$$

With an increase in power there is an increase in the depth of immersion of the electrodes and together with that an increase in the pressure exerted by the upper layers on the lower layers. Consequently, there is a reduction in the specific electrical resistance of the layer of the charge at the lower face of the electrode. In addition, the increase in pressure is instrumental in forming scum (crusts) in the furnace. Thus, the quantity ρ can be a function of power [1].

Accordingly,

$$\rho = M_1 P^{p}.$$

Considering equation (18),

$$U_l = A\left(\frac{M_1 M}{\eta_e}\right)^{2/3} \frac{j^{1/3}}{\cos\varphi} P.$$

If $\eta_э$, p, j and $\cos\varphi$ are constant, then equation (21) can be represented in the following form:

$$U_h = c_{0\,III} P^{n}. \tag{22}$$

In the same way it can also be shown that

$$I = A_0 j^{-1/3} \rho^{-2/3} P^{2/3}; \tag{23}$$

$$I = A_{0I} j^{-1/3} P^{2/3}; \tag{23a}$$

$$I = A_{0\,II} P^{2/3}; \quad I = A_{0\,II} P^{1-n}. \tag{23b}$$

The values of the coefficients c_{0I}, c_{0II}, as well as A_0 to A_{0II}, depend on the composition of the charge, the frequency and depth of stirring, the frequency of tapping and other factors. These coefficients can be found from practical data of the voltages and outputs of the furnaces which provide the best results.

Comparison of calculations with operating data

In published literature it is said that the value n in equation (22) is 0.5 for certain furnaces with different outputs. However, Kamentsev [8] states that it is a question of a change in output in one and the same furnace. Curtis [9] also came to the same conclusion without any explanation.

Equation (21) can be represented in the form

$$U_l = c_{0\,IV} \frac{I^{1/3}}{l^{2/3}} P^{1/3}.$$

Since d = const and $I = \frac{P}{U}$ in the case under consideration, it is found that

$$U = c_{0\,III} P^{0,5}. \tag{22a}$$

The value of ES with ρ and d constant corresponds to the equation

$$\frac{U}{I} = \text{const.} \tag{22b}$$

Thus equations (22a) and (22b) hold good for furnaces with the same method of production and electrode diameter.

The correctness of the foregoing relationships for furnaces with the same electrode diameter at different outputs does not contradict equation (21) or equations (23) and, being a special case, it actually confirms them. In view of this, it must be acknowledged that the conclusion of certain authors that the value $\frac{U}{I}$ cannot be taken as constant if d varies at the same time as U, but that it does not hold if the latter quantity remains constant when U and I vary.

It was pointed out in a previous paper [3] that the order of n in equation (22) can be less than 0.33. One of the reasons for the decrease in the order of n with increasing output is that j decreases in this case. The value of n can be influenced appreciably by this change under certain circumstances.

Consider the following example by way of illustration. Using equation (21), the value of n is found from the expression

$$n = \frac{\log \frac{U^2}{U_1}}{\log \frac{P_2}{P_1}} = \frac{0.33 \log \frac{I_2}{I_1}}{\log \frac{P_2}{P_1}}.$$

According to the LKB project of the Electrical Furnace Trust, the value of j is 4.4 and 5.5 A/cm^2 in 16,500 and 7,500 kVA furnaces respectively. A difference of 0.09 in the value of n is brought about by including the second term in the last equation. It is natural that if

$n = 0.33$ when j and other terms in equations (18) or (20) are equal, then the value n will be $0.33-0.09 = 0.24$ when only one multiplier is included, namely, the difference in the value of j.

Consequently, other published equations with other values of n than 0.33, are special cases of equation (21).

The following conclusion can therefore be drawn. Assuming that c_{0III} is constant in equation 22, which only corresponds to certain special cases, then n will no longer be 0.33, it will generally have a lower value, but in individual cases it can have higher values (for example, if j or the specific resistance of the charge increases with increasing power).

Since the coefficient c_{0III} is not a constant quantity [1,2,3] it is recommended that the value of this coefficient and the value of n should be found from two furnaces with different outputs.

More accurate values of ES and U_n

The next step in refining the criterion ES is to include the specific properties of the arc discharge in the circuit for which the following relationship holds good

$$U = a + bl,$$

where a is the drop in arc voltage at the electrode which depends in particular on the nature of the vapours in the sub-electrode space (this value differs depending upon the technological design of the furnace).

For a 100 kVA carbide furnace the expression for U can be written with averaged coefficients [10]:

$$U = 15.5 + 3.4l.$$

Under normal operating conditions 4 to 6% of the current is branched between the electrodes [4]. Therefore, in the subsequent calculations it can be assumed that the greater part of the current in ore smelting furnaces flows through the arc and charge or the melt in succession. Furthermore, in view of the closeness in value of ρ and $\rho_{eff.a}$, the voltage drop in the charge and the melt can be written in the form

$$U = a + I\rho\frac{l}{S}.$$

Consequently, the voltage drop in the melt and charge is

$$U_{vd} = U_h - \alpha = I\rho \frac{l}{S} = \frac{I\rho}{d}.$$

This new expression for ES differs from the previous one in that the term $U - \alpha$ is written in the first instead of U.

It is more convenient to express the value of U_{vd} in terms of P_{vd}. It is found like $U_h = f(P)$ in the way shown above, e.g. by equations (12), (18), (19), (20) and (21). Consequently,

$$U_{vd} = A_{III} P_{vd}^{1/3} j^{1/3}. \tag{24}$$

The following expression can be used instead of 24

$$U_{vd} = A_{IV} P_{vd}^{n}. \tag{24a}$$

Since

$$\frac{P_{vd}}{P_h} = \frac{U_{vd}}{U_h},$$

it is found that

$$U_{vd} = A_{III} P_{vd}^{1/3} \frac{U_{vd}^{1/3}}{U_{vd} + \alpha} \rho^{2/3} j^{1/3},$$

or

$$U_{vd}^3 + U_{vd}^2 \alpha = A_{VI} P \rho^2 j. \tag{25}$$

In large furnaces $\alpha < U_{vd}$ and therefore when calculating them it is necessary bear in mind that the term $U_{vd}^2 \alpha < U_{vd}^3$. It is therefore possible to solve equation (25) by trial and error if α is assumed to be a small parameter. As a result

$$U_{vd} = A_V P^{1/3} \rho^{2/3} j^{1/3} - \frac{\alpha}{3};$$

$$U_h = \frac{2}{3}\alpha + A_V P^{1/3} \rho^{2/3} j^{1/3}.$$

Current density in the electrode

It will be seen from equations (7) and (21) that it is necessary to increase j to increase U. An increase in j above a certain value is not permissible because the electrode can get much too hot or unfavourable coking conditions can arise. The need to include this factor has been dealt with by Alekseev [11].

An attempt will now be made to establish the link between j, P and d on the condition that the thermal balance of the electrode is preserved. One side of the balance contains the item q_1 for the generation of heat owing to the transmission of current through the electrode and q_2 for the influx of heat from the arc to the lower face of the electrode, whilst the other side of the balance contains q_3, the dissipation of heat through the side surface, q_4 the heat necessary for heating, coking and vapourizing the electrode, and q_5 the dissipation of heat from the lower face of the electrode to the electrode holder.

The equilibrium equations are

$$k_1'' I^2 \rho_e \frac{4L}{\pi d^2} + k_2'' \frac{\pi d^2}{4} - k_3''' \pi d L - \\ - k_4'' \frac{c\gamma \pi d^2}{4} l - k_5'' \frac{\pi d^2}{4L} = 0; \qquad (26)$$

$$k_0 I^2 \rho_e \frac{L}{d^2} + k_{20} d^2 - k_{30} d L - k_{40} d^2 l - \frac{k_{50} d^2}{L} = 0,$$

where L, ρ_e, c, γ and l are the length of the electrode from the lower face to the electrode holder, the specific resistance of the electrode, its thermal capacitance, the specific gravity, and the expenditure of electrodes per unit of time.

Considering equations (6) and (23),

$$k_{10} j^{2/3} P^{2/3} + k_{20} \frac{P^{2/3}}{j^{4/3}} - \frac{k_{30} P^{2/6} L}{j^{2/}} - \\ - \frac{k_{40} P^{2/3} l}{j^{4/3}} - \frac{k_{50} P^{2/3}}{j^{4/3} L} = 0.$$

Equations have been published which establish the link between d and P or I. It will now be shown that these relationships can be found if the items q_2, q_4 and q_5 are ignored in equations (26).

However, there is no foundation for ignoring these terms and in particular the item q_2. It therefore remains for the assumptions underlying the following relationships to be verified at a later date in order to see whether they correspond to operating data and to find out whether further refinement is necessary.

If q_2, q_4 and q_5 are ignored, then equation (26) takes the form

$$P^{1/3} = \frac{k_{30}}{k_{20} j^{4/3}}; \quad j = k_{50} P^{-4}. \tag{27}$$

Platonov [12] obtained a similar formulae from other considerations for furnaces with a constant specific power, i.e. the supply of power per unit area of the hearth for which we put g.

Ignoring q_2, q_4 and q_5 it is found from equation (26) that

$$\frac{I^2}{d^2} = Nd. \tag{28}$$

or

$$j^2 = \frac{N}{d}. \tag{29}$$

It should be pointed out that Kelley's [13] empirical equation has a similar form

$$j = 250\, d^{-1/2}, \tag{29a}$$

where j is expressed in amperes per square inch and d in inches.

But equations (29) and (29a) are only approximate.

The relationship between I and d can be established from equation (28):

$$I = Nd^{1,5}. \tag{30}$$

It must be mentioned that there is only any point in determining the empirical coefficients in accordance with equation (26) to (30) on the basis of the furnaces' operation where the values of j correspond to electrodes with the optimum thermal balance.

It has already been shown [3] if the criteria of electrical and

geometric similarity are observed, that

$$g = N_0 j^{1,33} P^{0,33} \cos\varphi^{0,66}. \tag{31}$$

Assuming that j and $\cos\phi$ are constant, equation (27) is then obtained. Considering equations (21) and (27), it can be inferred that the voltage U if g = const is equal to

$$U = c_{0III} j^{1/3} P^{1/3} = c_{IV} P^{-1/12} P^{1/3} c_{IV} P^{0,25}. \tag{32}$$

Thus, equations (27) to (30) and (32) correspond to a constant g if the electrical and geometric similarity is observed.

Since expressions (27) to (30) ignore certain items in the thermal balance, it should be pointed out that Morkramer [6] recommended that th following relationship should be used:

$$I = 20 d^{1,7}. \tag{33}$$

But an error was committed here in that he took a constant g along with this equation. It has already been established that equation (30) should have been used in this case instead. Incidentally, taking equation (33),

$$U = c_V P^{0,29}.$$

It is necessary to find expressions for the relationships between j and the other quantities for square electrodes. As before, the only items of the balance which are included are q_1, q_3 for ρ_e:

$$\left.\begin{aligned} I^2 \frac{L}{a_0 b_0} &= k_{e0} (a_0 + b_0) L; \\ \frac{I^2}{a_0^2 n_0} &= k_{e0} a_0 (1 + n_0). \end{aligned}\right\} \tag{34}$$

Since,

$$j = \frac{I}{a_0 b_0},$$

it follows that

$$j = k_{e0} \left(\frac{1 + n_0}{a_0 n_0^q}\right)^{1/2}. \tag{35}$$

To ensure the maximum values of U with increasing P, it is necessary to enlarge the heat dissipating surface of the electrodes. For example, it is possible to increase the power within limits without changing the thickness of the electrode (retaining the dimension a_0).

The relationship between the electrode dimensions a_0, n_0 and I follows directly from equation (34):

$$I = k_{70} a_0^{3/2} [n_0 (1 + n_0)]^{1/2}. \quad (36)$$

Translated by O.M. Blunn

REFERENCES

1. A.S. Mikulinskii; *Prom. energ.*, No.4, (1948).
2. A.S. Mikulinskii; *Determination of the parameters of electric furnaces.* In book: *Theory and practice of electric ore smelting, (K opredeleniiu parametrov elektricheskikh pechei. Sborn. "Teoriia i praktika rudnoi elektrotermii)".* Metallurgizdat (1948).
3. A.S. Mikulinskii; *Theory of carbide and ferro-alloy furnaces, (K teorii karbidnykh i ferrosplavnykh pechei).* Trud. UNIKhIM, No.II, Goskhimizdat (1954).
4. A.S. Mikulinskii, V.K. Ivanov and P.V. Gel'd; *The electrical field between cylinders in an inhomogeneous medium.* In book: *Technical physics, (Elektricheskoe pole mezhdu tsilindrami v neodnorodnoi srede. Sborn. "Teknicheskaia fizika")* (1947).
5. P.V. Sergeev; *Determination of the main electrical parameters of ore-smelting furnaces with a large slag capacity, (Opredelenie osnovnykh elektricheskikh parametrov rudnotermicheskikh pechei s bol'shim ob'emom shlakov).* Trud. Altai. gornomet. nauchno-issled. inst., IV (1957).
6. M. Morkramer; *J. du four elect.*, No.2 (1960).
7. V.K. Ivanov and A.S. Mikulinskii; *The distribution of current in ore-smelting furnaces.* In book: *Theory and practice of electrical ore smelting, (K raspredeleniiu toka v rudnotermicheskikh pechakh. Sborn. "Teoriia i praktika rudnoi elektrotermii).* Metallurgizdat (1948).
8. M.V. Kamentsev; *Synthetic abrasives, (Iskusstvennye abrazivnye materialy).* Mashgiz (1960).
9. H.A. Curtis; *J. electrochem. soc.*, 100 (1953).
10. A.S. Mikulinskii and L.V. Iumenova; *The transmission of current in a carbide furnace, (K voprosu prokhozhdeniia toka v karbidnoi pechi).* Trud. UNIKhIM, No.II. Goskhimizdat (1954).

11. E.M. Alekseev; *Stal'*, No.10, (1956).
12. G.F. Platnov; *Prom. energ.*, No.1 (1960).
13. W.M. Kelley; *Iron and steel engineer*, No.4 (1958).

A NEW SYSTEM OF GENERATING DIRECT AND STABLE FREQUENCY ALTERNATING CURRENT FROM MOTORS WHICH RUN AT DIFFERENT SPEEDS*

M.M. KRASNOSHAPKA

(Kiev)

(Received 5 September 1960)

Purpose, construction and operating principle

Modern aircraft use d.c. and stable frequency a.c. systems of electrical supply at the same time. In the majority of cases the d.c. source is a d.c. generator driven by the aircraft motors at a wide range of speeds. In order to obtain stable frequency a.c. in this case use is made of dynamo electric converters (motor-generators), provided with automatic voltage and frequency regulators.

If the consumption of a.c. is relatively large, it is better to use special generator plant for generating stable frequency a.c. at various running speeds of the primary motor. Such generator plant can be a synchronous generator with a hydraulic drive, a synchronous generator with an electromagnetic clutch, a twin-machine system consisting of a d.c. generator and a single-armature converter besides other types of plant and dynamo-electric systems [1-5].

There is also a need to generate stable frequency a.c. at a wide range of rotational speeds in other branches of engineering, such as wind-driven power stations, small hydro-electric power stations with non-controlled turbines, new types of railway passenger cars etc [1-4].

The general disadvantage of known types of aircraft systems of

* *Elektrichestvo*, No.6, 38-44, 1961.

generating stable frequency alternating current for varying rotational speeds is that the mechanical power of the primary motor developed by them is subject to a two-fold and even three- fold conversion. The efficiency of the system is therefore low and its weight is relatively large per kVA of output.

In this paper a study is made of a new system which is intended for the simultaneous generation of direct and stable frequency a.c. for varying rotational speeds. It consists of a special twin-generator unit with two automatic regulators and a single-armature converter of comparatively low power. The system is relatively light in weight and it is highly efficient, since more than 85% of the electrical power is obtained direct from the twin-generator unit and only a small proportion of it is converted in the single-armature converter. The system can be used for any ratio of the powers consumed in the a.c. and d.c. networks, and even in extreme conditions when only a.c. or only d.c. is being generated.

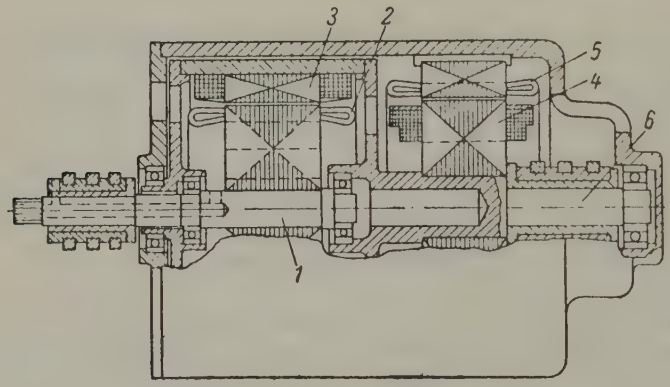

Fig. 1. Construction of generator unit.

Fig. 1 illustrates the construction of the unit and Fig. 2 the main circuit of the connexions of the unit's machines with the single-armature converter *SC*, the voltage regulator *VR* and the frequency regulator *FR*.

The generator unit consists of an electromagnetic slip clutch with an excitation winding *3* and a three phase winding 2 which is connected to the contact rings on the primary shaft *1*, and a three phase synchronous generator with a rotating inductor *4* and a fixed armature winding *5*. The d.c. supply of the excitation windings is via three contact rings on the secondary shaft of the unit *6*.

At a rotational speed n_1 of the primary shaft *1* the first machine of the unit *2* simultaneously operates as a synchronous generator supplying the a.c. network and as a clutch rotating at a speed n_2 the synchronous generator connected via rectifier *7* to the d.c. network. From now on we will refer to the second machine of the unit as the restraint generator.

Depending upon the relationship between the power consumption in the a.c. and d.c. networks and the rotational speed of the primary motor, the balancing single-armature converter can convert d.c. into a.c. or a.c. into d.c. and under no-load conditions it can operate with supply from both ends.

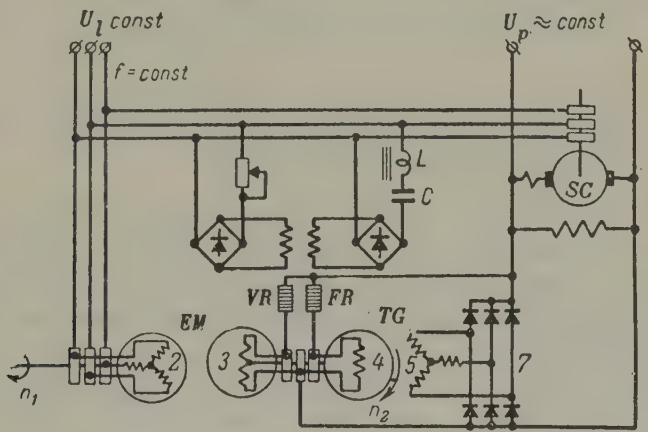

Fig. 2. Electrical connexions of machines and system regulators.

The frequency of the a.c. is stabilized at different running speeds of the primary motor and different loads by the automatic frequency regulator *FR* which varies the excitation current of the restraint generator. The frequency of the alternating current *F* depends upon the the number of pole pairs *p* and the difference between the speed of the driving and driven parts of the clutch.

To maintain the frequency stable it is necessary to maintain a constant speed difference between the driving and driven parts of the clutch since

$$f = \frac{p(n_1 - n_2)}{60}. \qquad (1)$$

Under steady state conditions the moving magnetic moment of the clutch is equal to the sum of the electro magnetic moment of the restraint generator and the moment of friction of the driven part of the clutch. If there is no frequency regulator, an increase in the active load on a.c., a decrease in the d.c. load and a reduction in the rotational speed of the primary motor n_1 will cause a decrease in the speed difference $n_1 - n_2$ and the frequency owing to the balance of the moments being upset. In order to maintain the frequency constant under these conditions it is necessary to increase the torque of the restraint generator by a corresponding increase in the excitation current. In the opposite case it is necessary to reduce the torque of the restraint generator by decreasing its excitation current.

The frequency is automatically stabilized if there is a frequency regulator *FR* connected as in the circuit in Fig. 2.

It will be seen from Fig. 2 that the voltage in the a.c. network is stabilized by regulating the excitation current of the electromagnetic clutch by the automatic voltage regulator *VR*.

The main circuit in Fig. 2 shows the voltage and frequency regulators in the form of conventional angle regulators as used in aircraft supply systems. Other types of automatic regulator could be used instead, including regulators with magnetic amplifiers which may be more reliable and convenient in use.

Relationship between machine output and system efficiency under different operating conditions: approximate weight of the system

The mechanical power from the primary motor to the primary shaft of the generator unit P_{m1} is partially converted in the electromagnetic clutch, as in a conventional generator, to electrical power P_{e1}. The rest of the power is transmitted to the secondary shaft of the unit in the form of mechanical power P_{m2}, in which case

$$P_{M2} = P_{M1} - P_{e1} = \frac{P_2}{\eta_{2y}} = M_{e1} \frac{\pi n_2}{30}. \qquad (2)$$

The electrical power of the clutch including the losses in the armature circuit and magnetic system is

$$P_{e1} = P_{1a} + \Delta P_{...m} + \Delta P_{1st} = \frac{P_{1a}}{\eta_{1y}} = M_{e1} \frac{\pi (n_1 - n_2)}{30}, \qquad (3)$$

where m_{el} is the electromagnetic moment of the clutch, n_1, n_2 the rotational speeds of the primary and secondary shafts, η_{l2v} the conditional efficiency of the restraint generator with the losses in the rectifier, the excitation circuit of the clutch and the friction losses of its driven part all included, P_{la} the electrical active power of the clutch, $\Delta P_{l\ arm}$ the electrical losses in the armature winding circuit, ΔP_{lst} the iron losses in the magnetic circuit of the clutch, η_{ly} the conditional efficiency of the clutch as an a.c. generator without the losses in the excitation circuit and the friction losses of its driven part included, and P_2 the useful power of the restraint generator.

The relationship between the d.c. power and the active a.c. power given off by the restraint generator and clutch respectively can be obtained from equations (2) and (3):

$$\frac{P_2}{P_{la}} = \frac{n_2\eta_{l2y}}{n_c\eta_{ly}} = kn_2, \tag{4}$$

where $n_c = n_1 - n_2 =$ const is the nominal difference in rotational speed.

It is presupposed that the active P_{la} when the armature of the electromagnetic clutch is greater than the active power consumed in the a.c. network $P_{m.a}$ by an amount which exceeds the no-load losses of the single-armature converter. In this case the power consumed in the d.c. network $P_{n.d}$ is equal to the sum of the powers given off by the restraint generator P_2 and the single-armature converter P_{sc}. Suppose that the unit of measurement is the total power consumed in the a.c. and d.c. networks $(P_{na} + P_{nd})$ and that x denotes the relative power in the d.c. network. Then

$$P_{nd} = P_2 + P_{sc} = x(P_{na} + P_{nd}); \tag{5}$$

$$P_{na} = P_{la} - \frac{P_{sc}}{\eta_{sc}} = (1 - x)(P_{na} + P_{nd}). \tag{6}$$

The joint solutions of equations (4) to (6) gives the following expressions for the outputs of the electromagnetic clutch P_{la}, the restraint generator P_2 and the single-armature converter P_{sc}:

$$P_{la} = \frac{[x(1 - \eta_{sc}) + \eta_{sc}](P_{na} + P_{nd})}{kn_2 + \eta_{sc}}; \tag{7}$$

$$P_2 = \frac{[x(1-\eta_{sc})+\eta_{sc}]\,kn_2(P_{na}+P_{nd})}{kn_2+\eta_{sc}}; \tag{8}$$

$$P_{sc} = \frac{[x(1+kn_2)-kn_2]\,\eta_{sc}(P_{na}+P_{nd})}{kn_2+\eta_{sc}}. \tag{9}$$

Formulae (7) to (9) hold good for all unit operating conditions under which the single-armature converter converts the a.c. into d.c. i.e. with $P_{sc} > 0$.

It is presupposed that the output of the restraint generator is greater than the power consumption in the d.c. network by an amount which exceeds the no-load losses of the single-armature converter, whilst the sum of the active power of the electromagnetic clutch P_{1a} and of the single-armature converter P_{sca} is equal to the active power of the a.c. network P_{na}. In this case the initial equations have the form:

$$P_{nd} = P_2 - \frac{P_{sca}}{\eta_{sc}} = x(P_{na}+P_{nd}); \tag{10}$$

$$P_{na} = P_{1a} + P_{nda} = (1-x)(P_{na}+P_{nd}). \tag{11}$$

As a result of the joint solution of equations (4), (10) and (11), to determine the active powers of the electromagnetic clutch, the single-armature converter, and the restraint generator, the corresponding formulae are:

$$P_{1a} = \frac{[x(\eta_{nd}-1)+1](P_{na}+P_{nd})}{kn_2\eta_{sc}+1}; \tag{12}$$

$$P_{sco} = \frac{[kn_2-x(1+kn_2)]\,\eta_{sc}(P_{na}+P_{nd})}{kn_2\eta_{sc}+1} \tag{13}$$

$$P_2 = \frac{[x(\eta_{sc}-1)+1]\,kn_2(P_{na}+P_{nd})}{kn_2\eta_{sc}+1}. \tag{14}$$

Formulae (12) to (14) hold good for all operating conditions of the unit when the balancing single-armature converter converts the direct current into alternating current, i.e. when $P_{sca} > 0$.

The efficiency of the generator unit with the balancing single-armature converter when the latter is converting a.c. into d.c. is given

by equation (15). In the other case it is given by (16):

$$\eta_c = \frac{1}{P_{na} + P_{nd}} \left[\left(P_{1a} - \frac{P_{sc}}{\eta_{sc}} \right) \eta_1 + P_{sc} \eta_1 \eta_{sc} + P_2 \eta_{12} \right]; \quad (15)$$

$$\eta_c = \frac{1}{P_{na} + P_{nd}} \left[P_{1a} \eta_1 + \left(P_2 - \frac{P_{sca}}{\eta_{sc}} \right) \eta_{12} + P_{sca} \eta_1 \eta_2 \eta_{sc} \right], \quad (16)$$

where $\eta_{s.c}$, η_1 and η_{12} are the real efficiencies of the single armature-converter, the first machine and the second machine.

When the system is operating in the middle range of speeds n_1 with a certain relationship between the loads in the a.c. and d.c. networks, the single armature-converter can operate under conditions of supply from both ends, consuming power equal to the no-load losses ΔP_{sc}.

In this case the total electrical power of the unit's machine is equal to the total power consumed in both networks with the no-load losses of the single-armature converter included:

$$P_{1a} + P_2 = P_{n.a} + P_{n.d} + \Delta P_{n.d}. \quad (17)$$

The outputs of the first and second machines of the unit, in this case in accordance with relationship (4), can be found from formulae (18) and (19):

$$P_{1a} = \frac{P_{na} + P_{nd} + \Delta P_{sc}}{kn_2 + 1}; \quad (18)$$

$$P_2 = \frac{(P_{na} + P_{nd} + \Delta P_{sc}) kn_2}{kn_2 + 1}. \quad (19)$$

The generator unit with a single-armature converter is not only suitable for simultaneously generating a.c. and d.c., but also for generating either a.c. or d.c. separately. The formulae for finding the power of the electromagnetic clutch, single-armature converter and restraint generator when generating only a.c. can be found from formulae (12) to (14) by substituting x = zero and $P_{n.d}$ = zero therein.

If only d.c. is being generated, the appropriate formulae are ob-

tained from (7) to (9) after substituting $x = 1$ and $P_{n.a}$ = zero, but this state of affairs has no practical significance.

When only a.c. is being generated, the efficiency of the system is defined by formula (20), but when only generating direct current it is given by formula (21):

$$\eta_c = \frac{P_{1a}}{P_{na}}\eta_1 + \frac{P_{sca}}{P_{na}}\eta_2\eta_1\eta_{sc}; \tag{20}$$

$$\eta_c = \frac{P_2}{P_{nd}}\eta_2 + \frac{P_{sc}}{P_{sc}}\eta_1\eta_{sc}. \tag{21}$$

Fig. 3 shows curves for the relative outputs

$$\frac{P_{1a}}{P_{n.a} + P_{n.d}}, \quad \frac{P_2}{P_{n.a} + P_{n.d}},$$

$$\frac{P_{s.c}}{P_{n.d} + P_{n.d}} \quad \text{and} \quad \frac{P_{s.c.a}}{P_{n.a} + P_{n.d}}$$

as a function of the rotational speed of the primary motor n_1 at $x = 0.4$ $\eta_{2y} = 0.7$ to 0.8, $\eta_{sc} = 0$ to 0.76, $\eta_{1y} = 0.92$, and $n_c = n_1 - n_2 = 4800$ rev/min.

The curves for relative machine outputs have been plotted from data calculated for a system intended for simultaneous supply of a 30 kVA a.c. network (f = 400 c/s cos $\varphi = 0.75$, and $P_{na} = 22.5$ kW) and a 15 kW d.c. network.

The curve η_c gives the efficiency of the system at rated load, and the inclined straight line n_2 the rotational speed of the restraint generator. It will be from Fig. 3 that the power of the restraint generator P_2 is increased by practically a factor of 2.5 with an increase in rotational speed n_1 from 6500 to 1300 rev/min and n_2 from 1700 to 8200 rev/min. Since the voltage of the d.c. network is practically constant, it follows that the curve P_2 simultaneously defines the limits of variation of the current in the stator winding of the restraint generator.

In order to reduce the theoretical dimensions and weight of the restraint generator intended for such operating conditions, it is necessary to change over the stator winding from the star system to the

delta system with an increase in rotational speed n_2 to 3200 rev/min. This changeover can be made by a 2-position 3 phase contactor with automatic control.

The 20-30 kVA alternators used in modern aircraft without an exciter for theoretical speeds of 6000 rev/min weight no more than 1 kg per 1 kVA of rated output (g_{rel} = 1 kg/kVA).

Bearing these data in mind, the total weight of a twin-machine unit for P_1 = 30 kVA and P_{nd} = 50 kW can be calculated quite closely by the formula

$$G_{\Sigma} = g_{rel} n \left(\frac{P_{1\,max}}{n_c} + \frac{P_{2\,max}}{n_{2p}} \right) =$$

$$= 6\,000 \left(\frac{35.8}{4\,800} + \frac{22}{3\,200} \right) = 86 \text{ kg}.$$

The approximate weight of the single-armature converter with a maximum output of 5.65 kW at $n_{s.c}$ = 8000 rev/min is about 9 kg, whereas the approximate weight of the germanium rectifiers can be taken as about 8 kg at a maximum output of 22 kW. In this case the total weight of the system without regulators is 103 kg and its weight per 1 kVA of the total power of the a.c. and d.c. networks is 2.29 kg.

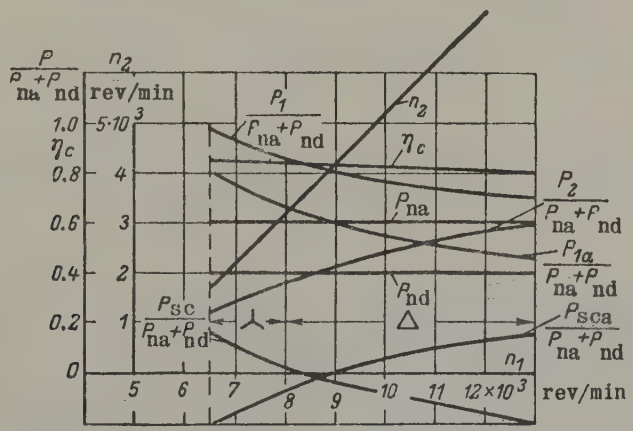

Fig. 3. Calculated characteristics of the system in a.c. and d.c. generation.

Fig. 4 shows calculated curves for a system solely intended for an a.c. network with an output 30 kVA, f = 400 c/s at $\cos\phi$ = 0.75, n_1 = 6250 to 12500 rev/min n_c = 6000 rev/min and n_2 = 250 to 6500 rev/min.

To ensure the necessary restraint torque of the second machine in the unit at n_2 = 250 to 1700 rev/min, provision is made for disconnecting the single-armature converter from the network and the shortcircuiting of the a.c. armature winding. In this case all the output is delivered to the a.c. network only by the first machine, and the relatively low output of the restraint generator is dissipated in the form of losses in the armature windings of the converter and restraint generator.

In the range of speeds n_2 = 1700 to 3300 rev/min the stator winding of the restraint generator is connected in star, but if n_2 = 3300 rev/min it is connected in delta.

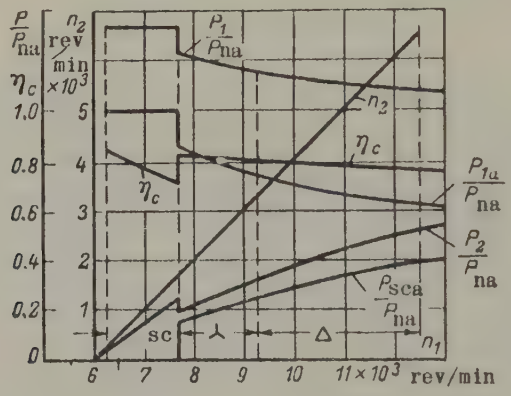

Fig. 4. Calculated characteristics of the system in the generation of a.c. alone

In accordance with Fig. 4 the first machine of the unit must be designed for a total power in the a.c. network P_1 = 30 kVA at n_c = 6000 rev/min, the second machine for a maximum power P_2 = 11.25 kW at n_{2p} = 3200 rev/min. The maximum power of the single-armature converter at n_1 = 12500 rev/min is 0.39 P_{na} = 8.7 kW. The total weight of the twin-machine unit of 30 kVA at cos φ = 0.75 is 49.5 kg in accordance with the formula given above.

The total weight of a single-armature converter of 8.7 kW at $n_{s.c}$ = = 8000 rev/min and the set of germanium rectifiers for a maximum output of 11.25 kW is about 18.5 kg.

The total weight of the system without including the weight of the regulators and contactors if the foregoing changes have to be made is about 68 kg and its weight per 1 kVA of rated output is 2.27 kg.

The weight indices of the dynamo-electric system are approximately equal to the wt. indices of an aircraft generator plant of equal power consisting of an alternator and differential – hydraulic drive. But the efficiency of the proposed system is considerably greater.

Distribution of reactive power between the first machine and the single-armature converter

The foregoing equations 7-9 and 12-14 and the curves in Figs. 3 and 4 define the relative active a.c. powers of the first machine and the single-armature converter as well as the relative output of the restraint generator. The active power can be delivered into the network either from the first machine of the element or from the single-armature converter. The relationship between the reactive powers of the first machine and single-armature converter when an automatic voltage regulator VR is present (see Fig. 2) depends upon the degree of excitation of the converter. At rated converter excitation ($\cos \varphi = 1$) active power only comes into the network from the first machine of the unit. If there is under-excitation, the single-armature converter is a consumer of reactive power, but if there is over-excitation it delivers active power into the network partially unloading the first machine.

If a.c. is being generated it is advisable to change the excitation of the single-armature converter in such a way that it delivers a certain reactive power into the network at low speeds of the primary motor when its active output is low.

With an increase in active load on the single-armature converter at high speeds of the primary motor the reactive power from the converter must gradually decline to zero owing to the weakening of its excitation. In this case the necessary reactive power will come in an ever increasing extent from the first machine of the unit, the active power of which decreases with increasing speed of the primary motor, as will be seen from Fig. 4.

The excitation of the single-armature converter can be changed automatically as required by mixed excitation with counter connexion of its parallel and series windings.

Test results

In order to check the operating characteristics, dynamic properties and weight indices of the system, an experimental equipment was produced on the basis of the batch produced SGS-7.5 type aircraft alternators.

The restraint generator was a SGS-7.5 alternator with 6 slip rings on the shaft so that the armature winding could be changed from star to delta and back by a 2-position contactor. In place of the single-armature converter use was made of an aircraft cascade converter of the PK-750 type which was reconstructed as a three phase converter with a line voltage of 120 V and a maximum output to 1000 VA at collector voltage of 28 V. The electrical power of the restraint generator was transmitted into the d.c. network and armature circuit of the converter via VG-50 type germanium rectifiers.

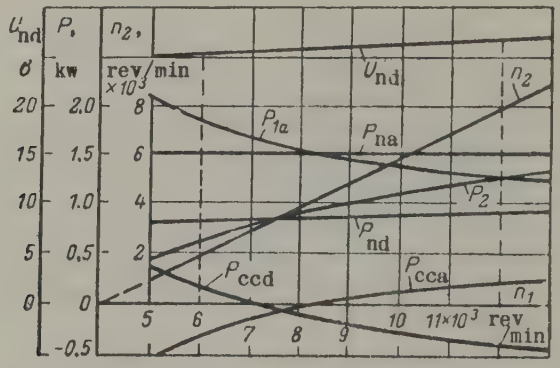

Fig. 5. Test curves of prototype system in a.c. and d.c. generation at 400 c/s and 120 V.

The load of the unit did not exceed 30% of its theoretical output owing to the lack of a suitable cooling system.

Fig. 5 shows the static characteristics of the experimental generator plant for the case of simultaneous generation of a.c. and d.c.

In order to investigate the dynamic properties of the system a prototype system was assembled consisting of the two machines described above, a 3-phase cascade converter, a 2-position contactor and two angle regulators. The electrical connexion of the machines and regulators differed from the system shown in Fig. 2 in that measuring devices and a three phase 2-position contactor were included to provide for changeover of the armature winding of the restraint generator.

The control winding of the frequency regulator was supplied from a tuned circuit via a magnetic amplifier, whilst the excitation winding of the first machine was supplied from a direct or constant source. Oscillograms of transient behaviour in the system are shown in Figs. 6-9.

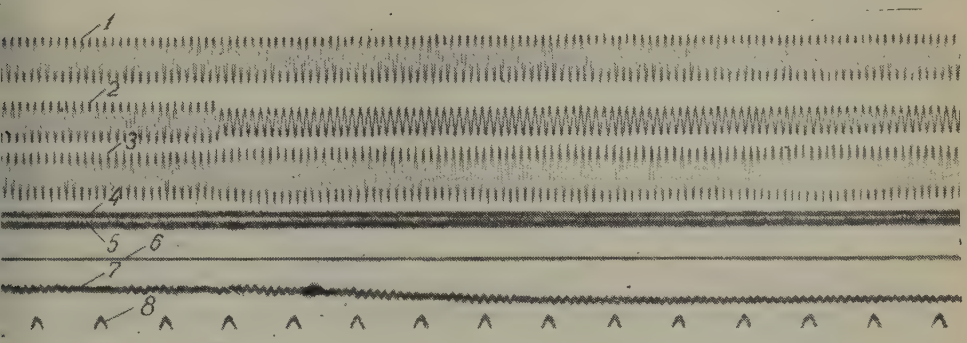

Fig. 6. Oscillograms of transient phenomena in system on disconnecting an a.c. load:
1 – line voltage of network 120 V, 400 c/s; *2* – phase current of first machine in the unit (initial value 2.8 A); *3* – phase current of cascade converter (initial value 2.8 A); *4* – voltage of d.c. network (initial value 24 V); rotational speed of primary motor (n_1 = 5300 rev/min); *6* – zero line; *7* – d.c. given off by converter; *8* – time indication (50 c/s).

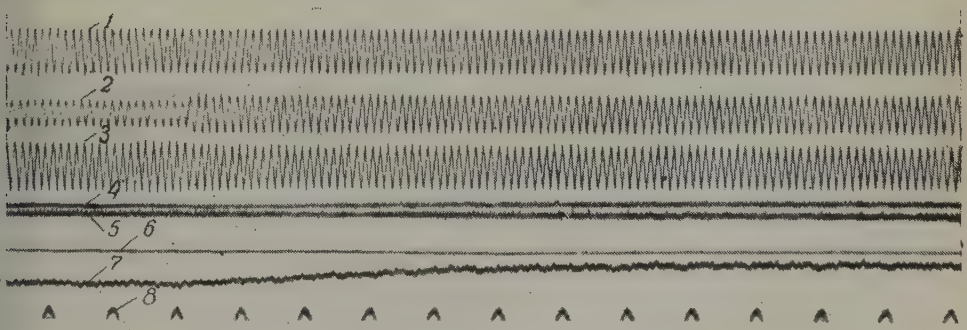

Fig. 7. Oscillograms of transient phenomena in system on connecting an a.c. load:
(Legend as in Fig.6)

The switching of the restraint generator's armature winding is accompanied by an instantaneous change in the collector voltage and

converter currents, but this has no practical effect on the frequency and the magnitude of the a.c. network voltage. Unlike Figs. 6 and 7, the second sine curve from the top in Figs. 8 and 9 shows the load current of the network, whilst the frequency of the time indicator is 500 c/s.

Conclusions

1. The proposed system of simultaneously generating d.c. and stable frequency a.c. widely different running speeds of the primary motor can be used for generating both types of current as well as for generating a.c. alone.

2. The proposed system is more efficient and lighter in weight per unit of output than other similar systems.

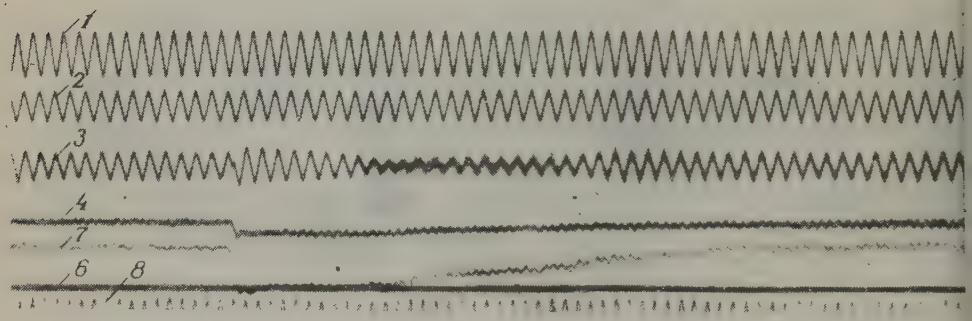

Fig. 8. Oscillograms of transient phenomena in system when changing the armature winding of restraint generator from star to delta.

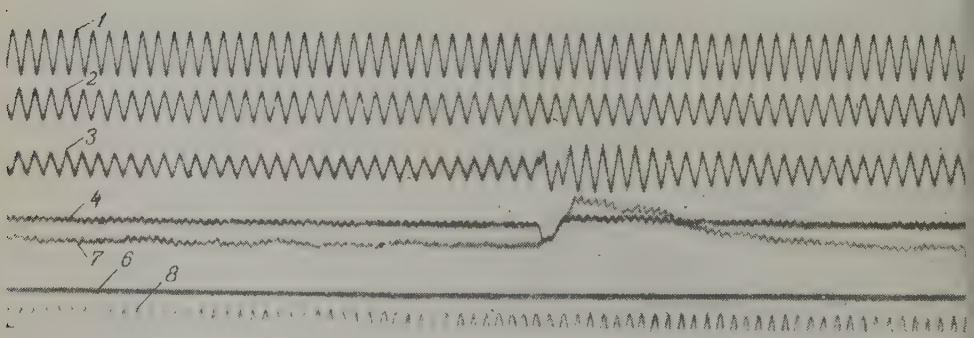

Fig. 9. Oscillograms of transient phenomena in system when changing the armature winding from delta to star.

3. Tests results of a prototype system are in full agreement with theoretical data and testify to the good stability obtained during transient conditions.

4. The proposed system can be used in all cases when it is necessary to generate stable frequency a.c. at different speeds of the primary motor.

Translated by O.M. Blunn

REFERENCES

1. M.P. Kostenko; *Elektrichestvo*, 2 (1948).
2. M.M. Krasnoshapka; *A twin-machine system of generating a.c. of constant frequency at varying rotational speeds of the drive, (Dvukhmashinnaia sistema generirovaniia peremennogo toka postoiannoi chastoty pri izmeniaiushcheisia skorosti vrashcheniia privoda)*. Iz. VVIA, im. N.E. Zhukovskogo, 545 (1955).
3. V.S. Kulebakin, V.T. Morozovskii and I.M. Sindeev; *The electrical supply of aircraft, (Elektrosnabzhenie samoletov)*. Oborongiz (1956).
4. M.M. Krasnoshapka; In book: *Automation of production processes in agriculture, (Avtomatizatsiia proizvodstvennykh protsessov v sel'skom khozhaistve)*. Akad. Nauk SSSR (1956).
5. B.N. Petukhov; *The electrical supply of aircraft, (Elektrosnabzhenie letatel'nykh apparatov)*. LK VVIA im. A.F. Mozhaiskogo (1960).

A HIGH-SPEED ELECTRO-DYNAMIC CIRCUIT BREAKER*

Yu. G. KOMAROV

(Leningrad)

(Received 31 December 1960)

The electrical industry now has to face the problem of producing high speed switchgear capable of limiting short-circuit currents of over 100 kA in large low-voltage networks with a build-up rate of several tens of millions of amperes per second. The necessary switchgear must be designed for rated currents up to 10 kA and higher, and should be as small and quick-acting as possible. In this paper a description is given of experimental circuit breakers which have been developed on the basis of previous patents [1, 2].

A simple type of breaker is illustrated in Fig. 1. The two short traverses *1* and *2* form a narrow loop in the main circuit. Contacts *3* are disposed on the ends of the traverse. Traverse *2* is fixed, but traverse *1* is secured by a current-conducting hinge *4*. The main spring *5* creates the necessary pressure on contact *3* and *4*. The breaker is supplied with current at points *6* and *7*.

The flow of current along the traverses gives rise to electrodynamic forces which tend to open the contacts *3*. It is possible to select the dimensions of the loop, the shape of the traverse and the amount of pressure on the contacts in such a way that no dangerous weakening of the pressure on the contacts occurs under normal conditions But at a definite short-circuit current the electrodynamic forces increase so much that they overcome the resistance of spring *5* and open contacts *3*. Traverse *1* is then rotated on axle *4* and is fixed in a disconnected position by the stop *8*.

---

* *Elektrichestvo*, 6, 53-55, 1961.

Experimental breakers for rated currents of 500 and 3,000 A have been produced on the basis of the methods shown in Fig. 1. The 3,000 A breaker has been provided with arc quenching contacts.

To determine the current limiting capacity of these breakers tests have been carried out on voltages of 10 to 300 V, short circuit currents of 13 to 100 kA and build-up current rates of (0.65 to 10) x 10^6 A/sec. Fig. 2 illustrates one of the results of the tests on the breakers with arc quenching contacts. It will be seen from the curves in this diagram that the breaker limited the short-circuit current to 38 kA at a steady state value of the circuit current of 100 kA. By way of comparison the dotted line in Fig. 2 shows the short-circuit current interrupted in the same circuit by a "universal" circuit breaker.

Tests with identical circuit parameters have shown that the proposed type of breaker is highly stable as regards the limitation of short-circuit currents. The average fundamental opening time of the breaker did not exceed 2 x 10^{-3} sec. Curves for the movement of the breaker's traverses were also determined during the tests. One such curve $h=f(t)$ is shown in Fig. 3. The fundamental opening time t_0 is plotted along the base and the arc quenching time t_a is also plotted there. This makes it possible to determine the motion of the traverse at different stages.

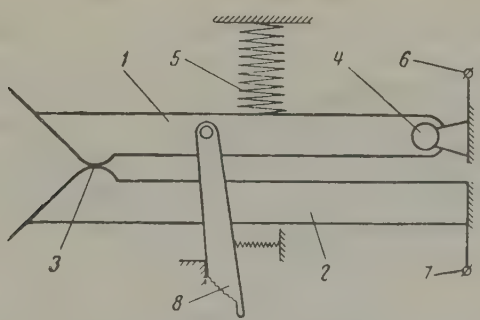

Fig. 1.

However, despite the advantages of this simple system, they have a number of short-comings. The contacts may stick if the short-circuit currents are small, with natural cooling the load does not exceed 5000 A and the system is sensitive to vibration.

To eliminate these shortcomings a new type of breaker was developed using the system illustrated in Fig. 4. The traverses 1 and 2 of this

breaker were water-cooled. Sectional main contacts *3* and arc quenching contacts *4* were fixed at the end of the traverse. Traverse *1* was balanced about axle *5* of the current conducting hinge. The main springs *6* provided the necessary pressure on contacts *3* and *5*. The current is supplied to conductors *7*. The breaker has an auxiliary disconnecting mechanism consisting of a free release device which is secured on shafts *8* and *9*, an electromagnetic release arrangement *10*, feedback *11* and a vibration plate *12*. The axle *13* which is secured to traverse *1*, passes through a slot in the plate *12*.

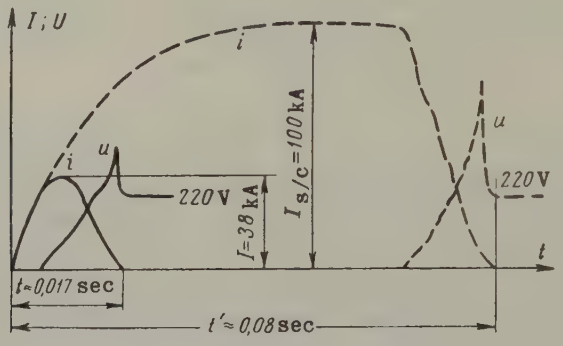

Fig. 2

The device operates (closes) when the interrupting roller *14* rotates 16°. The roller can be rotated from the release arrangement *10*, and through feedback *11* when moved by the electrodynamic forces of traverse *1*. The main springs *6* are secured at one end to traverse *1*, and at the other to lever *15* which is secured on shaft *9*. This was arranged in order to use the energy of the spring to accelerate the operation (closing) of the auxiliary device. Return springs are attached to lever *15*. These springs accelerate the rotation of shaft *9* when the auxiliary device operates (closes).

At small short-circuit currents which only cause small divergences of the traverse, the auxiliary device operates via feedback *11* or the release arrangement *10*, and opens the contacts of the breaker and sticking is thereby prevented.

The breaker is only tripped by the release arrangement at currents which are close to the setting of the release arrangement *10*.

At the first instant when the traverse begins to move the auxiliary device continues to remain in the "on" position and shaft *9* and plate *12* are fixed. When the main contacts have parted 2 to 3 mm the operation

of the auxiliary device takes place via feedback *11*. In this case the release *10* also operates and affects roller *14*. The effect of springs *6* and *16* is then to rotate *9* in a clockwise direction, plate *12* is shifted upwards, the movement of the traverse is accelerated and this fixed in the "off" position so that current limitation is effective and reclosure of the contacts is prevented.

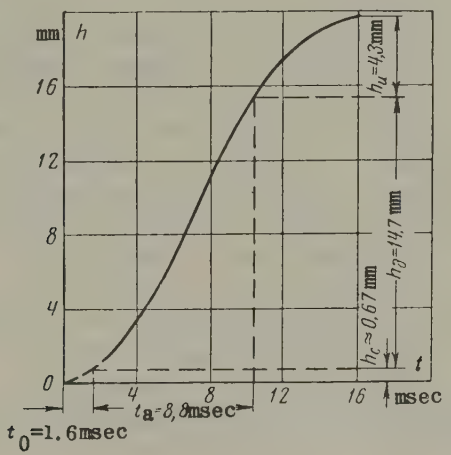

Fig. 3

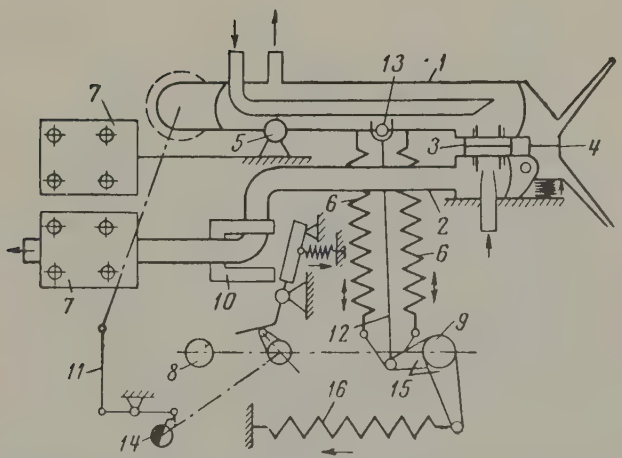

Fig. 4

Remote disconnection of the breaker is possible via the interrupting release arrangement which acts on roller *14*; remote connection can be carried out by a pneumatic drive, for instance, acting on shaft *8*. A

prototype breaker of 5000 A and 320 V has been made and tested on the system illustrated in Fig. 4. The setting of the release arrangement was 10,000 A. The dynamic setting which can be defined by the beginning of movement by the traverse, corresponds to 20 to 25 kA. Natural, or water cooling can be used depending upon the rated current of the circuit breaker. The moving parts of the breaker can be unbalanced in individual cases in use.

Fig. 5 shows an oscillogram of the breaking current with this kind of breaker in a circuit with a steady state value of the short-circuit equal to 133.2kA, at a build-up current rate of 10.6×10^6 A/set and a voltage of 310 V. It will be seen from the oscillogram, that the breaker limited a current up to 53 kA. No sticking of the contacts occurred at current values close to the dynamic setting or because of the vibration at currents of 5 to 10 kA. Under current limiting conditions the fundamental opening time did not exceed 1 m sec. The operating (closing) time of the breaker at over load currents was between 12 and 18 m sec depending on the value of the current to be tripped. At a load of 10 kA and a pressure on the main contacts of 30 kg the overheating of the main contacts of the test breaker do not exceed 53° C. Only about 150 litres of water were consumed for cooling at 5 kA for one hour. The breaker weighs 45 kg and its dimensions are 262 x 515 x 765 mm.

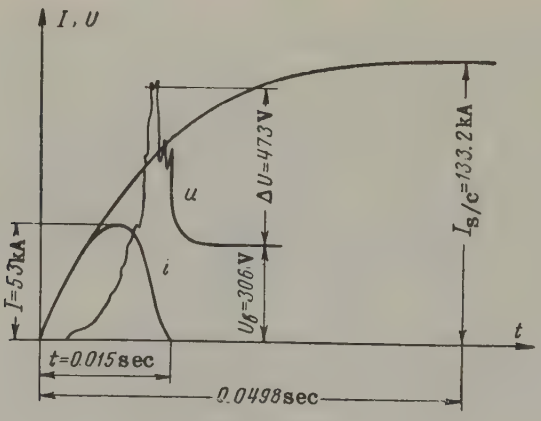

Fig. 5

The conclusion can be drawn from the tests that these experimental breakers can be used to develop actual production models.

Translated by O.M. Blunn

REFERENCES

1. Iu.G. Komarov; Russian patents Nos. 116138, 28 Nov. 1958, 117597, 12 Apr. 1959, 116139, 15 Dec. 1958, 120238, 11 June 1959, 124494, 27 May 1960.
2. Iu.G. Komarov; *Ways of producing an automatic high-speed electro-dynamic circuit breaker.* In book: *Low voltage switchgear. (Puti sozdaniia bystrodeistvuiushchego elektrodinamicheskogo vykliuchitelia. Sborn. "Elektricheskie apparaty nizkogo napriazheniia).* TsBTI elektropromyshlennosti (1959).

A METHOD OF DETERMINING THE LEAKAGE INDUCTANCE OF STATOR WINDINGS IN LARGE A.C. MACHINES WITHOUT THE ROTOR "OUT"*

R.R. PARTS

(Tallin)

(Received 18 June 1960)

The method of taking out the rotor is recommended by many authors for determining the inductive reactance of the stator windings [1,2,3]. The essence of this method is as follows.

A voltage of 3-phase current is supplied from an extraneous source at rated frequency to the stator. Having measured the phase voltages U_p and current I_p it is possible to obtain with a known phase resistance of the stator winding the inductive reactance

$$x_1 + x_{Sch} = \sqrt{\left(\frac{U_p}{I_p}\right)^2 - r_1^2}\,, \tag{1}$$

where x_1 is the inductive reactance of the stator winding, and x_{Sch} the inductive reactance due to the magnetic flux within the stator air gap (Schenkel's correction).

This method was first put forward by M. Schenkel [1]. The term x_{Sch} is therefore known by some authors as *Schenkel's correction*. In order to avoid measuring the magnetic flux inside the stator gap on every occasion, on the assumption that the inductive reactance x_{Sch} is due to the main magnetic flux, the following formula has been recommended by various authors [1,2,3].

---

* *Elektrichestvo*, 6, 88-90, 1961.

$$x_{Sch} = Afl_1 \frac{w_1^2 k_{ow1}^2}{p} \cdot 10^{-8}, \quad (2)$$

where f is the mains frequency, l_1 the length of the stator, w_1 the number of turns in the stator winding phase, k_{w1} the winding coefficient for the main harmonic, p the number of pole pairs and A a coefficient equal to 13.75 in Schenkel's article [1] and 15.1 in the article by Piotrovskii and Efremov [2].

Assuming that only the main magnetic field is present, as does Richter [4], the coefficient A = 15.079. The different values of the coefficient A are explainable by the accuracy of the calculations. The coefficient A = 13.75 was obtained by Schenkel as a result of artificially determining the mean amplitude of the first harmonic of the m.m.f.

Even though the removing of the rotor is a simple method, it has still not been recognized as a suitable method for determining the inductive reactance of the stator winding, since under rated conditions in the synchronous or asynchronous state the inductive reactance x_1 is clearly different from that determined by tests (by the method of rotor withdrawn) where the value $(x_1 + x_{Sch}) - x_{Sch}$.

In order to find the reasons for this discrepancy, the author has tested an A52-4 220/380 V induction motor (Table 1).

TABLE 1

x_1+x_{Sch}, Ω	x_{Sch}, Ω	$(x_1+x_{Sch})-x_{Sch}$, Ω	x_1, Ω
2.234	0.874	1.36	1.68

Schenkel's correction x_{Sch} (second column of Table 1) was calculated by formula (2) for A = 15.79. The inductive reactance of the stator winding $(x_1 + x_{Sch}) - x_{Sch}$ (third column of Table 1) was obtained with the rotor "out". The inductive reactance of the stator winding x_1 (fourth column of Table 1) was determined by the new method developed in the U.S.S.R. at the VNIIEM. If use is made of this method for calculating the operating characteristics of the motor, it can be seen that it corresponds to reality unlike the results obtained by Schenkel's method with the rotor out.

This circumstance is evidence of the fact that the distribution of the magnetic induction on the pole pitch is markedly different from a fundamental sinusoid with the rotor out.

When taking the curve for the distribution of the radial component of magnetic induction by oscillographing the e.m.f. in a rotating measuring coil with a diametral pitch at an instant when the current has its amplitudinal value in one phase, it was thereby confirmed that higher 3-dimensional harmonics were present [1] on the pole pitch with the rotor out.

When taking the curve for the distribution of the radial component of the magnetic induction in one section (Fig. 2) of the four-pole stator in an A 52-4 type motor by oscillographing, it was established that the magnetic induction varies practically along the inclined straight line above the slit in the semi-closed slot. Therefore, in the case of an induction motor it is advisable to proceed from the m.m.f. of the linear sectional sides of the sections on the surface of the stator instead of from points [5].

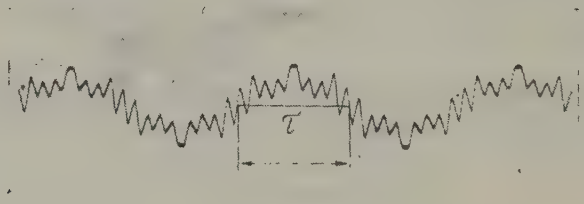

Fig. 1.

For a single phase winding with a linear sectional side, the m.m.f. on the pole pitch f_k is characterized by the expression

$$f_k = \frac{4\sqrt{2}}{\pi 2} \frac{I_0 w_k q}{\frac{\pi b}{\tau 2}} \left[\Sigma (-1)^{\frac{\nu-1}{2}} \frac{k_{o\nu} \nu}{\nu^2} \times \right.$$
$$\left. \times \sin \nu \frac{\pi}{\tau} \frac{b}{2} \cos \nu \frac{\pi}{\tau} x \right] \cos \omega t, \qquad (3)$$

where I_0 is the current in the turn, w_k the number of turns in the section, q the number of slots per pole and phase, ν the order of the three dimensional harmonic, b the width of a linear sectional side, τ the pole pitch, x the transient coordinate along the base with an origin in the middle of the pole, ω the angular frequency of the network, and t the time.

In its more general form the curve for the radial component of magnetic induction on the pole pitch is characterized by the expression

$$B=\left[B_{\delta 1}\cos\frac{\pi}{\tau}x+B_{\delta 3}\cos 3\frac{\pi}{\tau}x+\ldots+\right.$$
$$\left.+B_{\delta\nu}\cos\nu\frac{\pi}{\tau}x\right]\cos\omega t, \tag{4}$$

whilst the magnetic flux through the pole pitch equals:

$$\Phi=\left(\sum_{\nu}\Phi_{\nu}\right)\cos\omega t, \tag{5}$$

where

$$\Phi_{\nu}=(-1)^{\frac{\nu-1}{2}}\frac{2}{\pi}B_{\delta\nu}\frac{\tau_1}{\nu}l_1$$

is the higher three dimensional harmonic of magnetic flux, and $\Psi_{\nu}=\Phi_{\nu}w_1k_{ow\nu}$ is the flux coupling.

For a single phase winding the effective value of the e.m.f. will be

$$E=E_1+E_1\left[-\frac{1}{3}\cdot\frac{B_{\delta 3}}{B_{\delta 1}}\cdot\frac{k_{ow3}}{k_{ow1}}+\right.$$
$$\left.+\ldots+(-1)^{\frac{\nu-1}{2}}\frac{1}{\nu}\cdot\frac{B_{\delta\nu}}{B_{\delta 1}}\cdot\frac{k_{ow\nu}}{k_{ow1}}\right], \tag{6}$$

where

$$E_1=4fB_{\delta 1}\tau_1l_1w_1k_{ow1}.$$

Dividing expression (6) by the magnetization current,

$$x_{m0}+x_{h0}=\frac{E_1}{I_0}+$$
$$+\frac{E_1}{I_0}\left[\sum_{\nu\geqslant 3}(-1)^{\frac{\nu-1}{2}}\frac{B_{\delta\nu}}{\nu B_{\delta 1}}\cdot\frac{k_{ow\nu}}{k_{ow1}}\right], \tag{7}$$

where x_{m0} is the fundamental inductive reactance of the single phase winding and x_{h0} the inductive reactance of single phase winding due to the higher three dimensional harmonics.

In accordance with formula (7) the expression for the inductive

reactance x_{h0} can be written in the form

$$x_{h0} = x_{m0}\left[\sum_{\nu\geqslant 3}(-1)^{\frac{\nu-1}{2}}\frac{1}{\nu}\cdot\frac{B_{\delta\nu}}{B_{\delta 1}}\cdot\frac{k_{ow\nu}}{k_{ow1}}\right]. \tag{8}$$

For a symmetrical multi-pnase winding the inductive reactance x_h due to the higher three dimensional harmonics equals

$$x_h = x_m\left[\Sigma(-1)^{\frac{\nu-1}{2}}\frac{1}{\nu}\cdot\frac{B_{\delta\nu}}{B_{\delta 1}}\cdot\frac{k_{ow\nu}}{k_{ow1}}\right], \tag{9}$$

where x_m is the inductive reactance of the multi-phase winding due to the main magnetic field.

It will be seen from expressions (8) and (9) that to determine the inductive reactance of the higher three dimensional harmonics with known winding coefficients, it is sufficient to know the ratio of the amplitude of the magnetic induction of the higher three dimensional harmonic to the amplitude of magnetic induction of the fundamental harmonic, and to know the sign of the ratio in question.

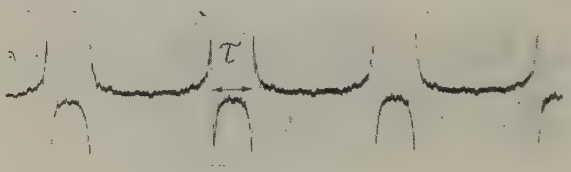

Fig. 2.

It can be seen that this is true for a symmetrical 3-phase winding with a whole number of slots per pole and phase when the curve for the magnetic induction on the pole pitch is a replica of the m.m.f. curve [6, page 1 2 4]. Expression (9) then takes the form

$$x_h = x_m\sum\frac{1}{\nu^2}\cdot\frac{k^2_{ow\nu}}{k^2_{ow1}}, \tag{10}$$

where $\nu = 5, 7, 11, 13, \ldots$.

It should be pointed out that x_h can be calculated by formula (10) by means of curves showing the relationship between the sum of the resistances and the number of slots per pole and phase [4 et al.]

Using expression (3), the amplitude of the harmonic m.m.f. of a

multiphase winding per pair of poles equals

$$F_\nu = m \frac{4\sqrt{2}}{\pi 2} \cdot \frac{I_0 w_k q (-1)^{\frac{\nu-1}{2}}}{\frac{\pi}{\tau} \cdot \frac{b}{2} \nu^2} k_{ow\nu} \sin \nu \frac{\pi}{\tau} \cdot \frac{b}{2}, \tag{11}$$

$$\frac{F_\nu}{F_1} = \frac{k_{ow\nu}}{\nu^2 k_{ow1}} \cdot \frac{\sin \nu \frac{\pi}{\tau} \cdot \frac{b}{2}}{\sin \frac{\pi}{\tau} \cdot \frac{b}{2}} (-1)^{\frac{\nu-1}{2}}. \tag{12}$$

With the rotor out the expression for the tangential component of the magnetic field intensity of the higher 3-dimensional harmonic can be represented in the form:

$$H_{\varphi\nu 1} = -\frac{B_{\delta\nu}}{\mu_0} \left(\frac{R}{R_1}\right)^{\nu p - 1} \sin \nu p \varphi, \tag{13}$$

whilst the m.m.f. of the higher 3-dimensional harmonic between the middles of two adjacent poles will be:

$$F_\nu = \int_{\nu p \varphi = \pi}^{\nu p \varphi = 0} (H_{\varphi\nu 1})_{R=R_1} R_1 d\varphi = \frac{2}{\nu p} \cdot \frac{B_{\delta\nu}}{\mu_0} R_1, \tag{14}$$

where R_1 is the radius of the internal surface of the stator stamping, μ_0 the magnetic permeability of the air and R, φ are transient cylindrical coordinates.

Hence it follows:

$$\frac{F_\nu}{F_1} = \frac{B_{\delta\nu}}{\nu B_{\delta 1}}. \tag{15}$$

From (12) and (15):

$$\frac{B_{\delta\nu}}{B_{\delta 1}} = \frac{k_{ow\nu}}{\nu k_{ow1}} \cdot \frac{\sin \nu \frac{\pi}{\tau} \cdot \frac{b}{2}}{\sin \frac{\pi}{\tau} \cdot \frac{b}{2}} (-1)^{\frac{\nu-1}{2}}; \tag{16}$$

and consequently, with the rotor out the inductive reactance due to the

high 3-dimensional harmonics equals

$$x_h = x_m \sum \frac{k^2_{o\nu}}{\nu^2 k^2_{o1}} \cdot \frac{\sin \nu \frac{\pi}{\tau} \cdot \frac{b}{2}}{\sin \frac{\pi}{\tau} \cdot \frac{b}{2}}. \qquad (17)$$

It should be pointed out that some authors consider that the reactance x_h found in this way is "static". The inductive reactance due to the main magnetic field equals

$$x_m = \frac{4mfw_1^2 k^2_{o1} \tau_1 l_1 \mu_0}{\pi R_1 k_{F_1}} \cdot \frac{\sin \frac{\pi}{\tau} \cdot \frac{b}{2}}{\frac{\pi}{\tau} \cdot \frac{b}{2}}, \qquad (18)$$

where k_{F_1} is a coefficient of saturation practically equal to unity.

Since the inductive reactance due to the higher 3-dimensional harmonics varies greatly as a function of the design of the rotor, it is therefore of interest to establish how accurately the withdrawn rotor method permits the determination of the inductive reactance of the stator which is in effect the sum of the inductive reactance of the slot x_{1s} and face x_{1f} parts.

From test results on an A 52-4 type motor

$$x_{1s} + x_{1f} = \sqrt{\left(\frac{U_p}{I_p}\right)^2 - r_1^2} - (x_m + x_h) =$$
$$= 2.234 - (0.874 + 0.153) = 1.207 \quad \Omega,$$

where x_m and x_h have been found from expressions (17) and (18). According to the proposed Russian method $x_{1s} + x_{1f} = 1.205\ \Omega$. Thus the test results are almost the same as the calculations in this case.

Conclusions

The leakage of the stator with the rotor out is not the same as the leakage in normal operation under synchronous or asynchronous conditions. This occurs particularly in induction machines where the differential leakage depends on the type of rotor circuit, saturation, the air gap, the bevel of the rotor slots and so on.

The numerical value of the inductive reactance for stator leakage with the rotor in will only be the same as its value with the rotor out

in particular cases.

Translated by O.M. Blunn

REFERENCES

1. M. Schenkel; *E und M*, 27, 201-203 (1909).
2. L.M. Piotrovskii and D.V. Efremov; *Elektrichestvo*, 8 (1930).
3. A.A. Vainfil'd; *ADP type controlled motors with hollow rotors, (Upravlaemye elektrodvigateli s polysn rotorom tipa ADP)*, Sudpromgiz (1957).
4. R. Rikhter; *Electrical machines, (Elektricheskie mashiny)*, Vol. 1, pp. 165, 166, 207 and 208 (1935).
5. L.M. Piotrovskii; *Elektrical machines (Elektricheskie mashiny)*, Gosenergoizdat, 317 (1949).
6. M.P. Kostenko and L.M. Piotrovskii; *Electrical machines Pt. II, (Electricheskie mashiny Ch. II)*. Gosenergoizdat, p.124 (1957).

ABSTRACTS FROM PAPERS PUBLISHED IN ELEKTRICHESTVO No.6, 1961

Leading article

A new era in the history of humanity. V.V. Dobronravov, (pp. 1-4).

A tribute is paid to all persons associated with Gagarin's flight in space. The significance of the achievement is then considered in general terms.

Amplifiers

Operation of a full-wave d.c. magnetic amplifier. R.A. Lipman et al., (pp. 74-78).

A new type of push-pull d.c. magnetic amplifier is described which it is claimed has a highly efficient performance.

A magneto-transistor power amplifier with a differentially connected load. M.E. Poiurovskii, (pp. 56-58).

A short description is given of a push-pull magneto-transistor power amplifier in which the transistors act as switches. Pulse-width modulation of the output signal is effected by a transformer with a core having a rectangular hysteresis loop.

Control engineering

Using critical generator self-excitation in closed motor-generator sets. V.I. Kliuchev, (pp. 26-32).

The author considers the use of negative voltage feedback from the generator in the state of critical self-excitation in order to improve the dynamic behaviour of amplifier-controlled motor-generator sets and make them more compact.

Dynamic self-regulation of multi-motor drives in paper-making plant. G.M. Levin, (pp. 49-53).

A graphical-analytical method is proposed for determining those dynamic properties of motor drives which will keep the tension of the paper within specified limits in paper-making plant.

Ignitrons

An electromagnetic ignition system for ignitrons. Yu.A. Shmain et al., (pp. 61-65).

An account is given of the research into the ignition systems of ignitrons at the All-Union Power Research Institute. A method has been developed for analysing the operation of electromagnetic pulse generators with a variable load impedance.

Power systems

A statistical appraisal of urban network operation. B.V. Gnedenko, et al., (pp. 71-74).

The authors confine themselves to the implications of using probability methods to assess the operating conditions of low voltage mains.

Increasing the steady state stability limit by regulating the d.c. transmission. V.G. Novitskii, (pp. 58-61).

The limit of static stability in the transmission of a.c. can be increased by automatically varying the static characteristics of the rectifiers. Here the transmission of d.c. is regulated in accordance with the parameters of the a.c. system.

Deformation of the waves in a multi-conductor line due to the earth and conductor resistance. M.V. Kostenko, (pp. 5-10).

A practical method is proposed for calculating the distortion of the wave in multi-wire overhead transmission lines. An approximate solution is obtained in terms of tabulated time functions which take into account balancing currents and earth losses. An accuracy to within 15% is claimed over a 10 km stretch of line.

Estimating the effect of meteorological conditions on the electrical strength of external insulation. N.N. Beliakov et al., (pp. 20-26).

Two correcting coefficients are produced which it is claimed

characterize the electrical strength of all types of external insulation. From tests it has been established that these coefficients define meterological conditions and altitude with different probabilities. These relationships can be used in the design of the external insulation of distribution gear and high voltage transmission lines.

Rotating machines

A method of studying steady state fault currents in a self-excited alternator. D.V. Vilesov et al., (pp. 45-49).

A new method is proposed for calculating the steady state short circuit current in an independent alternator system. The results are used to determine the transfer and super-transfer components of the short circuit current more accurately.

The voltage of a self-excited alternator with a suddenly applied load. M.I. Aliab'ev, (pp. 79-82).

An analysis is made of the equations of an idealized self-excited alternator with an automatic voltage control system.

Traction

Special operating conditions of power systems supplying a.c. electric locomotives. N.A. Mel'nikov et al., (pp. 10-15).

A statistical method is proposed for estimating the operating conditions of electrical equipment used on very long stretches of railway line to supply a.c. electric locomotives.

The effect of external voltage surges on H60 type electric locomotives. M.N. Novikov, (pp. 15-20).

An account is given of the research carried out at the Institute of Railway Engineers in Leningrad to establish the effect of external voltage surges on the insulation of gear used in the large H60 locomotive's low voltage transformer circuit.

Transformers

Some special characteristics of transformer insulation. G. Slovikovski, Warsaw, (pp. 82-87).

A study is made of the factors affecting a certain ratio r_{60}/r_{15} which is used to define the electrical characteristics of transforme

insulation. Here r_{60} is the resistance 60 sec after connecting the transformer and r_{15} that after 15 sec. The use of this criterion is considered for service tests and final factory tests.

An approximate method of calculating overvoltages across the secondary windings of current transformers.
Ya.S. Gel'fand, (pp. 66-71).

The proposed method is based on the approximation of the actual e.m.f. curve for the open secondary winding of the current transformer without losses by triangular pulses of alternate polarity with a large mark space ratio. The resulting curve is expanded into a Fourier series and the effect of losses and the load on the amplitude and phase of the individual harmonic components is then taken into account. Subsequent summation gives the required voltage amplitude across the secondary winding.

ABSTRACTS FROM PAPERS PUBLISHED IN ELEKTRICHESTVO No.7, 1961

Leading article

To new achievements in the development of Soviet science. (pp.1-6).

An account is given of a recent conference which was held in the Kremlin to discuss the future development of Soviet science. Development work, applied research and fundamental research was discussed.

Capacitors

Determining the initial conditions for sudden changes in voltages and currents. I.A. Zaitsev *et al.*, (pp.52-55).

A contribution is made to the determination of initial conditions when sudden changes occur in the currents in inductances or voltages across capacitors. Simple schemes are obtained by analysing commutation behaviour which make it possible to determine the initial conditions for sudden changes in voltages and currents quickly.

Determining the reactive power in capacitors. N.I. Nazarov *et al.* (pp.55-59).

It is considered that the specific dissipating surface of a capacitor varies with the shape of the housing and its dimensions. For a given volume, the dissipating surface is maximum for a rectangular parallelepiped with the minimum permissible width of base. The reactive power of the capacitor unit depends on the design of the capacitor as well as the physical characteristics of the material.

Control engineering

Joint selection of the motor criteria and the gear ratio. D.A. Popov, (pp.63-67).

A study is made of the problems connected with choosing the optimum gear ratio for an electric drive under starting conditions when the torque of the motor and the moment of mechanical resistance of the drive device are constant. The study is made from the point of view of minimizing weight.

Use of the phase plane method for studying transient mechanical behaviour in electric drives. L.I. Gandzha, (pp.68-72).

Phase diagrams of transient behaviour are constructed from an analysis of the equation of motion of the drive for the various possible types of load.

The use of saturable reactors to prevent variation in the torque of induction motors due to transient currents. M.M. Sokolov, (pp. 72-75).

An account is given of tests on electric drives with induction motors and saturable reactors which show that a smooth increase in motor torque and speed can be obtained on starting and reversing. The connexion of saturable reactors in the stator circuit only increases acceleration time slightly. Acceleration time depends on the magnetization current of the reactor.

A frequency-controlled drive for a horizontal planing machine. D.A. Zavalishin *et al.*, (pp.75-79).

It is argued that the best frequency-controlled asynchronous drive system for horizontal planing machines is one with a compensated collector generator excited on the stator side. A detailed account is given of a prototype system.

Elimination of zones of insensitivity in ferromagnetic pickups and amplifiers. B.K. Karpenko, (pp.84-86).

A cheap and effective way of eliminating dead bands in pick-ups and amplifiers with ferromagnetic cores is proposed by the use of an additional magnetic circuit.

Magnetism

The permeance of magnetic circuits with teeth. Yu.S. Rusin, (pp. 59-63).

Owing to the considerable leakage flux in magnetic circuits with teeth, the author proposes an approximate estimate of permeance which is based on a particular idealization of the field of the system. The space surrounding the pole ends is divided into separate regions and, depending on the shape of the poles, the field between the faces is studied separately from that between the ribs. The type of magnetic circuit in question is illustrated in a diagram.

Power systems

Long-distance power transmission with d.c. magnetized reactor-transformers and forced capacitor banks. D.I. Azar'ev, (pp. 24-30).

The cost of transmission can be reduced by combining a transformer with an automatically-controlled high-voltage reactor in a high-speed unit which is capable of reducing overvoltages and increasing carrying capacity. The magnetic system of the reactor is split into parallel branches which are magnetized by d.c. in such a way that the fluxes in the branches are in opposite directions.

Automatic equipment for power system continuity. I.A. Syromiatnikov, (pp. 18-24).

The author considers the main automatic Soviet equipment available for improving the reliability of power system operation, namely, excitation regulators, frequency unloading devices, reserve supply auxiliaries, automatic reclosure, starting devices which react to the rate of change in voltage and a hydraulic differentiator for turbine steam.

Zero sequence equivalent networks for transmission lines with different voltages. N.G. Geinin, (pp. 79-81).

It is shown how to compile a zero sequence equivalent network which includes the mutual inductance between two or several transmission lines when each of the nearby lines is of a different voltage.

Rotating machines

The effect of excitation systems on the stability of large interconnected turbo-generators. V.M. Bobrov *et al.*, (pp. 7-13).

A study is made of the stability of large turbo-generators with

different systems of excitation. The use of electrodynamic modelling has made it possible to use natural excitation regulators, find their optimum adjustment and study electromechanical phenomena during transient behaviour.

Artificial damping in large synchronous machines. I.D. Urusov *et al.*, (pp.13-18).

Instead of increasing the flywheel mass, it is proposed to use a system of artificial damping to reduce the oscillation of synchronous machines with a pulsating load. Artificial damping is based on the creation of an additional electromagnetic rotational torque on the shaft by introducing additional periodic currents in the rotor circuits. The theory of the method is given along with test results.

Analysis of dynamic stability with the effect of damper windings, speed governors and excitation included. K.I. Bogatev, (pp.31-34).

A refinement to the method of successive intervals is proposed which makes it possible to include the effect of damper windings, speed governors and excitation when an analytical estimate of dynamic stability is required for synchronous alternators.

Experimental determination of the m.m.f. of the armature commutation reaction in d.c. machines. V.A. Lifanov, (pp.81-84).

A method is proposed which dispenses with calculated data in the determination of the m.m.f. of the armature commutation reaction by a Hall e.m.f. transducer.

Traction

Reduction of wheel-spin on electric locomotives. B.P. Petrov, (pp.35-41).

A study is made of the factors affecting high adhesion factors for electric locomotives. Recommendations are made for automatically stopping wheel spin.

Transformers

Problems of voltage regulation in auto-transformers. A.G. Kraiz, (pp.41-48).

A method is described for comparing different systems of voltage regulation for large auto-transformers using the typical power of auto-transformers. A refined method of analysis is proposed for the

system of regulation in the neutral of the auto-transformer. It can be used to specify the limits of regulation with over- or under-excitation. A short description is given of a new 220 kV auto-transformer with built-in apparatus for regulating the voltage.

Voltage stabilizers

Ferroresonant voltage stabilizers using magnetic material with a rectangular characteristic. D.I. Bogdanov, (pp.48-51).

A theoretical study is made of the phenomena associated with the operation under load of ferroresonant voltage stabilizers in which the saturable core is made of cold-rolled steel or magnetic alloy with a high coefficient of rectangularity.

ABSTRACTS FROM PAPERS PUBLISHED IN ELEKTRICHESTVO No. 8, 1961

Computers

Electronic simulation of electrical circuits, V.G. Vasil'ev *et al.*, (pp.41-45).

Certain aspects of the simulation of R, L and C circuits are considered on the basis of a simple example. The rules of the "dual circuit" method of analysis are formulated. An electrical circuit with one voltage source is simulated without forming equations for the circuit or the model. A minimum of amplifiers and integrating elements is required.

Regulation of the excitation of two synchronous machines operating in parallel, G.V. Mikhnevich *et al.*, (pp.31-35).

An analogue computer method is proposed for determining the optimum structure of the control signals with respect to their derivatives and assessing their effect on a coefficient of regulation for the excitation of two synchronous machines operating in parallel. The results for generators at the Stalingrad hydro-electric station are given by way of illustration.

Control engineering

The motor drive of a reversible cold rolling mill, I.M. Tolmach *et al.*, (pp.79-81).

An account is given of the motor drive which has been installed on a four-roll mill for low and medium carbon steel strip up to 300 mm wide with reduction from 3 to 0.2 mm in up to nine passes. The drive features the use of e.m.f. and current regulators to maintain rolling tension.

Measuring amplifiers for centralized automatic control systems, R.R. Kharchenko *et al.*, (pp.7-13).

Attention is concentrated on those d.c. measuring amplifiers which

are used to convert the signals of pick-ups in group data-processing circuits. The authors review six types of system covering the combined transmission of the amplified signal without a device for correcting zero drift, and wideband amplifiers with a device for correcting zero drift.

Electrical steel

The properties of 1 mm cold rolled electrical steel, A.I. Beliakov *et al.*, (pp.82-83).

A short account is given of the properties of the 1 mm gauge cold-rolled grain-oriented steel for the poles of d.c. electrical machines now being produced in Novosibirsk.

Insulation

Interdependence of the physical properties of organic and inorganic polymers, N.I. Vorob'ev *et al.*, (pp.76-78).

To simplify the problem of investigating the large number of polymers which are available, the author takes the magnitude of the inter-molecular forces as the main criterion defining the physical properties of many polymer substances.

The dielectric permeability and tangent of the loss angle for paper dielectrics, S.K. Medvedev, (pp.66-72).

Formulae are produced for calculating ϵ, tan δ and other characteristics of paper on the basis of the actual structure of the paper on the assumption that the relative thickness of the cellulose in the space between the layers varies between 0 and 1 according to a certain law. The pores are assumed to be in series in each individual volume of cellulose.

Power systems

Determining optimum operating conditions for power systems, V.M. Gornshtein, (pp. 19-24).

A study is made of common errors which are said to be made in the economic analysis of power system analysis.

Tuned power transmission systems, V.K. Shcherbakov, (pp.25-30).

It is stated that theory and laboratory investigations indicate that half-wave tuned transmission lines of 2000 and 2500 km can

ensure high steady state stability and relative voltage stability at line ends. The author disputes the reasons which have been given for not using this system and advocates its use on the grounds of efficiency and the possibility of intermediate off-take of power along the line.

Rotating Machines

Turbo-generators of large unit capacity, V.V. Titov, (pp.1-4).

A short account is given of the work which has been done at the Electrosila works in the U.S.S.R. on the development of 300 and 500 MW turbo-generators. The new 300 MW generators are described and it is stated that 500 MW generators can be made on the same principles when the demand arises. Extremely high efficiency is claimed and it is an interesting paper. Unfortunately, this account does not explain how the efficiency is achieved or how it is calculated and some of the main features have their counterpart in recent American, Swiss and British innovations.

The problems of developing new small and F.H.P. motors, N.P. Ermolin, (pp. 4-7).

This paper classifies the problems involved in the development of small and f.h.p. motors into those which are common to all types of such motor and those which are special for particular applications. The main purpose of the article is to draw attention to the need for keeping State Standards up to date and co-ordinating research.

New 100 kW amplidynes, B.F. Tokarev *et al.*, (pp.14-18).

Two new types of amplidyne are to be produced in the U.S.S.R., namely, three-stage amplidynes with a longitudinal field, and multipole amplidynes with a transverse field (four and eight poles) with increased magnetization of the winding along the transverse axis or with additional poles along the longitudinal and transverse axes. The equipment is compared and the respective merits assessed.

A new principle of obtaining constant advance times in automatic synchronizers, N.N. Vostroknutov *et al.*, (pp.35-40).

In this article the synchronizers are defined as devices which select the angle of lead and stop action if the amount of slip is too large. A new approach to the design of the time advance elements of such synchronizers is proposed in which the angle of lead is directly converted into a proportional d.c. voltage. This provides the possibility of twice-differentiating this voltage, as required for considering acceleration of slip. A detailed account

is given of a device for the exact synchronization of generators.

A two-motor machine-valve stage with semiconductor rectifiers, M.G. Chilikin *et al.*, (pp. 50-56).

An appraisal is made of the advantages of replacing one large slip ring motor by two smaller motors of the same total power in high speed drives of 1000 to 10,000 kW and 5000-7000 rev/min. In the proposed system the slip energy is converted by semiconductor diodes and it then passes into the network.

Calculation of the steady state errors in speed governors for d.c. motors, S.S. Roizen, (pp. 56-62).

Two fundamental methods of speed control for d.c. motors are considered with a view to determining the accuracy with which speed governors operate in the automatically controlled drives of rolling mills and lathes etc. Formulae are produced for calculating the degree of error under steady state conditions.

A study of the e.m.f. induced in electrical machines using an electrolytic tank, K.S. Demirchian *et al.*, (pp. 62-66).

In the proposed method the model of the rotor is fixed on a plate which slides along the bottom of the tank. A layer of vaseline is placed between the bottom of the tank and the plate to keep out the electrolyte and reduce friction. The model of the stator is secured to a fixed plate. In order to determine the potential differences accurately, the linear displacement of the rotor is measured and not the angle of rotation.

Switchgear

The measurement of large transient currents, V.D. Liashenko, (pp. 46-50).

In short-circuit tests on switchgear it has been possible to combine the advantages of shunts and current transformers in the measurement of the large transient currents which arise. The Switchgear Laboratory of the All-Union Electrical Engineering Institute has developed a successful method of measurement with air-cored current transformers using a toroidal core with a high-impedance winding, a d.c. amplifier with an integrating capacitance at the input and an electromagnetic oscillograph vibrator.

The leader stage of a spark discharge, V.P. Larionov, (pp. 72-76).

The author develops the notion of a leader stage in spark discharges

in long air gaps which precedes the main discharge and forms a leader channel between the electrodes. The mean longitudinal potential channel between the electrodes. The mean longitudinal potential gradients in the leader channel are determined along with the conductance of the leader channel, the concentration of the electrons and the time necessary for the formation of the leader channel.

Translated by O. Blunn

ELEKTRICHESTVO

Editor-in-Chief: N. G. DROZDOV

EDITORIAL BOARD

ELECTRIC TECHNOLOGY, U.S.S.R.

1961 VOLUME 2

CONTENTS

Printed in Great Britain by Pergamon Printing & Art Services Ltd., London